

TECHNISCHE UNIVERSITÄT MÜNCHEN
Professur für Biotechnologie der Naturstoffe

METABOLISM OF ABSCISIC ACID IN STRAWBERRY FRUITS

NICOLÁS FIGUEROA FUENTEALBA

Vollständiger Abdruck der von der Fakultät TUM School of Life Sciences der Technischen Universität München zur Erlangung des akademischen Grades eines

Doktors der Naturwissenschaften (Dr. rer. nat.)

genehmigten Dissertation.

Vorsitzender: Prof. Dr. Erwin Grill

Prüfer der Dissertation: 1. Prof. Dr. Wilfried Schwab

2. Prof. Dr. Brigitte Poppenberger-Sieberer

Die Dissertation wurde am 10.06.2020 bei der Technischen Universität München eingereicht und durch die Fakultät TUM School of Life Sciences am 12.10.2020 angenommen.

ACKNOWLEDGMENTS

I would like to express my sincere gratitude to Prof. Dr. Schwab for giving me the possibility to join the BiNa team and for supporting me during the entire process since the application for the scholarship until now. Thank you so much for your infinite patience and willingness with the corrections, and particularly I will always remember your constant motivational and positive words.

I am also very grateful to my mentor, Prof. Dr. Carlos Figueroa, for his continuous support since I was a bachelor student. Thanks for always believing in me and appreciating my work. It means a lot to me.

Special thanks to Prof. Dr. Poppenberger for her willingness to kindly help me with the recommendation letters and participating as a member of my examining committee.

Furthermore, I would like to thank Dr. Thomas Hoffmann, Dr. Katja Härtl, Dr. Rafal Jonczyk, and Dr. Fong-Chin Huang for providing me their scientific support at different stages of my research and sharing all their experience and knowledge with me. Thanks to Dr. Ruth Habegger, Heike, Anja, Hannelore, and Mechthild. Your work is essential for each student and the functioning of the team.

Johanna and Annika, without your invaluable help with the LC-MS analyses, this research would not have been possible. I appreciate your patience and time, not only with the LC-MS but also with the German language. Along with Shuai, you made me feel at home. Thank you for your friendship!

Emilia, Kate, Soraya, Martina, Jieren, Dr. Guangxin Sun, Dr. Elisabeth Kurze, Dr. Julian Rüdiger, Dr. Isabelle Effenberger, thanks to all of you for your kindness and friendship.

I cannot thank my family and wife enough for all the support and love during all these years. Thank you for always being there.

Finally, thanks to the National Commission for Scientific and Technological Research (CONICYT - Chile) and the German Academic Exchange Service (DAAD) for funding.

ABSTRACT

Fruit ripening is a complex and highly regulated process characterized by several physiological changes, which finally determine the organoleptic and nutritional properties of fleshy fruits. Based on physiological differences in their ripening pattern, fruits are classified as climacteric or non-climacteric. At the onset of ripening, climacteric fruits exhibit a peak in respiration rate along with a remarkable increase of autocatalytic ethylene production, while non-climacteric fruits do not display significant changes in respiration rate or ethylene production during the ripening process. Moreover, in climacteric fruits, ethylene regulates most ripening aspects, but in non-climacteric fruits, the ripening does not necessarily depend on ethylene, therefore much less information is available concerning to the mechanisms triggering and coordinating ripening in non-climacteric fruits. In this regard, strawberry has emerged as a model system for the study of non-climacteric ripening.

Besides auxin, abscisic acid (ABA) is a key hormone in non-climacteric *Fragaria spp*, regulating multiple physiological processes during fruit ripening such as fruit softening and red color acquisition but its metabolism in the fruit is largely unknown. Here, we analyzed the levels of ABA and its catabolites at different developmental stages of strawberry ripening in diploid and octoploid genotypes and identified two functional ABA glucosyltransferases (FvUGT71A49 and FvUGT73AC3) and two regiospecific ABA 8'-hydroxylases (FaCYP707A4a and FaCYP707A1/3). ABA glucose-ester content increased during ripening in all analyzed diploid *F. vesca* varieties but decreased during the ripening in octoploid *F. x ananassa* cv. Elsanta. Dihydrophaseic acid content increased throughout ripening in all analyzed receptacle samples, while 7'-hydroxy-ABA and neophaseic acid did not show significant changes during fruit ripening. The receptacle is the main tissue for ABA biosynthesis, but also for ABA metabolism, as the content of ABA metabolites in the receptacle was generally 100 times higher than in achenes. The increase in ABA content in the receptacle during ripening is due to an increase in ABA biosynthesis and to a decrease in ABA oxidation in the fruit.

On the other hand, even when previous studies suggested that cytokinins (CKs) might play a role during strawberry ripening, they have been poorly studied during this process. We identified and characterized the kinetic properties of a *trans*-zeatin glucosyltransferase (FvUGT85A80) and investigated the content of two active cytokinins throughout fruit ripening in receptacle tissue: *trans*-zeatin and N₆-isopentyladenine. Besides, we also quantified *trans*-zeatin-glucoside content. The *trans*-zeatin concentration peaked at the intermediate developmental stage and then decreased towards the end of the ripening. This behavior was conserved in *F. vesca* as well as in *F. x ananassa*. In contrast, we found a burst of N₆-isopentyladenine production at the ripe developmental stage of *F. vesca* fruits, however, a basal level of N₆-isopentyladenine was present in *F. x ananassa* during the whole ripening process. Furthermore, levels of zeatin glucoside decreased during the ripening except in one variety of *F. vesca*, where it slightly increased.

The accumulation patterns of different ABA catabolites and CKs along with the transcript abundances from the literature of the involved genes suggest the existence of conserved behaviors among species and varieties but also show that strawberry fruit can prefer a particular metabolic pathway in a certain tissue, variety, and species. This contrast can be present not only in phytohormone metabolism but also at the biosynthetic level in the case of CKs. The study highlights the significance of ABA metabolites during the ripening of non-climacteric fruit and provides metabolomic data to support the hypothesis of a probable antagonistic relationship between ABA and *trans*-zeatin. Further studies are needed to elucidate if contrasting levels related to hormone biosynthesis or metabolism are associated with physiological differences among *Fragaria spp.*

ZUSAMMENFASSUNG

Die Fruchtreifung ist ein komplexer und hochgradig regulierter Prozess, der durch mehrere physiologischen Veränderungen gekennzeichnet ist, die schließlich die organoleptischen und ernährungsphysiologischen Eigenschaften der fleischigen Früchte bestimmen. Aufgrund der physiologischen Unterschiede in ihrem Reifungsmuster werden Früchte als klimakterisch oder nicht-klimakterisch klassifiziert. Zu Beginn der Reifung zeigen klimakterische Früchte eine hohe Atmungsrate zusammen mit einer bemerkenswerten Zunahme der autokatalytischen Ethylenproduktion, während nicht-klimakterische Früchte während des Reifeprozesses keine signifikanten Veränderungen der Atmungsrate oder der Ethylenproduktion aufweisen. Darüber hinaus reguliert Ethylen bei klimakterischen Früchten die meisten Aspekte der Reifung, während bei nicht-klimakterischen Früchten die Reifung nicht vom Ethylen abhängt, weshalb viel weniger Informationen über die Mechanismen zur Verfügung stehen, die die Reifung bei nicht-klimakterischen Früchten auslösen und koordinieren. In dieser Hinsicht hat sich die Erdbeere als Modellsystem für die Untersuchung der nicht-klimakterischen Reifung herauskristallisiert.

Neben Auxin ist Abscisinsäure (ABA) ein Schlüsselhormon im Reifungsprozess von nicht-klimakterischen *Fragaria*-Arten. ABA reguliert zahlreiche physiologische Prozesse während der Fruchtreifung, wie z.B. die Erweichung der Früchte und die Rotfärbung, aber der Metabolismus von ABA in der Frucht ist noch weitgehend unbekannt. In dieser Arbeit analysierten wir die Gehalte von ABA und seinen Kataboliten in verschiedenen Entwicklungsstadien der Erdbeerfruchtreifung in diploiden und octoploiden Genotypen und identifizierten zwei funktionelle ABA-Glucosyltransferasen (FvUGT71A49 und FvUGT73AC3) sowie zwei regiospezifische ABA-8'-Hydroxylasen (FaCYP707A4a und FaCYP707A1/3). Der ABA-Glucose-Ester-Gehalt stieg während der Reifung in allen analysierten diploiden *F. vesca*-Sorten an, nahm jedoch während der Reifung in der octoploiden *F. x ananassa* cv. Elsanta ab. Der Dihydrophaseinsäuregehalt stieg während der Reifung in allen analysierten Fruchtfleischproben an, während die Konzentrationen an 7'-Hydroxy-ABA und Neo-Phaseinsäure keine signifikanten Veränderungen während der Fruchtreife

zeigten. Das Fruchtfleisch ist das Hauptgewebe für die ABA-Biosynthese, aber auch für den ABA-Stoffwechsel, da der Gehalt an ABA-Metaboliten im Fruchtgewebe im Allgemeinen 100 Mal höher war als in den Achänen (Samen). Der Anstieg des ABA-Gehalts im Fruchtfleisch während der Reifung ist auf eine Zunahme der ABA-Biosynthese und auf eine Abnahme der ABA-Oxidation in der Frucht zurückzuführen.

Andererseits sind die Cytokinine (CKs), auch wenn frühere Studien nahelegten, dass sie während der Erdbeerfruchtreifung eine Rolle spielen könnten, während dieses Prozesses nur unzureichend untersucht worden. Wir identifizierten und charakterisierten die kinetischen Eigenschaften einer *trans*-Zeatin-Glucosyltransferase (FvUGT85A80) und untersuchten den Gehalt von zwei aktiven Cytokinin während der gesamten Fruchtreife im Fruchtgewebe: *trans*-Zeatin und N6-Isopentyladenin. Darüber hinaus quantifizierten wir auch den Gehalt an *trans*-Zeatin-Glucosid. Die *trans*-Zeatin-Konzentration erreichte ihren Höhepunkt im mittleren Entwicklungsstadium und nahm dann gegen Ende der Reifung ab. Dieses Verhalten war sowohl bei *F. vesca* als auch bei *F. x ananassa* Arten zu beobachten. Im Gegensatz dazu fanden wir einen Anstieg der N6-Isopentyladeninergehalte im späten Entwicklungsstadium von *F. vesca*-Früchten, jedoch war während des gesamten Reifeprozesses ein basaler Gehalt an N6-Isopentyladenin in *F. x ananassa* vorhanden. Darüber hinaus nahm der Zeatinglucosid-Gehalt während der Reifung ab, außer bei einer Sorte von *F. vesca*, wo er leicht erhöht war.

Die Akkumulationsmuster verschiedener ABA-Kataboliten und CKs sowie die Transkriptgehalte der beteiligten Gene lassen auf eine konservierte Regulation der Arten und Sorten schließen, zeigen aber auch, dass die Erdbeerfrüchte einen bestimmten Stoffwechselweg in einem bestimmten Gewebe, einer bestimmten Sorte und einer bestimmten Art bevorzugen können. Dieser Kontrast kann nicht nur im Phytohormon-Stoffwechsel, sondern auch auf der biosynthetischen Ebene bei CKs beobachtet werden. Die Studie unterstreicht die Bedeutung von ABA-Metaboliten während der Reifung von nicht-klimakterischen Früchten und liefert metabolomische Daten zur Unterstützung der Hypothese einer wahrscheinlichen antagonistischen Beziehung zwischen ABA und *trans*-Zeatin. Weitere Studien

sind erforderlich, um zu klären, ob kontrastierende Gehalte, die mit der Hormonbiosynthese oder dem Metabolismus zusammenhängen, mit physiologischen Unterschieden bei *Fragaria* spp. in Verbindung gebracht werden können.

CONTENTS

1. INTRODUCTION	1
1.1 Strawberry plant	1
1.2 Fruit ripening	1
1.3 Glycosyltransferases and hormonal regulation	4
1.4 Abscisic acid biosynthesis and its role in strawberry ripening	5
1.5 Abscisic acid catabolism	8
1.5.1 Abscisic acid glucosylation	8
1.5.2 Abscisic acid hydroxylation	10
1.6 Biosynthesis and metabolism of cytokinins	11
1.7 Aim of the thesis	13
2. MATERIALS	15
2.1 Plant material	15
2.2 Chemicals	15
2.3 Microorganisms	15
2.4 Primers	16
2.5 Vectors	18
2.6 Equipment	19
2.6.1 Liquid chromatography ultraviolet electro-spray ionization mass spectrometry	19
2.6.2 Laboratory equipment	20
2.7 Software	21
2.8 Internet Resources	21
3. METHODS	22
3.1 Extraction of secondary metabolites from strawberry tissues for quantification by LC-MS	22
3.2 RNA isolation from strawberry fruits	22
3.3 cDNA synthesis	23
3.4 Plasmid isolation from microorganisms	23
3.4.1 Plasmid isolation from <i>E. coli</i>	23
3.4.2 Plasmid isolation from <i>S. cerevisiae</i>	23
3.5 Polymerase chain reaction	24

3.6	Real-time PCR	26
3.7	Construction of plasmids	27
3.8	Transformation of plasmid in microorganisms	27
3.8.2	Transformation of <i>S. cerevisiae</i>	28
3.8.3	Transformation of <i>A. tumefaciens</i>	28
3.9	Isolation of microsome protein.....	29
3.10	<i>In vitro</i> and biotransformation assays with P450 enzymes	30
3.11	Heterologous expression and purification of recombinant UGTs in <i>E. coli</i>	31
3.12	Sodium dodecyl sulfate polyacrylamide gel electrophoresis (SDS-PAGE).....	32
3.13	<i>In vitro</i> UGT activity assay	33
3.14	UDP-Glo assay and kinetics	34
3.15	Phylogenetic tree	34
3.16	Statistical analysis.....	36
4.	RESULTS	37
4.1	Selection and cloning of candidate glycosyltransferases and hydroxylases.....	37
4.2	Characterization of isolated UGTs.....	38
4.2.1	Enzymatic activity of isolated UGTs.....	38
4.2.2	Kinetic properties of isolated UGTs.....	40
4.2.3	Substrate specificity of UGTs with activity towards ABA	42
4.3	Enzymatic activity of <i>FaCYP707A1/3</i> and <i>FaCYP7074a</i>	43
4.4	Extended incubation of UGT71A49 with ABA.....	46
4.5	Quantification of ABA and its metabolites during strawberry ripening .	46
4.6	Analysis of ABA and ABA-GE content in agroinfiltrated fruits	51
4.7	Phylogenetic tree	52
4.8	Cytokinins quantification during strawberry ripening.....	55
5.	DISCUSSION.....	58
5.1	Enzymatic activity of isolated UGTs	58
5.2	Enzymatic activity of P450s enzymes.....	59
5.3	Dynamic of ABA and ABA metabolites during strawberry ripening	60
5.4	Transient overexpression of UGT71A49 in strawberry fruit	63

5.5	CKs content and metabolism during strawberry ripening.....	63
5.6	Phylogenetic tree	68
6.	CONCLUSION	70
7.	REFERENCES	71
8.	SUPPLEMENTAL DATA	82

LIST OF FIGURES

Figure 1. Fruit developmental stages of <i>F. x ananassa</i>	2
Figure 2. Fruit developmental stages of <i>F. vesca</i> varieties.	3
Figure 3. General scheme of the UDP glucosyltransferase reaction.	5
Figure 4. Biosynthetic pathway of ABA in higher plants.	6
Figure 5. ABA catabolic pathways.	8
Figure 6. Current model of CK biosynthesis.	12
Figure 7. Vector used for production of recombinant UGTs in <i>E. coli</i>	18
Figure 8. Vector used for production of recombinant P450s in <i>S. cerevisiae</i> ..	18
Figure 9. Vector used for transient overexpression	19
Figure 10. SDS-PAGE analysis of all UGT-GST fusion proteins expressed in <i>E. coli</i> for this work.	37
Figure 11. LC-MS analysis of products formed by FvUGT71A49, FaUGT71A34, and FaUGT71W2 incubated with (+)-ABA and UDP-glucose.	41
Figure 12. Structure of ABA analogues	42
Figure 13. Enzymatic activity of FvUGT71A49 and FvUGT73AC3 towards different ABA analogues.	43
Figure 14. EIC and MS2 spectra of the products formed by recombinant hydroxylases incubated with ABA.	44
Figure 15. Time curve of PA formation in biotransformation systems.	45
Figure 16. In vitro activity of UGT71A49 towards ABA (extended incubation). 46	
Figure 17. Quantification of ABA and its catabolites in receptacle tissue from <i>F. vesca</i>	48
Figure 18. Quantification of ABA and its catabolites in achenes tissue from <i>F. vesca</i>	49
Figure 19. Quantification of ABA and its catabolites in <i>F. x ananassa</i> cv. Elsanta.	50
Figure 20. MS and MS2 spectra of ABA and its metabolites.	51
Figure 21. Changes in relative mRNA levels of <i>FvUGT71A49</i> and (+)-ABA content in agroinfiltrated fruits.	52
Figure 22. Phylogenetic trees using full-length aminoacidic sequences of biochemically characterized phytohormone-related UGTs and hydroxylases. .	54
Figure 23. MS and MS2 spectra of N ₆ -isopentenyladenine.	55
Figure 24. Quantification of tZ, tZG, and iP in <i>F. x ananassa</i> cv. Elsanta.	56
Figure 25. Quantification of tZ, tZG and iP in receptacle tissue from <i>F. vesca</i> . 57	
Figure 26. Expression profiles of genes involved in ABA catabolism in achenes and receptacle tissues from <i>F. vesca</i> varieties.	61
Figure 27. Expression profiles of the <i>IPT</i> genes in receptacle tissue from <i>F. vesca</i>	64
Figure 28. Expression profiles of <i>LOG</i> gene in receptacle tissue from <i>F. vesca</i> varieties.	66
Figure 29. Expression profiles of <i>CKX</i> genes in receptacle tissue from <i>F. vesca</i> varieties.	67

Figure 30. Expression profiles of *FvUGT85A80* in receptacle tissue from *F. vesca* varieties. 68

LIST OF TABLES

Table 1. Primers used for cloning UGTs and P450 enzymes	16
Table 2. Primers used for real-time PCR analyses	17
Table 3. Additional settings of MS system	20
Table 4. Laboratory equipment	20
Table 5. CTAB buffer	23
Table 6. Breaking buffer	24
Table 7. PCR reaction mixture for gene cloning	24
Table 8. PCR program for gene cloning	25
Table 9. Colony PCR reaction mixture	25
Table 10. PCR conditions for colony PCR	26
Table 11. Conditions for real-time PCR	26
Table 12. Double-digestion reaction mixture	27
Table 13. SOC medium composition	28
Table 14. SC-U selective medium composition	28
Table 15. LB medium composition	29
Table 16. SC-U induction medium	30
Table 17. Glass Bead Disruption Buffer	30
Table 18. TEG Buffer	30
Table 19. Reaction mixture for in vitro hydroxylase activity	31
Table 20. Composition 1x GST Wash/Binding Buffer	32
Table 21. Composition 1x GST Elution Buffer	32
Table 22. 7% SDS stacking gel	32
Table 23. 12% SDS resolving gel	33
Table 24. 1x Running Buffer	33
Table 25. Colloidal Coomassie Solution	33
Table 26. Reaction mixture for in vitro UGT activity assay	34
Table 27. UDP-Glo Assay - General reaction mixture	34
Table 28. References of the enzymes used for constructing the phylogenetic trees	35
Table 29. Summary of the substrate tolerance of the isolated UGTs	39
Table 30. Optimal reaction conditions of the selected UGTs	40
Table 31. Kinetic data of the catalytic activity of examined UGTs	41

ABBREVIATIONS

1-NAA	1-naphthaleneacetic acid
3,7-diHF	3,7-dihydroxyflavone
3-HF	3-hydroxyflavone
7'-OH-ABA	7'-hydroxy-ABA
8'-OH-ABA	8'-hydroxy-ABA
9'-OH-ABA	9'-hydroxy-ABA
<i>A. tumefaciens</i>	<i>Agrobacterium tumefaciens</i>
ABA	abscisic acid
ABA-GE	ABA glucose ester
ABA-GTs	UGT with activity towards ABA
APS	ammonium persulfat
Arg	arginine
Asp	aspartate
BG	β -glucosidase
cDNA	complementary DNA
CDS	coding sequence
CKs	cytokinins
Cf	chloroform
Cys	cysteine
cZ	<i>cis</i> -zeatin
dH ₂ O	distilled water
DNA	deoxyribonucleic acid
dNTPs	deoxynucleoside triphosphates
DPA	dihydrophaseic acid
DTT	dithiothreitol
DZ	dihydrozeatin
<i>E. coli</i>	<i>Escherichia coli</i>
EDTA	ethylenediaminetetraacetic acid
EIC	extracted ion chromatogram
Fw	forward
GA ₃	gibberellic acid
GAPDH	glyceraldehyde 3-phosphate dehydrogenase
GST	glutathione S-transferase
HCl	hydrochloric acid
His	histidine
I-3-AA	indole-3-acetic acid
IAA	isoamyl alcohol
Ile	isoleucine
iP	N ₆ -isopentenyladenine
JA	jasmonic acid

LB	Luria Bertani
LC-MS	liquid chromatography electro-spray ionization mass spectrometry
Leu	leucine
LiCl	lithium chloride
Lys	lysine
Met	methionine
MEP	methylerythritol phosphate
mRNA	messenger RNA
mQ	milli-Q ultrapure water
MS	mass spectrometry
MVA	mevalonate pathway
NaCl	sodium chloride
NADPH	nicotinamide adenine dinucleotide phosphate
NCED	9'- <i>cis</i> -epoxycarotenoid dioxygenase
neoPA	neo-phaseic acid
NSY	neoxanthin synthase
OD ₆₀₀	optical density measured at 600 nm
PA	phaseic acid
PCR	polymerase chain reaction
Phe	phenylalanine
PMSF	phenylmethylsulfonyl fluoride
Pro	proline
qPCR	real-time PCR
RNA	ribonucleic acid
RT	room temperature
Rv	reverse
<i>S. cerevisiae</i>	<i>Saccharomyces cerevisiae</i>
SC-U	synthetic minimal medium for yeast cultivation without uracil
SDS	sodium dodecyl sulfate
SDS-PAGE	sodium dodecyl sulfate polyacrylamide gel
Ser	serine
SOC	super optimal broth with catabolite repression
TEMED	tetramethylethylenediamin
Thr	threonine
Tris	2-amino-2-(hydroxymethyl)-1,3-propanediol
Trp	tryptophan
Tyr	tyrosine
tZ	<i>trans</i> -zeatin
tZG	<i>trans</i> -zeatin-glucoside
UDP	uridine diphosphate
UDP-gluc	uridine-diphosphate-5'-glucose

UGT	UDP-glucose dependent glucosyltransferase
UTR	untranslated region
UV	ultraviolet
Val	valine

1. INTRODUCTION

1.1 Strawberry plant

The strawberry genus (*Fragaria*) belongs to the order *Rosales*, family *Rosaceae*, and subfamily *Rosoideae*. Strawberry plants are perennial, herbaceous, low-growing plants with vegetative propagation capacity via the production of stolons, to produce clonal daughter plants (Davis et al. 2007). The strawberry “fruit” corresponds to the expanded receptacle of the strawberry flower, while the achenes, described as dry indehiscent fruits, are the authentic fruits. The *Fragaria* genus is characterized by interspecific hybridization and polyploidy, with a natural range of ploidy levels from diploids to decaploids (Liston et al. 2014).

The most popular cultivated strawberry, the garden strawberry *Fragaria x ananassa* Duch. is the result of accidental hybridizations between two octoploid species, the beach or Chilean strawberry *Fragaria chiloensis* (L.) Mill. ssp *chiloensis* f. *chiloensis* and the scarlet or Virginia strawberry, *Fragaria virginiana* Mill. ssp *virginiana* in European gardens. However, the first systematic breeding of strawberries was performed by Thomas A. Knight in England in 1817 (Darrow 1966).

In 2017, the world production of strawberry reached ~9.2 million tons (FAOSTAT, 2019). The strawberry species *Fragaria vesca* (L.), *Fragaria moschata* (L.), and *F. chiloensis* are also cultivated but on a much smaller scale (Hancock et al. 2008).

1.2 Fruit ripening

Fruit ripening involves several changes in the color, texture, flavor, and aroma of fleshy fruits (Symons et al. 2012). The modification of color occurs through the alteration of chlorophyll, carotenoid and/or anthocyanin accumulation, while the modification of texture occurs via alteration of the cell wall structure and/or metabolism. Moreover, import/accumulation and modification of sugars, acids and volatiles influence changes in flavor and aroma (Giovannoni 2004).

Fruits are categorized according to physiological differences in their ripening pattern as climacteric or non-climacteric. Climacteric fruits such as tomato, avocado, banana, and mango are characterized by the occurrence of a peak in respiration with a parallel burst of ethylene at the onset of ripening. On the other hand, non-climacteric fruits, for example, strawberry, citrus and grape, do not exhibit a remarkable change in respiration rate, while the production of ethylene remains stable at a basal level during the ripening process (Cherian et al. 2014). However, it does not exclude that ethylene may play some role during the ripening in non-climacteric fruits, for example, in grape berry ripening (Chervin et al. 2004) or strawberry ripening (Villarreal et al. 2010). In contrast to climacteric fruits, less progress has been made in understanding the regulatory mechanisms of fruit ripening in non-climacteric fruits (Cherian et al. 2014).

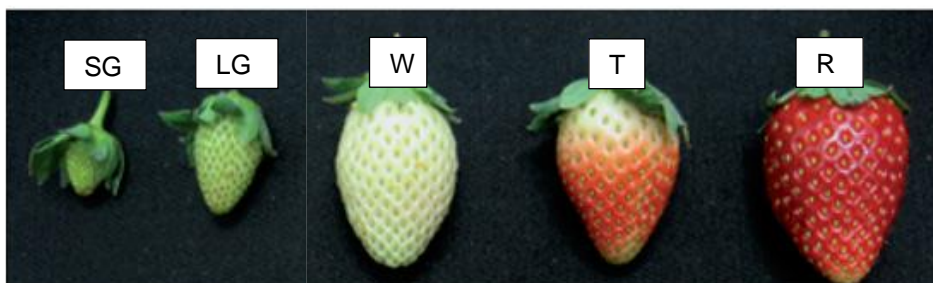


Figure 1. Fruit developmental stages of *F. x ananassa*. From left to right: small green (SG), large green (LG), white (W), turning (T) and red (R). Adapted from Fait et al. (2008).

In recent years, strawberry has been widely accepted as model species for the study of non-climacteric ripening (Giovannoni 2001; Concha et al. 2013; Cherian et al. 2014). The ripening process of strawberry fruit can be divided into different developmental stages. Although each author defines his own developmental stages according to changes in size and color of the receptacle, the agreed main developmental stages of *F. x ananassa* fruit are small green (SG), large green (LG), white (W), turning (T) and ripe (R) (Fait et al. 2008; Symons et al. 2012; Garrido-Bigotes et al. 2018) (Figure 1). For *F. vesca* fruit ripening, it is not possible to clearly differentiate all developmental stages defined for *F. x ananassa*, mainly due to a large genetic variability, which includes not only red- but also white-colored fruit varieties. Härtl et al. 2017 defined three developmental

stages for the ripening of *F. vesca* fruits: green (G), white or intermediate (W), and ripe (R) (Figure 2).

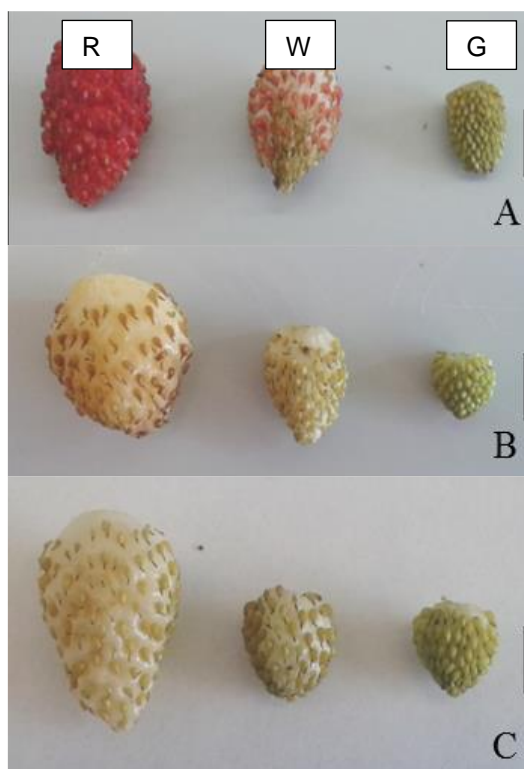


Figure 2. Fruit developmental stages of *F. vesca* varieties (A) Reine des Vallées (RdV), (B) Yellow Wonder (YW) and (C) Hawaii4. From right to left green (G), white or intermediate (W) and ripe (R). Adapted from Härtl et al. (2017).

Unlike climacteric fruits and other non-climacteric fleshy fruits, the ripening process of strawberry is much more complex, and several aspects must be taken into consideration. The receptacle and the achene tissues, with a diverse origin, physiological role, and metabolism, form the strawberry fruit, which is botanically an aggregate accessory fruit. Therefore, the analysis of the whole strawberry fruit and how each organ at each developmental stage contributes to the development of the whole fruit is complicated (Merchante et al. 2013).

The ripening of strawberry fruits is regulated by the coordinated action of several phytohormones through the entire ripening process. In the early developmental stage, the concentrations of auxin and gibberellic acid increase, while abscisic acid (ABA) is present in minimal amounts (Symons et al. 2012, Liao et al. 2018).

During this phase, the enlargement of the receptacle and the chlorophyll degradation takes place, whereby the color changes from green to white. At the intermediate developmental stage, the levels of auxins and gibberellic acid decrease, and the concentration of abscisic acid quickly increases with a concomitant color acquisition due to accumulation of anthocyanins (Jia et al. 2011, Symons et al. 2012) and loss of firmness due to the action of multiple cell wall modifying enzymes (Ramos et al. 2018).

All these changes are remarkably fine-tuned, and each phytohormone plays a temporal-specific role. For example, the application of gibberellic acid at the intermediate developmental stage of strawberry ripening decreases the rate of color acquisition by inhibiting chlorophyll degradation (Martinez et al. 1996). Moreover, the application of the synthetic auxin, 1-Naphthaleneacetic acid (NAA) at the white developmental stage delayed the ripening of the strawberry fruit (Symons et al. 2012).

1.3 Glycosyltransferases and hormonal regulation

The regulation of hormone levels in plants is crucial for plant growth, development, and adaptation to environmental changes (Tiwari et al. 2016). The conjugation of plant hormones with sugars, amino acids, or proteins contributes to this regulation and to maintain the homeostasis (Ostrowski and Jakubowska, 2014). Bajguz and Piotrowska (2009) suggest that the conjugation can lead to a loss of hormone activity and could serve as a method to conserve an inactive pool of the phytohormone, which can later be converted to an active form after an enzymatic hydrolysis reaction. In this sense, glycosylation is a particularly relevant mechanism of phytohormone regulation.

The glycosylation reaction is mediated by glycosyltransferases (GTs), enzymes which can transfer sugars from activated donor molecules to O (-OH or -COOH groups), C (C-C), N (-NH₂), and S atoms (-SH) of a wide range of substrates (aglycones or acceptor molecules) (Ostrowski and Jakubowska, 2014; Osmani et al. 2009; Lim and Bowles, 2004). In general, GTs are classified according to their sequences into (until now) 109 families that can be found at the Carbohydrate-active Enzymes (CAZY) database (www.cazy.org/glycosyltrans-

reaction is also possible, and zeaxanthin can be produced from violaxanthin in high light conditions by the action of the enzyme violaxanthin de-epoxidase (VDE) (Nambara and Marion-Poll 2005; Endo et al. 2014).

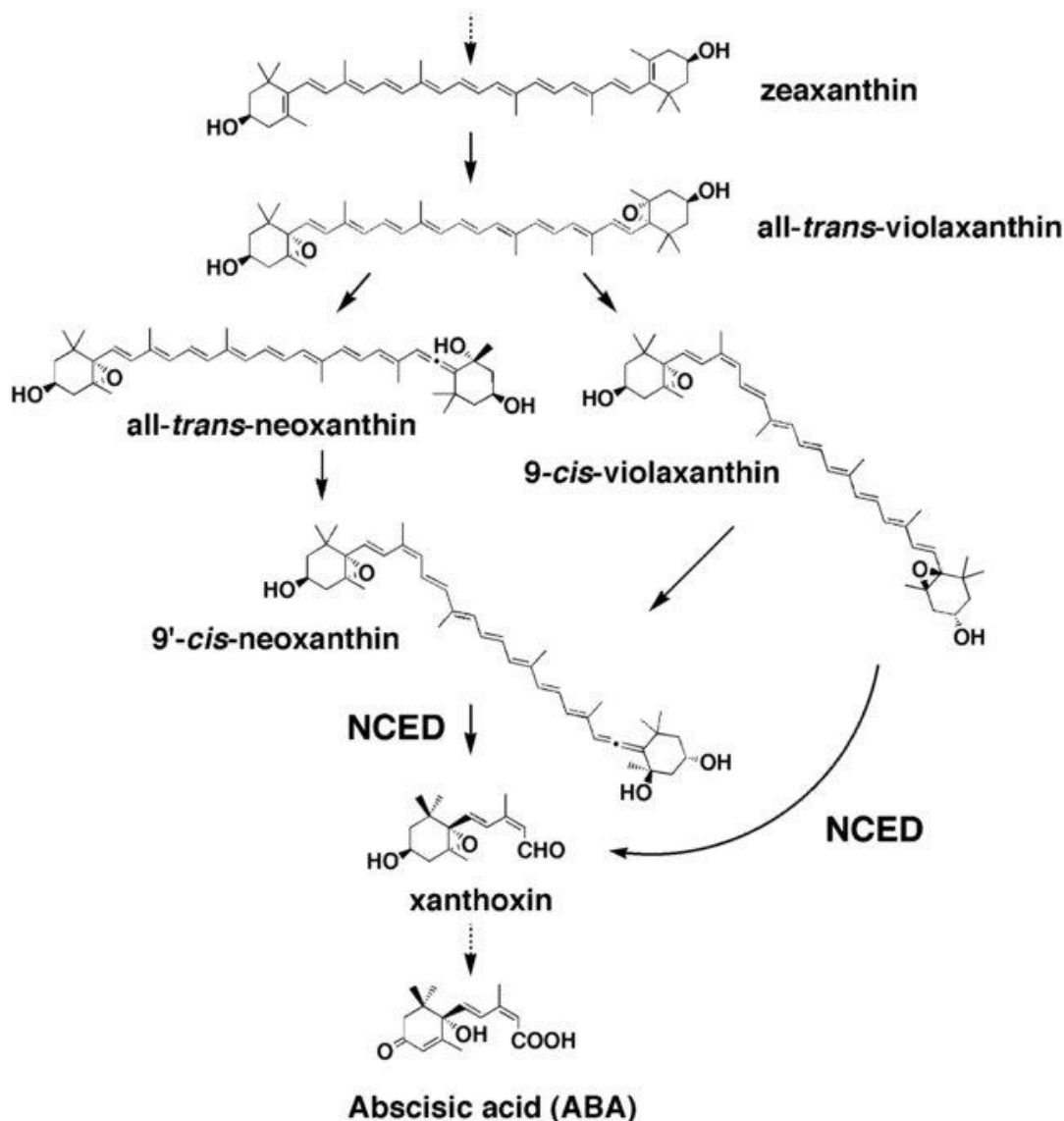


Figure 4. Biosynthetic pathway of ABA in higher plants (Han et al. 2004). NCED, 9-*cis*-epoxycarotenoid dioxygenase.

Then, all-*trans*-violaxanthin can take two pathways: 1) it is converted to the 9'-*cis* isomer before oxidative cleavage to produce xanthoxin catalyzed by 9'-*cis*-epoxycarotenoid dioxygenase (NCED) or 2) it is converted to all-*trans*-neoxanthin, which is subsequently converted to 9'-*cis*-neoxanthin, which is also a substrate for NCED in the production of xanthoxin. In both cases, an isomerase is required to produce the 9'-*cis*-epoxycarotenoids, and in the second case, an

extra neoxanthin synthase (NSY) is required. However, no conclusive information is available, and little progress has been made in the identification and characterization of the isomerase and the NSY.

Towards the end of the biosynthetic pathway, xanthoxin is translocated from the plastid to the cytosol and converted to the abscisic aldehyde by short-chain alcohol dehydrogenase (ABA2). Finally, the abscisic aldehyde is oxidized and converted to ABA by an abscisic aldehyde oxidase (AAO3). (Nambara and Marion-Poll 2005; Endo et al. 2014).

ABA has been described as an inducer of strawberry ripening for more than 30 years (Kano and Asahira 1981). Jiang and Joyce (2003) reported that ABA treatment accelerates fruit color intensity by increasing the anthocyanin content and increases the activity of the enzyme phenylalanine ammonia-lyase (PAL). These results were confirmed and complemented by Jia et al. (2011), showing that endogenous ABA levels increase in the receptacle during strawberry fruit ripening, and the exogenous application of ABA promoted fruit development, while fluoridone (an ABA biosynthesis inhibitor) remarkably delayed fruit development.

Besides, recent studies have contributed to the identification and characterization of key genes for ABA biosynthesis and signaling in the strawberry fruit. Jia et al. (2011) have functionally characterized a 9-*cis*-epoxycarotenoid dioxygenase gene (*FaNCED1*), which is considered an essential gene in ABA biosynthesis. The downregulation of this gene resulted in uncolored fruits, while the uncolored phenotype of the *FaNCED1*-downregulated fruit was rescued by the application of exogenous ABA. Furthermore, they downregulated a putative ABA receptor gene encoding the magnesium chelatase H subunit (*FaCHLH/ABAR*), altering the ABA content and producing an uncolored phenotype, which could not be rescued by the application of ABA.

Chai et al (2011) showed that the downregulation of the ABA receptor gene *FaPYR1* not only delayed fruit ripening but also altered the ABA content, ABA sensitivity and a set of ABA-responsive gene transcripts, in addition to producing

an uncolored phenotype, which could not be rescued by exogenous ABA application.

1.5 Abscisic acid catabolism

The catabolism of ABA during strawberry ripening is only partially characterized, and there is limited information about the dynamic of ABA catabolites during strawberry ripening, which is important to understand how homeostasis of ABA is maintained globally. ABA catabolism is categorized into two types of reactions, hydroxylation and conjugation (Nambara and Marion-Poll 2005) (Figure 5).

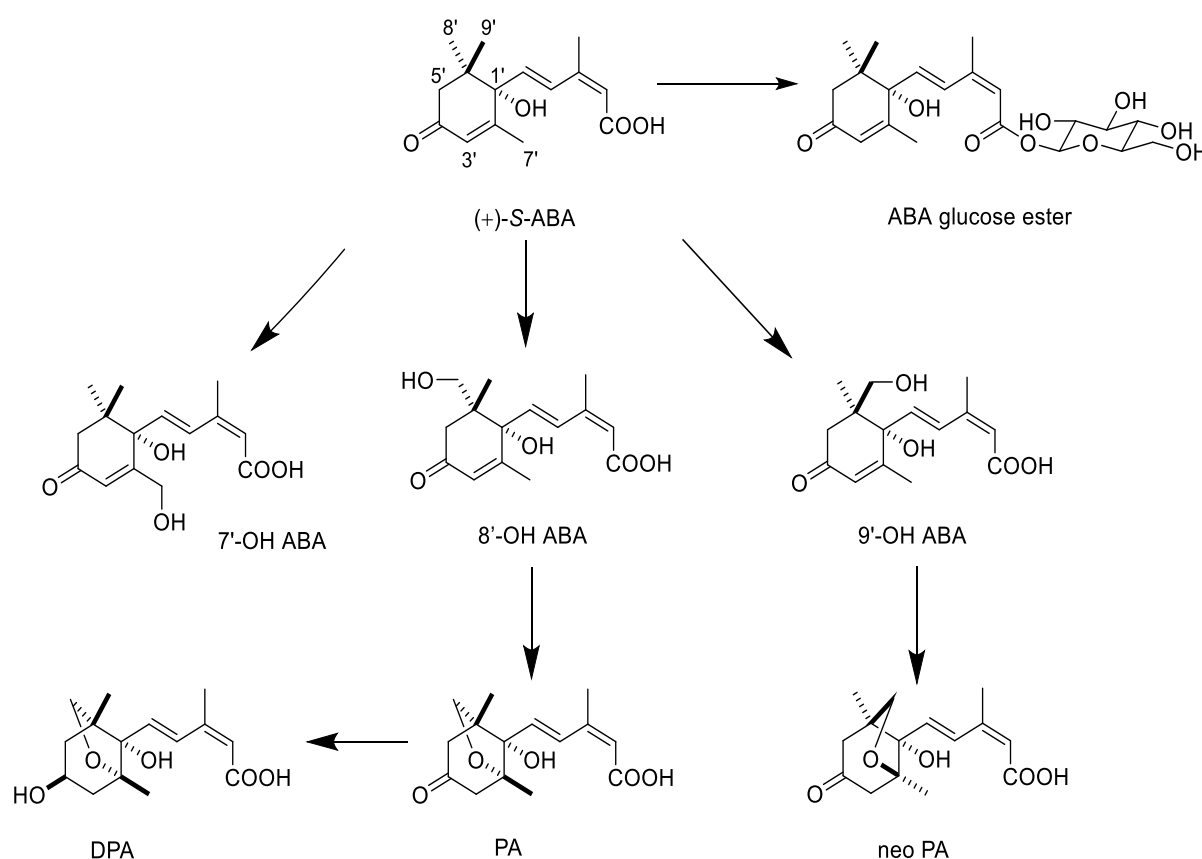


Figure 5. ABA catabolic pathways. ABA, abscisic acid; PA, phaseic acid; DPA, dihydrophaseic acid; neoPA, neo-phaseic acid.

1.5.1 Abscisic acid glucosylation

The principal conjugate of ABA is its glucose ester (ABA-GE), which is produced by ABA glucosyltransferases (ABA-GTs) through the direct glucosylation of the carboxyl group (at the C-1) (Liu et al. 2015). ABA-GE probably serves as a storage/transport form of ABA (Sauter et al., 2002), accumulates in vacuoles

(Bray and Zeevaart, 1985), and is considered as an inactive product of ABA catabolism (Zeevaart, 1999). Dietz et al. (2000) reported on the release of ABA after incubation of ABA-GE with intracellular washing fluid of *Hordeum vulgare* (L.) and the identification of two β -glucosidases (BG) in *Arabidopsis thaliana* (L.) Heynh. (*At*BG1 and 2), which were able to hydrolyze ABA-GE and release active free ABA, led to the conclusion that this pathway could be a mechanism to rapidly increase ABA levels (Lee et al. 2006; Xu et al. 2012). In strawberry fruit, two BGs with regulatory effects on endogenous ABA content have been described (Li et al. 2013; Zhang et al. 2014).

Several GTs from different species are capable of glycosylating ABA (Tiwari et al. 2016). In *A. thaliana*, ABA-GTs are encoded by the gene *UGT71B6* (Lim et al. 2005) and its two closely related homologs *UGT71B7* and *UGT71B8* (Dong et al. 2014). They show functional redundancy and play a role in the regulation of ABA homeostasis and adaptation to abiotic stress (Priest et al. 2006; Dong et al. 2014). Also, the gene *UGT71C5* has been described as a significant contributor to ABA homeostasis in *A. thaliana* (Liu et al. 2015). In strawberry, four GTs glucosylated ABA, while three (*UGT71A33*; *UGT71A35* and *UGT71W2*) preferred the naturally occurring (+)-ABA over racemic form (\pm)-ABA (Song et al. 2015). *UGT71W2* was successfully downregulated in *F. x ananassa* cv. Mara des Bois, however, the concentration of ABA-GE was only slightly reduced, probably due to enzymatic redundancy (Song et al. 2015).

Besides glucosylation of ABA, other ABA catabolites have been identified as acceptors of a glucose moiety. Milborrow and Vaughan (1982) reported the isolation of dihydrophaseic acid (DPA) 4'-O- β -D-glucoside in tomato (*Solanum lycopersicum*) shoots. Moreover, del Refugio Ramos et al. (2004) identified 8'-hydroxy-ABA- β -D-glucoside and epi-DPA- β -D-glucoside in avocado (*Persea americana* Mill.) seeds. Although several authors have tested if UGTs with activity towards ABA can also glucosylate PA or DPA (Xu et al. 2002, Priest et al. 2005), these attempts have not been successful, and up to date, no UGT with activity towards ABA catabolites have been described.

1.5.2 Abscisic acid hydroxylation

The oxidation of ABA is catalyzed by members of the CYP707A cytochrome P450 monooxygenase family and follows three different pathways, oxidizing the methyl group of C-7', C-8' or C-9' of the ring structure (Krochko et al. 1998; Zhou et al., 2004; Okamoto et al., 2011). The 8'-hydroxylation of ABA is considered the predominant catabolic pathway (Nambara and Marion-Poll 2005), resulting in unstable 8'-OH-ABA, which is spontaneously isomerized to form phaseic acid (PA). PA can be subsequently reduced at the 4' position to form dihydrophaseic acid (DPA) (Cutler and Krochko, 1999). Zhou et al. (2004) reported the isolation of the product of cyclized 9'-OH-ABA, which was named as neophaseic acid (neoPA). Later, Okamoto et al. (2011) demonstrated that in *Arabidopsis*, 9'-hydroxylation of ABA is catalyzed by CYP707As as a side-reaction. Regarding 7'-hydroxy-ABA, it has been found in several plant species, but as a minor ABA catabolite (Nambara and Marion-Poll 2005)

In strawberry, five members of the CYP707A family have been identified by bioinformatic and transcriptomic analyses (Ji et al. 2012; Kang et al. 2013; Liao et al. 2018). Among them, only *FvCYP707A4a* has been further studied and its transient overexpression in *F. vesca* cv. Yellow Wonder receptacle resulted in a reduction of free ABA content (Liao et al. 2018).

Weng et al. (2016) studied a putative hormonal activity of PA in *Arabidopsis*. They found a dihydroflavonol reductase (DFR)-like gene named ABA HYPERSENSITIVE 2 (*ABH2*), which is due to the ABA-hypersensitivity phenotypes produced by loss-of-function *abh2* mutants. The recombinant ABH2 protein catalyzed the reduction of PA to DPA *in vitro*, these mutants over-accumulated PA. Besides, they overexpressed an ABA hydroxylase in the *abh2* mutant background, resulting in an *Arabidopsis* strain that produced about 10-fold more PA and 3-fold less ABA. However, the strain was similar to the wild type, suggesting that high PA levels were able to compensate for the ABA deficiency in the plants.

1.6 Biosynthesis and metabolism of cytokinins

Compared to other phytohormones, little information is available on the role of cytokinins in non-climacteric ripening (Cherian et al. 2014). Cytokinins (CKs) are a group of phytohormones that play different roles in plant growth and development. They regulate leaf senescence, apical dominance, control of shoot/root balance, stress response, and nutritional signaling among others (Takei et al. 2002; Werner et al. 2003; Kim et al. 2006; Tanaka et al. 2006; Nishiyama et al. 2011). The naturally occurring CKs are derivatives of adenine carrying an isoprene-derived or an aromatic side chain at the N₆ terminus (Mok and Mok, 2001; Strnad 1997) and are called isoprenoid CKs and aromatic CKs, respectively. However, isoprenoid CKs are present in larger quantities (Sakakibara 2006).

The naturally occurring isoprenoid CKs widely found in higher plants consist of isopentenyl adenine (iP), *trans*-zeatin (tZ), *cis*-zeatin (cZ), and dihydrozeatin (DZ) (Figure 6) (Mok and Mok, 2001; Sakakibara 2006), all of them differing just in the side-chain structure. Among them, tZ and iP are generally most common in plants, but their concentrations vary depending on plant species, tissue, and developmental stage (Sakakibara 2006, Hirose et al. 2008). Sidechains of the isoprenoid CKs mainly originate from the methylerythritol phosphate (MEP) pathway, while the cZ sidechain derives from the mevalonate (MVA) pathway (Kasahara et al. 2004). The first step of isoprenoid CK biosynthesis is catalyzed by adenosine phosphate-isopentenyltransferase (IPT), which catalyzes the N-prenylation of adenosine 5'-phosphate (preferably ATP or ADP but also AMP is used) at the N-terminus with dimethylallyl diphosphate (DMAPP) or 1-hydroxy-2-methyl-2-(*E*)-butenyl 4-diphosphate (HMBDP) to form iP nucleotides (Kakimoto, 2001). Afterward, the iP nucleotides are converted into tZ nucleotides by hydroxylation at the prenyl side chain. This reaction is stereo-specifically catalyzed by two P450 monooxygenases: CYP735A1 and CYP735A2 (at least in *Arabidopsis*), whereby no cZ nucleotides are produced (Takei et al. 2004). Finally, the CK-nucleotides are converted to their free-base form to become biologically active. Kurawa et al. (2007) reported a CK-activating enzyme in rice

named LOG (Lonely guy). LOG has phosphoribohydrolase activity and is able to use all four CK nucleoside 5'-monophosphates (but not di- or triphosphates).

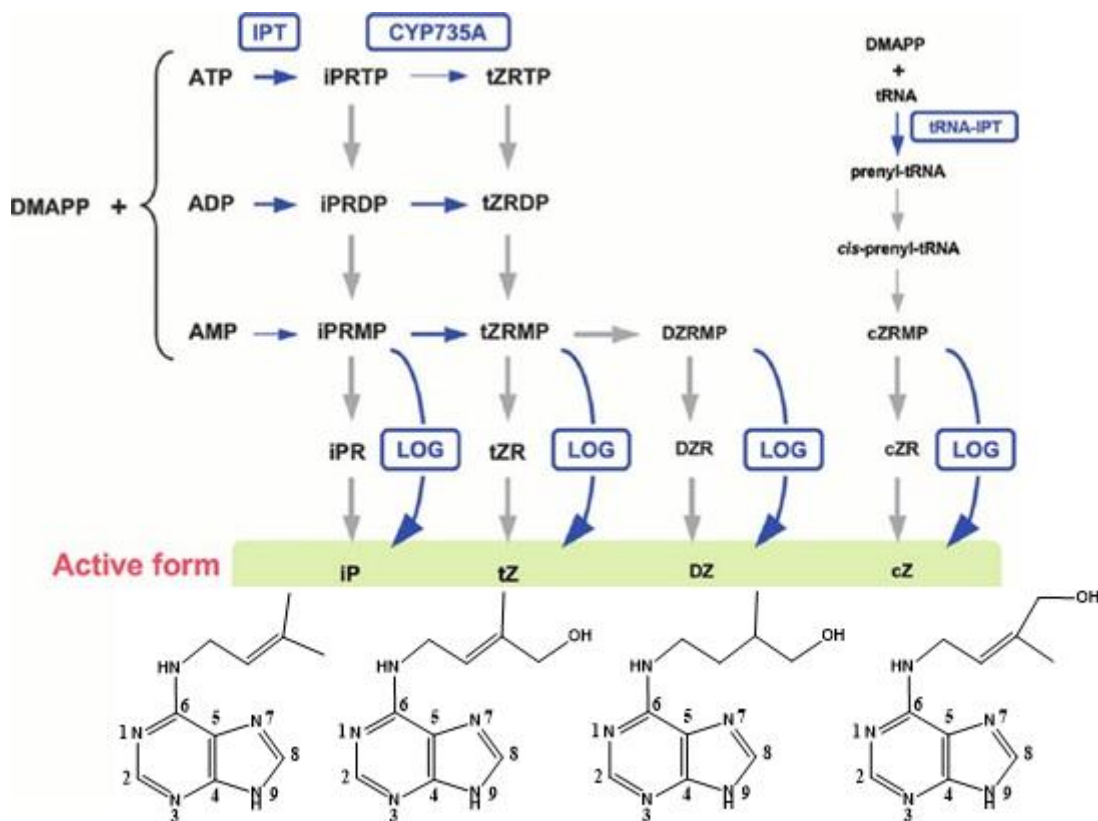


Figure 6. The current model of CK biosynthesis. DMAPP, dimethylallyl pyrophosphate; ATP, adenosine triphosphate; ADP, adenosine diphosphate; AMP, adenosine monophosphate; iP, isopentenyladenine; iPRTP, iP riboside 5'-triphosphate; iPRDP, iP riboside 5'-diphosphate; iPRMP, iP riboside 5'-monophosphate; iPR, iP riboside; tZ, trans-zeatin; tZRTP, tZ riboside 5'-triphosphate; tZRDP, tZ riboside 5'-diphosphate; tZRMP, tZ riboside 5'-monophosphate; tZR, tZ riboside; DZ, dihydrozeatin; DZRMP, DZ riboside 5'-monophosphate; DZR, DZ riboside; cZ, cis-zeatin; cZRMP, cZ riboside 5'-monophosphate; cZR, cZ riboside; IPT, phosphate-isopentenyltransferase; LOG, monophosphate phosphoribohydrolase (LONELY GUY). Adapted from Hirose et al. (2008).

The content of active CKs is determined by the rate of formation of free CKs and their degradation and conjugation. CKs are irreversibly degraded by cleavage of their side chains. This reaction is catalyzed by CK oxidases/dehydrogenases (CKX). Specifically, CKX removes the N₆-isoprenoid chain of CK molecules, converting them to adenine and the corresponding unsaturated aldehyde (Galuszka et al. 2001). Active isoprenoid CKs and their ribosides, 9-glucosides,

nucleotides and aromatic CKs can be degraded by different CKX isoforms (Galuszka et al. 2007).

CKs can be glycosylated at the N3, N7, and N9 position of the purine moiety (as N-glucosides) and the hydroxyl group of the side chains of cZ, tZ, and DZ (as O-glucosides or O-xylosides) (Sakakibara 2006). Glucosyl conjugates at N7 and N9 are usually inactive in most of the bioassays (Bajguz and Piotrowska, 2009). Hou et al. (2004) reported two genes *UGT76C1* and *UGT76C2*, which encode CK N-glucosyltransferases in *Arabidopsis*. *In vitro* assays showed that both enzymes form N7- and N9-glucosides and prefer glucosylation at N7. Also, Hou et al. (2004) studied the *in vitro* activity of enzymes UGT85A1, UGT73C5, and UGT73C1. All of them produced O-glucosides of tZ and DZ. Moreover, specific CK O-glucosyltransferases have been reported in *Phaseolus lunatus* L. (Martin et al. 1999) and *Zea mays* (Martin et al. 2001). The CK-UGT encoded by the *P. lunatus* *ZOG1* gene displayed a high affinity for tZ while the enzyme encoded by *Z. mays* preferred cZ (Veitch et al. 2003). Brzobohaty et al. (1993) reported that O-glucosylation is reversible by the activity of a β -glucosidase in *Z. mays* L. named Zm-p60.1. The β -glucosidase can accept a broad range of substrates; however, the enzyme is not able to hydrolyze N7- or N9-glucosides. Later, Falk and Rask (1995) found a β -glucosidase in *Brassica napus* L. with activity towards zeatin-O-glucoside; however, the enzyme activity and specificity has not been further studied. The physiological effects of the stability differences of O- and N-glucosides are not clear, but it is assumed that they represent inactive stable storage forms because of the natural cleavage of O-glucosides by glucosidases (Sakakibara 2006).

1.7 Aim of the thesis

In this study, we attempted to clarify the dynamic of CKs and ABA metabolism during strawberry fruit ripening. Based on transcriptomic data from literature and phylogenetic data, we cloned a set of genes encoding putative phytohormone-related UGTs from strawberry, which were expressed in *E. coli* and its substrate tolerance tested *in vitro*. Two promiscuous UGTs with *in vitro* activity towards ABA and one with *in vitro* activity towards tZ were further functionally

characterized. Also, two ABA hydroxylases were cloned and expressed in *S. cerevisiae*, and the *in vitro* substrate tolerance studied. The products of ABA catabolism (ABA-GE, PA, DPA, neoPA, and 7'-OH-ABA), CKs (iP and tZ), and tZG were quantified at different developmental stages of fruit ripening in red- and white-fruited varieties of *F. vesca* as well as *F. x ananassa* cv. Elsanta. These analyses contribute to complete the global perspective of the balance between biosynthesis and catabolism of ABA and active CKs during strawberry fruit ripening.

2. MATERIALS

2.1 Plant material

The strawberry varieties used in this study were grown in greenhouses: *F. x ananassa* cv. Elsanta was grown at the Greenhouse Laboratory Center Dürnast, Freising, Germany (48° 24' 18.5" N 11° 41' 33.1" E), while *F. vesca* cv. Reine des Valleys (RdV), Red Wonder (RW), Korsika (K), Yellow Wonder (YW), and Hawaii4 (HW4) were grown at Hansabred GmbH & Co. KG in Dresden, Germany (51°09'09.2"N 13°47'41.7"E). Fruits were collected at different developmental stages and classified according to Härtl et al. (2017) and Fait et al. (2008). For qPCR, fruits were immediately cut into small pieces and frozen with liquid nitrogen after harvest and stored at -80 °C until use. For LC-MS analyses, after harvest, the fruits were stored at -20 °C until use.

2.2 Chemicals

All chemicals were purchased from either Carl Roth (Karlsruhe, Germany), Sigma-Aldrich (Steinheim, Germany), Merck (Darmstadt, Germany), and Fluka (Steinheim, Germany) unless otherwise stated. ABA catabolites mass spectrometry standards were kindly provided by Dr. S.R. Abrams (Department of Chemistry, University of Saskatchewan, Canada) or purchased from the National Research Council of Canada (Saskatchewan, Canada). On the other hand, *trans*-zeatin and N₆-isopentenyladenine were purchased from Sigma-Aldrich (Steinheim, Germany) and OlchemIm (Olomouc, Czech Republic), respectively.

2.3 Microorganisms

- *E. coli* BL21 (DE3) pLYsS (Promega, Mannheim, Germany).
- *E. coli* NEB 10-beta (New England BioLabs, Frankfurt, Germany)
- *S. cerevisiae* INVSc1 (Invitrogen, Karlsruhe, Germany)
- *A. tumefaciens* AGL0 (Lazo et al. 1991).

2.4 Primers

Table 1. Primers used for cloning UGTs and P450 enzymes

Target	Organism	Forward primer sequence	Reverse primer sequence	Destination	Amplicon size (bp)
UGT75L26-UTR	<i>F. vesca</i> var RdV	TCGTCACCTCAAACGTCATC	CCCCTACATTTTTCTCCAA		1806
UGT75L26-CDS		ACGC <u>GTGACCC</u> CATGCTCTCCTATCTT	TTTAG <u>CGGCCGCT</u> TAGGCTAGAAAACA	pGEX-4T1	1575
UGT75L27-UTR	<i>F. vesca</i> var RdV	CTCCAGACTCCACAACCACC	TTCCCCAAGCAGTCAAGCTC		1489
UGT75L27-CDS		ACGC <u>GTGACTG</u> GTTCAACATCGC	TTAG <u>CGGCCGCT</u> CTAGCGTAAGCGTT	pGEX-4T1	1450
UGT71A48-UTR	<i>F. vesca</i> var RdV	ACTAGCAGAAACCGCACTCC	AAGCTTTCCGATCGATCCCG		1631
UGT71A48-CDS		CG <u>GGATCC</u> ATGAAGCAATCGGTA	TTTAG <u>CGGCCGCT</u> TAAATTTGATCAAT	pGEX-4T1	1451
UGT85A80-UTR	<i>F. vesca</i> var RdV	AGAATGGGTTCCAACGCCTC	AGATGAACCACAGGAGCTGT		1632
UGT85A80-CDS		CG <u>GGATCC</u> ATGGGTTCCAACGCC	CCG <u>CTCGAGCT</u> ACTTGCCATCCTC	pGEX-4T1	1466
UGT71A49-UTR		CACCCCTCGTAGCCTCTACT	TCGTTTACACCAATCTTGAACCT		1518
UGT71A49-CDS	<i>F. vesca</i> var RdV	CGC <u>GGATCC</u> ATGAAGAAAGCTTCAGAGC	TTTAG <u>CGGCCGCT</u> CACGAGGTTTGAAT	pGEX-4T1	1461
UGT71A49-CDS		GC <u>TCTAGA</u> ATGAAGAAAGCTTCAGAGCTAATC	TCC <u>CCCGGGT</u> CACGAGGTTTGAATTT	pBI121-2x35S	1457
UGT73AC3-UTR	<i>F. vesca</i> var RdV	CCCTACCTCAATCTCGCGTC	AGAAATGCTTGCGGGTACGA		2043
UGT73AC3-CDS		CG <u>GGATCC</u> ATGGATTCAGAACCT	CCG <u>CTCGAGT</u> CAGTTCTTCTCAG	pGEX-4T1	1451
CYP707A1/3-UTR	<i>F. x ananassa</i> cv Elsanta	TGCCTCTCTGTGTCTGCTTC	TTCTGAAGCTTTTCGGGGGTG		1532
CYP707A1/3-CDS		CG <u>GGATCC</u> AACACAATGTTTGCTGCTT	CCG <u>GAAATTC</u> CATTCCCTTGAGGATAATATG	pYES2	1403
CYP707A4a-UTR	<i>F. x ananassa</i> cv Elsanta	TTTCGCAGTCACTCTCACCC	AAGTTGGGGAGGGTATGGCT		1507
CYP707A4a-CDS		GGGGTACCAACACAATGAAGAAGAGC	ATAGTTTAG <u>CGGCCGCT</u> ATTCTAATTT	pYES2	1413

Table 2. Primers used for real-time PCR analyses

Description	Forward primer sequence	Reverse primer sequence	Amplicon size (bp)
Total expression of Fv <i>UGT71A49</i> .	TAACGAGTTCGGGCTCCCTA	TCGGTGCAGTCCTTGTTCTC	111
Total expression of Fa <i>GAPDH</i>	TCCATCACTGCCACCCAGAAGACTG	AGCAGGCAGAACCTTTCCGACAG	143
Screening for pBI121- 2x35S:Fv <i>UGT71A49</i> in cDNA of agroinfiltrated fruits. Primers targeted the end of 35S promoter and the beginning of CDS region	CTATCCTTCGCAAGACCCTTC	TGCGGTGAAGGGGAATTTCA	216

2.5 Vectors

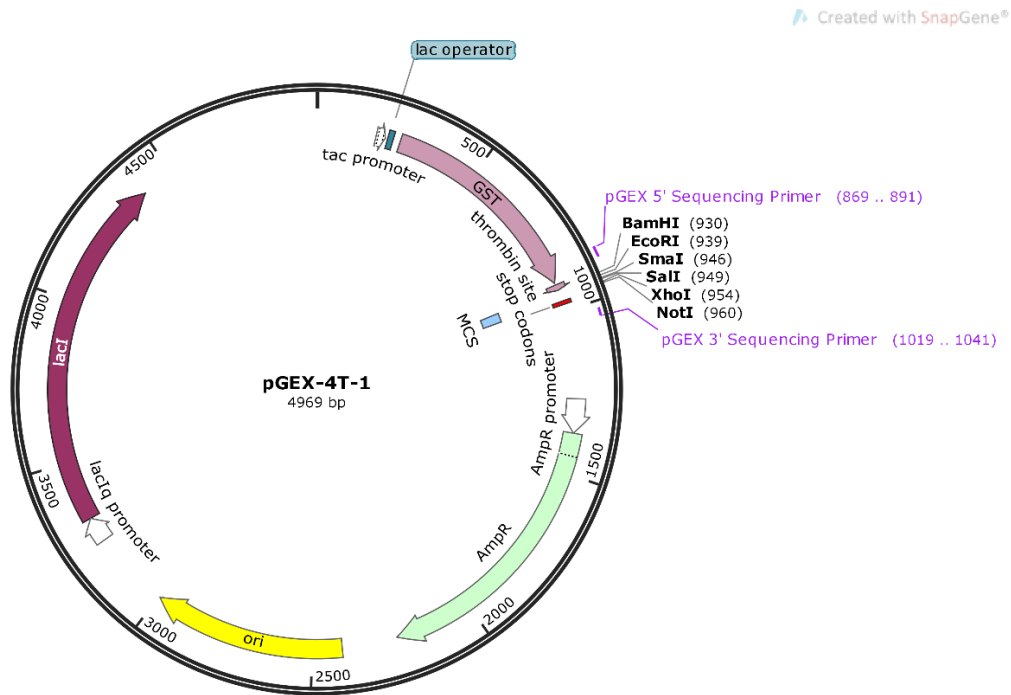


Figure 7. Vector used for the production of recombinant UGTs in *E. coli*

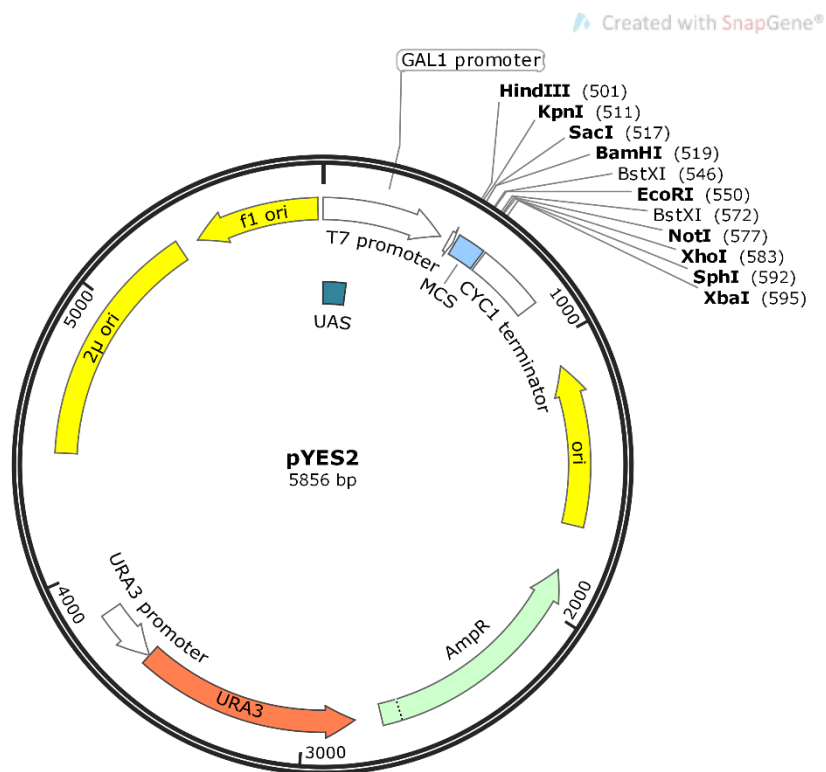


Figure 8. Vector used for the production of recombinant P450s in *S. cerevisiae*

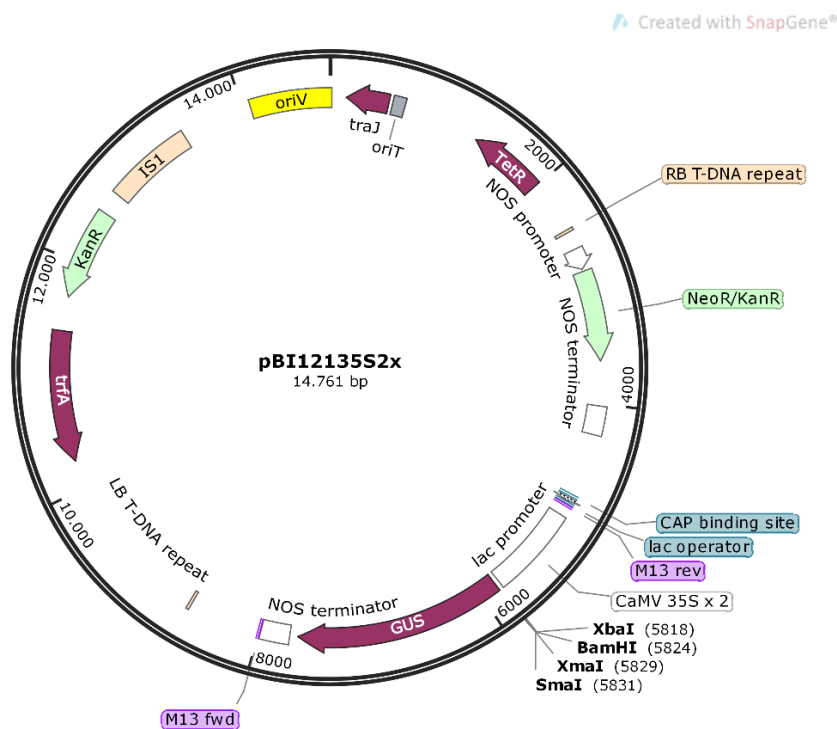


Figure 9. Vector used for transient overexpression

2.6 Equipment

2.6.1 Liquid chromatography ultraviolet electro-spray ionization mass spectrometry

All samples were analyzed using an Agilent 1100 HPLC/UV system (Agilent Technologies Inc., Santa Clara, US-CA) equipped with a pre-column SecurityGuard Cartridge C18 4 x 2 mm (Phenomenex, Aschaffenburg, Germany) and reverse-phase column Luna 3 μ m C18 (2) 100 \AA 150 x 2 mm (Phenomenex). The system was connected to a Bruker Daltonics Esquire 3000^{plus} Ion Trap (Bruker, Bremen, Germany). For the mobile phase, (A) water with 0.1% formic acid and (B) methanol with 0.1% formic acid were utilized. The injection volume was 5 μ l, and the flow rate was 0.2 ml·min⁻¹. Two different gradient elution programs were used, (1) for substrate screening, the gradient was as follows: 10% B and 90% A, went to 50% B in 7 min, went to 100% B in 3 min, 100% B was kept for 5 min. Afterward, B was decreased to 10% within 5 min, and this condition was maintained for 10 min. The stop time was 30 min. The MS spectra were recorded in alternating polarity mode. The program (2) for detection and/or quantification of phytohormones and its metabolites was as follows: 100% A,

went to 50% B in 30 min, went to 100%B in 5 min, 100 % B was kept for 15 min. Finally, B was decreased to 0% within 5 min. This condition was maintained for 10 min. MS spectra were recorded in the negative mode for ABA and its metabolites and positive mode for CKs. Further details of the MS system are described in Table 3.

Table 3. Additional settings of the MS system

Component	Setting
Nebulizer gas	Nitrogen at 30 p.s.i.
Dry gas	Nitrogen at 330 °C 9 l·min ⁻¹
Capillary voltage	-4000 V
End plate voltage	-500 V
Skimmer voltage	40 V
Capillary exit voltage	121 V
Scan range	100 to 800 m/z
Resolution	13,000 m/z·s ⁻¹
Ion accumulation	Until ion charge control target achieved 20,000 (positive mode) or 10,000 (negative mode) or maximum time 200 ms
Collision gas	Helium at 4·10 ⁻⁶ mbar
Collision voltage	1 V

2.6.2 Laboratory equipment

Table 4. Laboratory equipment

Utility	Equipment
Centrifuges	Sigma K415, Sigma 1-14, Sigma 2K15 (Sigma, Osterode am Harz, Germany) Eppendorf 5415R, MiniSpin (Eppendorf AG, Hamburg, Germany)
Thermocycler	SensoQuest labcycler (SensoQuest GmbH, Göttingen, Germany) Step One Plus (Applied Biosystems, Foster City, USA)
Spectrophotometers	Nanodrop 1000 (Peqlab Biotechnologie, Erlangen, Germany) Nicolet evolution 100 (Thermo Fisher Scientific Inc., Waltham, USA)
Freeze dryer	Savant ModulyoD (Thermo Fisher Scientific Inc., Waltham, USA)
Vacuum concentrator	Christ RVC 2-18 (Martin Christ Gefriertrocknungsanlagen GmbH, Osterode am Harz, Germany)
Mixer mill	MM-200 (Retsch GmbH, Haan, Germany)
Plate reader	CLARIOstar Plus (BMG Labtech, Ortenberg, Germany)
Ultrasonic probe	Bandelin UW2070 / HD2070 (Bandelin Electronic GmbH & Co. KG, Berlin, Germany)
Ultrasonic bath	Sonorex RK103H (Bandelin Electronic GmbH Co. KG, Berlin, Germany)

2.7 Software

- Geneious Pro 5.3.4 (Biomatters Ltd.)
- DataAnalysis 6.2 (Bruker Daltonik GmbH)
- QuantAnalysis 6.2 (Bruker Daltonik GmbH)
- ChemDraw Pro 16.0 (PerkinElmer Informatics)
- BioEdit Sequence Alignment Editor (Hall 1999)
- GraphPad Prism 6.01 (GraphPad Software Inc.)
- StepOne Software 2.1 (Applied Biosystem)
- R 3.5.2 (R Core Team)

2.8 Internet Resources

- Strawberry Genomic Resources

<http://bioinformatics.towson.edu/strawberry/>

- KO (KEGG Orthology) Database

<http://www.genome.jp/kegg/ko.html>

- National Center for Biotechnology Information (NCBI)

<http://www.ncbi.nlm.nih.gov>

- Primer-BLAST

<http://www.ncbi.nlm.nih.gov/tools/primer-blast/>

- The Sequence Manipulation Suite – Reverse Complement

https://www.bioinformatics.org/sms/rev_comp.html

- ExPASy Bioinformatics Resource Portal - Translate Tool

<https://web.expasy.org/translate/>

- Primer3Plus

<http://www.bioinformatics.nl/cgi-bin/primer3plus/primer3plus.cgi>

3. METHODS

3.1 Extraction of secondary metabolites from strawberry tissues for quantification by LC-MS

The extractions of metabolites were performed according to Ring et al. (2013). Achenes were separated from the receptacle using liquid nitrogen to keep both tissues frozen. Tissues were ground to a fine powder using a laboratory mixer mill with pre-cooled grinding jars in liquid nitrogen. The powder was freeze-dried for 48 h, and 50 mg of each sample was aliquoted in a microtube. To each sample, 250 μ l of a solution containing Biochanin A diluted in methanol (0.2 mg·ml⁻¹) and 250 μ l of methanol were added. Samples were vortexed for 1 min, sonicated for 10 min, and centrifuged at 16,000 *g* for 10 min at 4 °C. The supernatant was retained, and the residue was extracted again with 500 μ l of methanol. The supernatants were combined, concentrated to dryness in a vacuum concentrator, and resuspended in 35 μ l of mQ-water. The samples were centrifuged at 16,000 *g* for 10 min at 4 °C, and the supernatant was used for LC-MS analysis. Quantified compounds were expressed as ng- or μ g-equivalents of Biochanin A per gram of dry weight.

3.2 RNA isolation from strawberry fruits

RNA isolation was performed combining the method described by Gasic et al. (2004) with some modifications and the RNeasy Plus Mini Kit (Qiagen, Hilden, Germany). Two grams of frozen strawberry powder were added to a 50 ml polypropylene tube containing 15 ml of prewarmed (60 °C) CTAB buffer (Table 5). The samples were incubated at 60 °C for 15 min and mixed by inversion every 5 min. One volume of cold chloroform (Cf) containing isoamyl alcohol (IAA) (24:1 v/v) was added and vortexed until homogenized. The samples were centrifuged at 13,000 *g* for 40 min at 4 °C. The supernatant was transferred to a new 50 ml tube and extracted again with 1 volume of cold Cf:IAA. The supernatant was transferred to a new 50 ml tube and 1/4 volume of cold LiCl (7.5 M) was added. The samples were mixed by inversion and incubated overnight at 4 °C. The next day, the samples were centrifuged at 13,000 *g* for 40 min at 4 °C, and the

supernatant was discarded. The pellet was resuspended in 600 µl of RLT Plus Buffer and purified according to the manufacturer's instructions.

Table 5. CTAB buffer

Component	Concentration
NaCl	2 M
PVP	2% (w/v)
Tris-HCl pH 8	100 mM
EDTA	25 mM
CTAB	2% (w/v)

3.3 cDNA synthesis

One microgram of total RNA was used for cDNA synthesis. Oligo (dT) primer was used for annealing a quantity of 1 µg. The reverse transcription was carried out using M-MLV Reverse Transcriptase (Promega, Madison, USA) following the producer's specifications.

3.4 Plasmid isolation from microorganisms

3.4.1 Plasmid isolation from *E. coli*

Bacterial DNA isolation was performed using the PureYield Plasmid Miniprep System (Promega, Madison, USA) according to the manufacturer's instructions. No alterations were made.

3.4.2 Plasmid isolation from *S. cerevisiae*

Yeast DNA was isolated using the method described by Hoffman (1997) to confirm positively transformed colonies isolated from plates. A single colony was used to inoculate 2 ml of SC-U medium (Table 14), and the solution was incubated overnight at 30 °C and 150 rpm. A 1.5 ml-aliquot was centrifuged at maximum speed for 10 sec. The supernatant was discarded, and the pellet was resuspended by vortexing in 200 µl of breaking buffer (Table 6). Then, 0.3 g of acid-washed glass beads and 200 µl of phenol:Cf:IAA (25:24:1 w/v/v) were added. The mixture was vortexed at maximum speed for 3 min and centrifuged for 5 min at maximum speed. For PCR, 1.5 µl of the aqueous layer was used.

Table 6. Breaking buffer

Component	Concentration
Triton X-100	2% (v/v)
SDS	1% (v/v)
NaCl	100 mM
Tris-HCl pH 8	10 mM
EDTA pH 9	1 mM

3.5 Polymerase chain reaction

In general, two polymerase chain reaction mixtures were employed. For the cloning of CDS regions, the strategy of nested PCR was used. For this purpose, a Q5 High-Fidelity DNA Polymerase (New England Biolabs, Ipswich, USA) was employed for all reactions (Table 7). First, a PCR with primers targeting the 5'- and 3'-UTRs of each gene (Table 1) was performed with an annealing temperature equal to the melting temperature of the primers + 3 °C (Table 7). The product of this reaction was diluted in sterile mQ-water (1:50 v/v) and used as the template for the next PCR, which was performed using primers including restrictions sites and targeting the CDS region (Table 1). PCR conditions were the same as described above (Table 8). Amplicons were evaluated by agarose gel electrophoresis.

Table 7. PCR reaction mixture for gene cloning

Component	Volume
cDNA template	0.5 µl
Fw primer (10 µM)	1.25 µl
Rv primer (10 µM)	1.25 µl
dNTPs (2.5 mM)	0.5 µl
5X Q5 Reaction Buffer	5 µl
Q5 HF DNA Polymerase	0.25 µl
sterile mQ-water	16.25 µl

Table 8. PCR program for gene cloning

Step	Temperature	Time	Cycles
Initial Denaturation	98 °C	1 min	1
Denaturation	98 °C	15 s	35
Annealing	T _m + 3 °C	20 s	
Elongation	72 °C	1 min 30 sec	
Final elongation	72 °C	2 min	1
Hold	8 °C	∞	-

Colony PCRs were performed to confirm *E. coli* colonies carrying *UGT* genes and *A. tumefaciens* colonies harboring corresponding gene constructs. For this purpose, a mixture containing *Taq* Polymerase (New England Biolabs, Ipswich, USA) was used (Table 9). In the case of *UGTs*, which were expressed using a pGEX-4T-1 vector, the primers used for colony PCR were pGEX3 and pGEX5.

Table 9. Colony PCR reaction mixture

Component	Volume
Fw primer (10 µM)	1 µl
Rv primer (10 µM)	1 µl
dNTPs (2.5 mM)	1 µl
10X ThermoPol Reaction Buffer	2 µl
<i>Taq</i> DNA Polymerase	0.5 µl
sterile mQ-water	14.5 µl

On the other hand, for Agroinfiltration assays, the constructs were based on the pBI121-2x35S vector (modified pBI121 vector under containing twice the 35SCaMV 35S promoter), and the primers used for colony PCR were the M13 Fw and M13 Rv primers. The PCR conditions are detailed in Table 10.

Table 10. PCR conditions for colony PCR

Step	Temperature	Time	Cycles
Initial Denaturation	98 °C	2 min	1
Denaturation	98 °C	1 min	35
Annealing	55 °C	1 min	
Elongation	72 °C	2 min	
Final elongation	72 °C	10 min	1
Hold	8 °C	∞	-

3.6 Real-time PCR

The relative expression of *FvUGT71A49* (mean of 6 biological replicates) was normalized against the mean calculated for the expression level of the housekeeping gene (*GAPDH*) according to the method described by Pfaffl (2001) and expressed in arbitrary units. Each biological replicate corresponded to a different fruit from the same or different plants and was measured three times (technical replicates), and blank control (water instead of cDNA from agroinfiltrated fruit) was included in each run. The fluorescence was measured at the end of each extension step. The absence of the pBI121-2x35S vector in isolated RNA from agroinfiltrated fruits was checked by PCR with primers targeting the end of the 35S region and the beginning of *FvUGT71A49* CDS region (data not shown). The PCR conditions are detailed in Table 11. Primers employed for these experiments are described in Table 2.

Table 11. Conditions for real-time PCR

Step	Temperature	Time	Cycles
Initial Denaturation	95 °C	10 min	-
Denaturation	95 °C	15 sec	40
Annealing	60 °C	15 sec	
Elongation	72 °C	30 sec	
Melting curve			
Step 1	95 °C	15 sec	1
Step 2	60 °C	1 min	
Step 3	95 °C	15 sec	

3.7 Construction of plasmids

All plasmids were constructed by the same procedure. After nested PCR with primers described in Table 1, a PCR clean-up was performed using the NucleoSpin Gel and PCR Clean-up Kit (Macherey-Nagel, Düren, Germany). The eluted purified product was double digested in parallel with the corresponding destination vector (Figures 7, 8, 9 and Table 1) using the set of FastDigest (Thermo Fisher Scientific, Waltham, USA) restriction enzymes according to the manufacturer's instructions (Table 12). Afterward, a PCR clean-up of restriction products was performed, using diluted Binding Buffer NT1 (1:5 (v/v) with mQ water) to eliminate small DNA fragments. The eluted purified products were ligated using T4 DNA Ligase Kit (Promega, Madison, USA) for 3 h at RT or 4 °C overnight following the producer's specifications.

Table 12. Double-digestion reaction mixture

Component	Volume
DNA	10 µl (800 ng)
10x Fast Digest Buffer	3 µl
Restriction enzyme 1	1 µl
Restriction enzyme 2	1 µl
mQ water	15 µl

3.8 Transformation of plasmid in microorganisms

3.8.1 Transformation of *E. coli*

Fifty microliters of chemically competent cells, stored at -80 °C were thawed on ice, mixed with plasmid and incubated on ice for 30 min. Subsequently, cells were heat-shocked at 42 °C for 45 sec in a water bath, cooled on ice for 5 min and supplemented with 500 µl of SOC medium (Table 13). Afterward, the samples were incubated for 90 min at 37 °C and 150 rpm. Transformants were plated on LB-agar plates containing appropriate antibiotics and incubated at 37 °C overnight.

3.8.2 Transformation of *S. cerevisiae*

Competent INVSc-1 cells frozen at -80 °C were transformed with the *S. c.* EasyComp Transformation Kit and plated on SC-U selective agar plates (Table 14), prepared following the instructions of the pYES2 vector manual, and incubated at 30 °C for 48 h.

3.8.3 Transformation of *A. tumefaciens*

Competent cells frozen at -80 °C were thawed on ice and mixed with 1 µg of plasmid DNA by flicking the tube. The mixture was placed on ice for 5 min and transferred to liquid nitrogen for 5 min, followed by incubation in a 37 °C water bath for 5 min. The mixture was transferred to a 15 ml polypropylene tube, and 1 ml of LB medium was added (Table 15). The mixture was incubated at 28 °C for 2 h at 150 rpm. The cells were harvested by spinning 2 min at 5,000 *g* and resuspended in 200 µl of LB medium. Finally, the samples were plated on LB agar plates containing appropriated antibiotics and were incubated at 28 °C for 48 h.

Table 13. SOC medium composition

Component	Concentration
Yeast extract	5 g·l ⁻¹
Tryptone	20 g·l ⁻¹
NaCl	0.5 g·l ⁻¹
KCl	2.5 mM
MgCl ₂	10 mM
MgSO ₄ x 4 H ₂ O	10 mM
Glucose	20 mM

Table 14. SC-U selective medium composition

Component	Concentration
Yeast nitrogen base	0.67% (w/v)
Glucose	2% (w/v)
Amino acid Mix A (Adenine, Arg, Cys, Leu, Lys, Thr, Trp)	0.01% (w/v)
Amino acid Mix B (Asp, His, Ile, Met, Phe, Pro, Ser, Tyr, Val)	0.005% (w/v)
Agar *	2 % (w/v)

*for preparing selective SC-U agar plates

Table 15. LB medium composition

Component	Concentration
Yeast extract	5 g·l ⁻¹
Tryptone	10 g·l ⁻¹
NaCl	10 g·l ⁻¹
Agar *	15 g·l ⁻¹
pH	7

* for preparing selective LB agar plates

3.9 Isolation of microsome protein

The procedure was conducted according to the methods described by Huang et al. (2014), Olsen et al. (2010), and Dunn and Wobbe (1993). A single yeast colony was used to inoculate 25 ml of SC-U selective medium and grown at 30 °C for 24 h and shaking at 150 rpm. The culture was transferred to 200 ml of SC-U selective medium and grown overnight at 30 ° at 150 rpm. An aliquot of the overnight culture sufficient to achieve an OD₆₀₀ of 0.4 in 200 ml of SC-U induction medium (Table 16) was taken, the cells were pelleted (1,500 g, 5 min at 4 °C) and resuspended in 200 ml of SC-U induction medium. The cells were grown for 24 h at 30 °C and 150 rpm orbital shaking. Microsomes were isolated in the following way: The cells were pelleted as previously described in pre-weighed tubes and 1 g of cells was considered as 1 ml of volume. Cells were resuspended in 2 volumes of ice-cold water and immediately pelleted. Cells were resuspended in 2 volumes of Glass Bead Disruption Buffer (Table 17) and 4 volumes of chilled acid-washed glass beads (0.42 –0.625 µm) were added. The mixture was shaken in an automatic shaker mixer mill in 4 cycles of 2 min and vibration frequency of 30. Between two shaking cycles, the sample was placed on ice for 3 min. Subsequently, the glass beads were allowed to settle, and the supernatant was retained. The beads were washed twice with 1 volume of Glass Bead Disruption Buffer. The supernatants were pooled and centrifuged at 10,000 g for 10 min at 4 °C. The supernatant was diluted with 1 volume of Glass Bead Disruption Buffer and the microsomes were precipitated by adding NaCl to a final concentration of 0.15 M and polyethylene glycol (PEG)-4000 to a final concentration of 0.1 g·ml⁻¹. The mixture was placed for 1 h on ice and centrifuged at 12,500 g for 20 min at

4 °C. The pellet was dissolved in 1 ml of TEG buffer (Table 18) and homogenized using a Teflon pestle.

Table 16. SC-U induction medium

Component	Concentration
Yeast nitrogen base	0.67% (w/v)
Galactose	2% (w/v)
Raffinose	1% (w/v)
Aminoacid Mix A (Adenine, Arg, Cys, Leu, Lys, Thr, Trp)	0.01% (w/v)
Aminoacid Mix B (Asp, His, Ile, Met, Phe, Pro, Ser, Tyr, Val)	0.005% (w/v)

Table 17. Glass Bead Disruption Buffer

Component	Concentration
Tris-HCl pH 7.9	20 mM
MgCl ₂	10 mM
EDTA	1 mM
Glycerol	5% (v/v)
DTT	1 mM
Ammonium Sulfate	0,3 M
Protease inhibitor cocktail I*	1 tablet per 25 ml of buffer
PMSF	1 mM

* cOmplete EDTA-free Protease Inhibitor Cocktail (Roche, Germany)

Table 18. TEG Buffer

Component	Concentration
Glycerol	30% (w/v)
Tris-HCl pH 7.5	50 mM
EDTA	1 mM

3.10 *In vitro* and biotransformation assays with P450 enzymes

To confirm the hydroxylase activity of the recombinant enzymes produced, the reaction mixture (Table 19) was incubated at RT for 18 h while shaking at 400 rpm. The reaction was stopped by the addition of 1 volume of ethyl acetate. The products were extracted 4 times with 1 volume of ethyl acetate each, the combined extracts were concentrated to dryness in a vacuum concentrator and resuspended in 40 µl of methanol. Finally, the samples were analyzed by LC-MS.

Table 19. Reaction mixture for *in vitro* hydroxylase activity

Component	Concentration
Potassium Phosphate Buffer pH 7.25	50 mM
(+)-ABA or (±)-ABA	200 µM
NADPH	200 µM
Recombinant CYP707A microsomes	1 µg·µl ⁻¹
mQ-water	to 200 µl

The biotransformation experiments were performed according to Huang et al. (2014) with modifications. Briefly, yeast colonies were inoculated into 15 ml liquid SC-U medium containing 2% (w/v) glucose and were grown at 30 °C with shaking at 150 rpm until an OD₆₀₀ of 2 to 4 was reached. The necessary amount of culture to obtain 20 ml of induction medium with an OD₆₀₀ 1.2 was centrifuged at 1,500 g for 5 min at 4 °C and resuspended in 20 ml of induction medium containing 2 mg of (+)-ABA or (±)-ABA. The cells were grown at 30 °C with shaking at 150 rpm. for 2 days. For each sampling point, 2 ml of culture were used and 100 µl of biochanin A (2 mg/l w/v) were added as internal standard. The products were extracted and were analyzed as previously described for the *in vitro* assays, but 100 µl of biochanin A (2 mg/l w/v) were added as internal standard. Results were expressed as the ratio of integrated peaks areas of phaseic acid : internal standard, and the values correspond to the average of three independent biotransformation systems.

3.11 Heterologous expression and purification of recombinant UGTs in *E. coli*

A single colony of *E. coli* was used to inoculate 10 ml of LB medium containing appropriate antibiotics and was grown overnight at 37 °C with shaking at 150 rpm. The next day, 0.5 l of LB medium with antibiotics was inoculated with 5 ml of the overnight culture and was incubated at 37 °C and 150 rpm until an OD₆₀₀ of 0.7 was achieved. The protein expression was induced by the addition of IPTG to a final concentration of 1 mM and the culture was incubated for 24 h at 19 °C and 150 rpm. Afterward, the cells were collected by centrifugation (5,000 g, 4 °C, and 20 min) and incubated at –80 °C for 30 min. The pellet was resuspended in 10 ml 1x GST Wash/Binding Buffer (Table 20) and sonicated for 10 min for cell

disruption. Cell debris was pelleted by centrifugation at 13,500 g for 20 min at 4 °C. The recombinant GST fusion proteins in the supernatant (crude protein extract) were finally purified by affinity chromatography incubating the sample for 2 h at 4 °C with GST•Bind Resin (Novagen, Darmstadt, Germany) and were eluted with 1x GST Elution Buffer (Table 21).

Table 20. Composition 1x GST Wash/Binding Buffer

Component	Concentration
NaCl	137 mM
KCl	2,7 mM
Na ₂ HPO ₄	4.3 mM
KH ₂ PO ₄	1.47 mM

Table 21. Composition 1x GST Elution Buffer

Component	Concentration
Reduced Glutathione	10 mM
Tris-HCl pH 8.0	50 mM

3.12 Sodium dodecyl sulfate polyacrylamide gel electrophoresis (SDS-PAGE)

After purification, the protein samples were analyzed by SDS-PAGE. Five micrograms of each protein fraction were mixed with 2x Laemmli Buffer (Bio-Rad, Hercules, USA) prepared with 2-mercaptoethanol following the manufacturer's instructions. Afterward, the samples were denatured by heating at 95 °C for 5 min. Samples were run on 7% stacking gel (Table 22) and 12% resolving gel (Table 23) using 1x Running Buffer (Table 24) at 100 V for approximately 3 h. Five microliters of PageRuler Plus Prestainder Protein Ladder (Thermo Fischer Scientific, Waltham, USA) was used as the marker.

Table 22. 7% SDS stacking gel

Component	Volume
dH ₂ O	925 µl
30% Acrylamide	350 µl
1 M Tris (pH 6.8)	187.5 µl
10% SDS	15 µl
10% APS	15 µl
TEMED	2,5 µl

Table 23. 12% SDS resolving gel

Component	Volume
dH ₂ O	2.45 ml
30% Acrylamide	3 ml
1.5 M Tris (pH 8.8)	1,9 ml
10% SDS	75 μ l
10% APS	75 μ l
TEMED	3 μ l

Table 24. 1x Running Buffer

Component	Concentration
Tris	3 g·l ⁻¹
Glycine	14.4 g·l ⁻¹
SDS	1 g·l ⁻¹

Subsequently, the gel was placed into a plastic box and stained overnight at RT using Colloidal Coomassie Solution (Table 25) as described by Kang et al. (2002). Excess staining was removed by incubation in the destaining solution (20% (v/v) ethanol, 10% (v/v) acetic acid in dH₂O).

Table 25. Colloidal Coomassie Solution

Component	Concentration
Al ₂ (SO ₄) ₃ x16 H ₂ O	5 g·l ⁻¹
Ethanol	10 ml·l ⁻¹
H ₃ PO ₄	2.5 ml·l ⁻¹
Coomassie G250	0.02 g·l ⁻¹

3.13 *In vitro* UGT activity assay

The reaction mixture (Table 26) was incubated overnight at 30 °C and 400 rpm. The next day, the reaction was stopped by heating at 75 °C for 10 min and centrifuged at 12,000 g for 5 min. Finally, 50 μ l of supernatant was transferred to an inner tube of an LC vial and analyzed by LC-MS.

Table 26. Reaction mixture for *in vitro* UGT activity assay.

Component	Concentration
Purified Protein	25 ng· μ l ⁻¹
1 M Tris-HCl (pH 7.5)	100 mM
UDP-gluc	1 mM
Substrate	450 μ M
mQ-H ₂ O	up to 200 μ l

3.14 UDP-Glo assay and kinetics

The kinetics of purified UGTs were studied using the UDP-Glo Glycosyltransferase Assay (Promega, Madison, USA) according to the manufacturer's manual. The general reaction conditions are detailed in Table 27. Briefly, the released UDP of the glucosyltransferase reaction is transformed into ATP, which produces luminescence in a luciferase reaction. Therefore, the measured luminescence is proportional to the concentration of UDP and the glycosyltransferase activity. The optimal reaction conditions (pH, temperature, and incubation time) were determined by the same method.

Table 27. UDP-Glo Assay - General reaction mixture.

Component	Concentration
Buffer of optimal Buffer	50 mM
Substrate	Variable
Purified protein	5 μ g
mQ-water	up to 45 μ l
UDP-gluc 1 mM	5 μ l

A UDP standard curve was used to calculate the concentration of UDP. Subsequently, the data were fitted to the Michaelis-Menten equation by using a nonlinear regression calculated with the Microsoft Excel complement Solver. The obtained K_m and V_{max} values were used to calculate k_{cat} and k_{cat}/K_m .

3.15 Phylogenetic tree

For the phylogenetic analysis, we selected previously biochemically characterized enzymes with *in vitro* or *in planta* activity towards different phytohormones, in addition to those enzymes characterized in this work. The trees were constructed employing the full-lengths amino acidic sequences by the

Maximum Likelihood method and JTT matrix-based model in MEGA X software (Kumar et al. 2018). The bootstrapping values are based on 1,000 replicates. The sequences used and their respective references are listed in Table 28.

Table 28. References of the enzymes used for constructing the phylogenetic trees.

Protein	Reference
AtUGT71C5	Liu et al. 2015
PvABA-GT	Palaniyandi et al. 2015
GhUGT73C14	Gilbert et al. 2013
VaQ8W3P8	Xu et al. 2002
FaUGT71A33	
FaUGT71A34	Song et al. 2015
FaUGT71A35	
FaUGT71W2	
AtUGT71B6	Priest et al. 2005
AtUGT71B7	
AtUGT71B8	Dong et al. 2014
OsiAGT1	Liu et al. 2019
PsABAUGT1	Zdunek-Zastocka and Grabowska 2019
ZmIAGLU	Szerszen et al. 1994
PIZOG	Rodó et al. 2008
InGTase1	Suzuki et al. 2007
NtSAGTase	Lee and Raskin 1999
AtSGT1	Song 2006
SIUGT75C1	Sun et al. 2017
AtUGT84B1	Jackson et al. 2001
AtUGT85A1	Hou et al. 2004
CsUGT85A53	Jing et al. 2020
AtUGT75B1	Jackson et al. 2001 and Chen et al. 2020
AtUGT73C5	Poppenberger et al. 2005
PacCYP707A1	
PacCYP707A2	
PacCYP707A3	Ren et al. 2010
PacCYP707A4	
SICYP707A1	Nitsch et al. 2009
SICYP707A2	Ji et al. 2014
FvCYP707A1/3	
FvCYP707A4a	Liao et al. 2018
AtCYP707A1	
AtCYP707A2	Kushiro et al. 2004 and Okamoto et al. 2006
AtCYP707A3	

AtCYP707A4	
PvCYP707A1	
PvCYP707A2	Yang and Zeevart 2006
PvCYP707A3	
OsCYP714B1	
OsCYP714B2	Magome et al. 2013
AtCYP714A1	
AtCYP714A2	Zhang et al. 2011
AtCYP735A2	
AtCYP94C1	Takei et al. 2014
AtCYP94B3	Heitz et al. 2012
PtCYP714A3	Wang et al. 2016

3.16 Statistical analysis

The data were subjected to analysis of variance (ANOVA), the normality and equality of variances were tested by the Shapiro-Wilks test and F-test, respectively and differences were considered statistically significant at $p < 0.05$ (Tukey HSD test or t-test). For analyses of agroinfiltrated fruits, it has been reported that levels of metabolites and transcripts are not normally distributed; therefore, we used the Wilcoxon-Mann-Whitney U test, and differences were considered statistically significant at $p < 0.05$ (Hart, 2001; Hoffmann et al. 2006).

4. RESULTS

4.1 Selection and cloning of candidate glycosyltransferases and hydroxylases

Sequencing of total mRNA from the receptacle and achenes of fruits of *F. vesca* varieties Reine des Vallées (RdV; red-fruited), Yellow Wonder (white-fruited), and Hawaii 4 (white-fruited) was performed by Härtl et al. 2017. Based on this data set, data available at the KO (KEGG orthology) database and further comparisons using BLAST with UGTs sequences from other plants, we selected a group of six UDP-dependent glycosyltransferases (UGTs) putatively involved in phytohormone glucosylation, namely UGT71A48, UGT71A49, UGT73AC3, UGT75L26, UGT75L27, and UGT85A80. Full-length sequences were amplified employing cDNA from different developmental stages of *F. vesca* RdV fruit, depending on the expression levels.

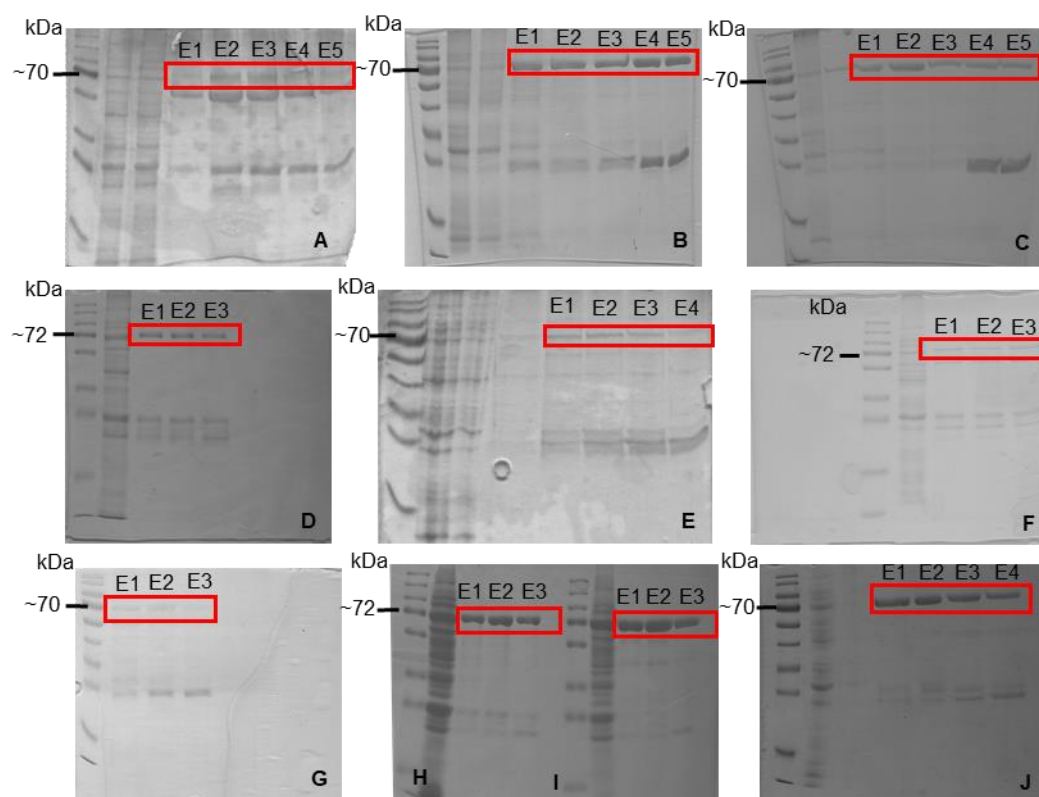


Figure 10. SDS-PAGE analysis of all UGT-GST fusion proteins expressed in *E. coli* for this work. The first lane of each gel corresponds to the molecular weight marker. “E” indicates elution fraction. Proteins are UGT75L26 (**A**), UGT71A49 (**B**), UGT71A48 (**C**), UGT73AC3 (**D**), UGT75L27 (**E**), UGT85A80 (**F**), UGT71W2 (**G**), UGT71A33 (**H**), UGT71A34 (**I**), and UGT71A35 (**J**).

All coding sequences (CDS) were successfully expressed in *E. coli* and the recombinant proteins purified by GST-tag affinity chromatography (Figure 10). Furthermore, we isolated two CDS encoding 8'-ABA-hydroxylases from *F. x ananassa* cv. Elsanta leaves, *FaCYP707A4a*, and *FaCYP707A1/3* due to sequence similarity to ABA-hydroxylases from *F. vesca* (Liao et al. 2018).

4.2 Characterization of isolated UGTs

4.2.1 Enzymatic activity of isolated UGTs

The *in vitro* substrate tolerance of the purified recombinant UGTs was studied by LC-MS. A broad range of substrates, previously found in plants, was selected to test the catalytic activity of UGTs (Table 29). All putative GTs were capable of glucosylating naringenin, while UGT71A48 transferred up to three glucose moieties to the substrates kaempferol, quercetin, and galangin (Supplementary Figure 1). Furthermore, UGT71A48 attached two glucose molecules to naringenin and 3,7-dihydroxyflavone. Similarly, di-glucosylated products were found when kaempferol, quercetin, galangin, naringenin, and 3,7-dihydroxyflavone were incubated with UGT71A49. UGT71A48 and UGT71A49 showed similar catalytic preferences and exhibited high activities towards the substrates kaempferol, quercetin, 3-hydroxyflavone, galangin, 3,7-dihydroxyflavone, and naringenin converting between 75–100 % of each substrate provided.

The phytohormone *trans*-zeatin was glycosylated by the enzymes UGT71A49 and UGT85A80, but enzyme UGT85A80 exhibited a remarkably higher activity (51% of the offered substrate) compared to UGT71A49 (1% of the offered substrate; Table 29, Supplementary Figure 1). Besides, we found that UGT71A49 and UGT73AC3 glycosylated (+)-ABA; however, UGT71A49 was much more effective than UGT73AC3 and converted 49% of (+)-ABA versus 1% (Table 29).

Table 29. Summary of the substrate tolerance of the isolated UGTs. Values are expressed in the percentage of the converted substrate and were calculated based on the integration of peak areas of the extracted ion chromatograms (EIC) obtained by LC-MS. I-3-AA: indole-3-acetic acid, 1-NAA 1-naphthaleneacetic acid; GA₃: gibberellic acid; 3-HF: 3-hydroxyflavone, 3,7-diHF: 3,7-dihydroxyflavone; JA: jasmonic acid.

Enzyme	Substrate	Carvacrol	Farnesol	Benzyl alcohol	2-Phenylethanol	Geraniol	cis-3-hexen-1-ol	Kaempferol	I-3-AA	β -Apo-8'-carotenal	Quercetin	<i>trans</i> -Zeatin	α -Ionol	β -Ionol	S-Perillyl alcohol	Scopoletin	Hydroquinone	Astaxanthin	1-NAA	(+)-ABA	GA ₃	3-HF	Galangin	3,7-diHF	Naringenin	JA
UGT75L26	x	x	x	x	x	x	x	31.16	x	x	x	x	x	x	x	x	x	x	x	x	x	x	x	x	17.15	x
UGT85A80	x	x	x	x	x	x	x	17.83	x	x	x	50.54	x	x	x	x	x	x	x	x	x	x	13.34	55.96	6.02	x
UGT75L27	x	x	x	x	x	x	x	x	x	x	x	x	x	x	x	x	x	x	x	x	x	x	x	x	5.22	x
UGT71A49	x	x	x	x	x	x	x	97.09	x	x	100	0.90	x	x	x	x	x	x	x	48.55	x	100	97.26	99.41	85.53	x
UGT71A48	x	x	x	x	x	x	x	93.47	x	x	100	x	x	x	x	x	x	x	x	x	x	100	96.99	100	75.48	x
UGT73AC3	x	x	x	x	x	x	x	66.33	x	x	x	x	x	x	x	x	x	x	x	0.76	x	x	88.07	45.78	12.76	x

4.2.2 Kinetic properties of isolated UGTs

The kinetic properties of UGT71A49 and UGT73AC3 towards (+)-ABA were studied using the UPP-Glo assay, and the values were compared to those obtained for previously described strawberry enzymes with *in vitro* activity towards (+)-ABA, UGT71A33, UGT71A34, UGT71A35, and UGT71W2 (Song et al. 2015). The enzymes without (+)-ABA UGT activity were not further analyzed, except for UGT85A80, whose kinetic properties towards *trans*-zeatin were also quantified. The optimal reaction conditions were determined for each enzyme, using (+)-ABA (or *trans*-zeatin in case of UGT85A80) as substrate (Table 30).

Table 30. Optimal reaction conditions of the selected UGTs.

Enzyme	pH	Buffer	Temperature (°C)
FvUGT73AC3	6	Phosphate	45
FvUGT71A49	6	Phosphate	45
FvUGT71A33	6	Phosphate	35
FvUGT71A34	8	Phosphate	35
FvUGT71A35	6	Phosphate	30
FvUGT71W2	8	Phosphate	35
FvUGT85A80	7	Phosphate	40

It was not possible to determine the kinetic properties of UGT71A34 and UGT71W2 towards (+)-ABA using the UDP-Glo assay due to the high background signal caused by the inherent UDP-glucose hydrolase activity of the enzymes, particularly at low (+)-ABA concentrations. As an alternative, a simple comparison of the signal intensities in the LC-MS chromatograms was performed (Figure 11). The peak corresponding to ABA-GE was considerably higher when (+)-ABA was incubated with UGT71A49 than with proteins UGT71A34 and UGT71W2 (Figure 11). The same problem arose when the kinetic properties of UGT71A49 towards *trans*-zeatin were studied. Among the enzymes whose activities were successfully analyzed by the UDP-Glo assay, UGT71A49 exhibited the lowest K_m value as well as the highest specificity constant k_{cat}/K_m towards (+)-ABA, while UGT73AC3 exhibited the second highest specificity constant, but a K_m value 10 times higher than UGT71A4 (Table 31).

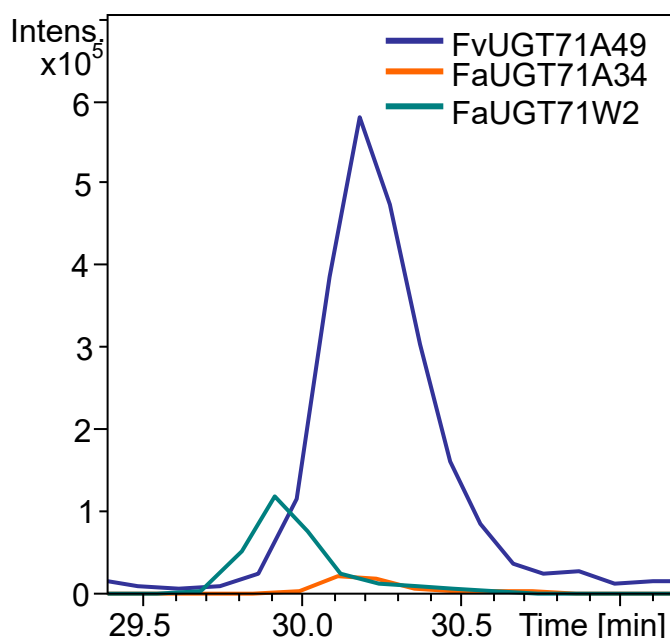


Figure 11. LC-MS analysis of products formed by FvUGT71A49, FaUGT71A34, and FaUGT71W2 incubated with (+)-ABA and UDP-glucose. The peaks of the ABA glucose ester in the extracted ion chromatograms are compared.

In general, the enzyme UGT85A80 was the most effective enzyme towards its corresponding putative substrate (*trans*-zeatin), displaying the second-lowest K_m value (635.17) and the highest specificity constant value: $18.0 \text{ s}^{-1} \text{ M}^{-1}$. However, we cannot distinguish if the glucoside corresponds to an O- or N-glucoside (Table 31).

Table 31. Kinetic data of the catalytic activity of UGT85A80 with *trans*-zeatin and of UGT71A49, UGT73AC3, and previously characterized UGT71A33 and UGT71A35 with (+)-ABA. Data indicate the mean \pm SD ($n = 3$).

Enzyme	Substrate	K_m (μM)	V_{max} (nkat/mg)	k_{cat} (s^{-1})	k_{cat}/K_m ($\text{s}^{-1} \text{ M}^{-1}$)
UGT71A49	(+)-ABA	100.57 ± 17.8	0.017 ± 0.002	0.0014 ± 0.0002	13.7
UGT73AC3	(+)-ABA	1047.87 ± 124.6	0.154 ± 0.007	0.0062 ± 0.0003	5.9
UGT71A33	(+)-ABA	2345.98 ± 165.6	0.055 ± 0.004	0.0022 ± 0.0002	0.9
UGT71A35	(+)-ABA	1061.49 ± 64.6	0.031 ± 0.001	0.0024 ± 0.0001	2.3
UGT85A80	<i>trans</i> -zeatin	635.17 ± 154.2	0.142 ± 0.01	0.0115 ± 0.0008	18.0

4.2.3 Substrate specificity of UGTs with activity towards ABA

To further analyze the substrate specificity of UGT71A49 and UGT73AC3, the activity of both enzymes was tested *in vitro* towards (+)-ABA and a set of structural analogues (Priest et al., 2005; Figure 12) by using the UDP Glo assay (Figure 13). For this assay, the samples were incubated for 30 min.

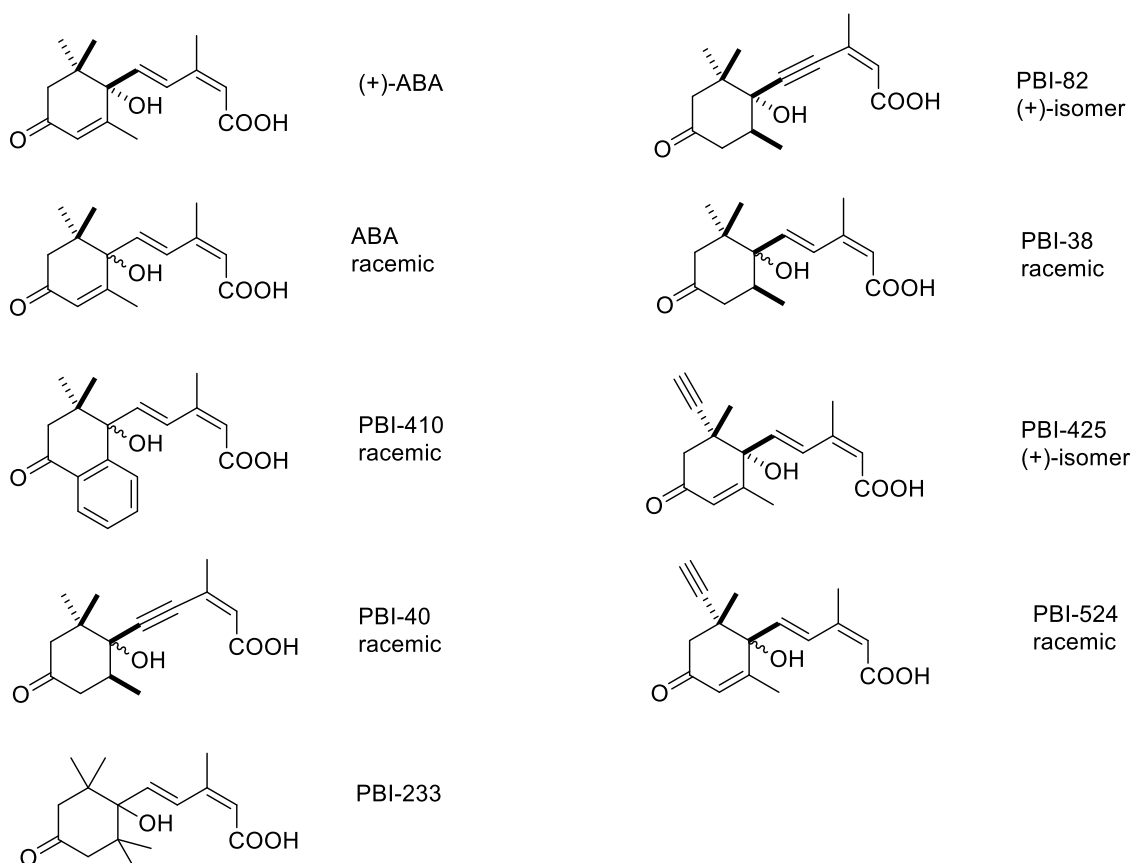


Figure 12. Structure of ABA analogues

UGT71A49 accepted all ABA analogues except for PBI-425 and PBI-524 (isomeric 8'-acetylene-ABA). Although the enzymatic activity of UGT71A49 towards PBI-425 was not detected with the UDP-Glo assay, a small amount of the product was found by LC-MS analysis after prolonged overnight incubation (data not shown). Moreover, UGT71A49 exhibited a significantly higher activity towards PBI-410 than for (+)-ABA. PBI-410 was the preferred substrate for this enzyme (Figure 13). Similarly, UGT73AC3 accepted all the substrates, except for PBI-524 and PBI-425 but no analogue was a better substrate than (+)-ABA added as naturally occurring form or racemic form.

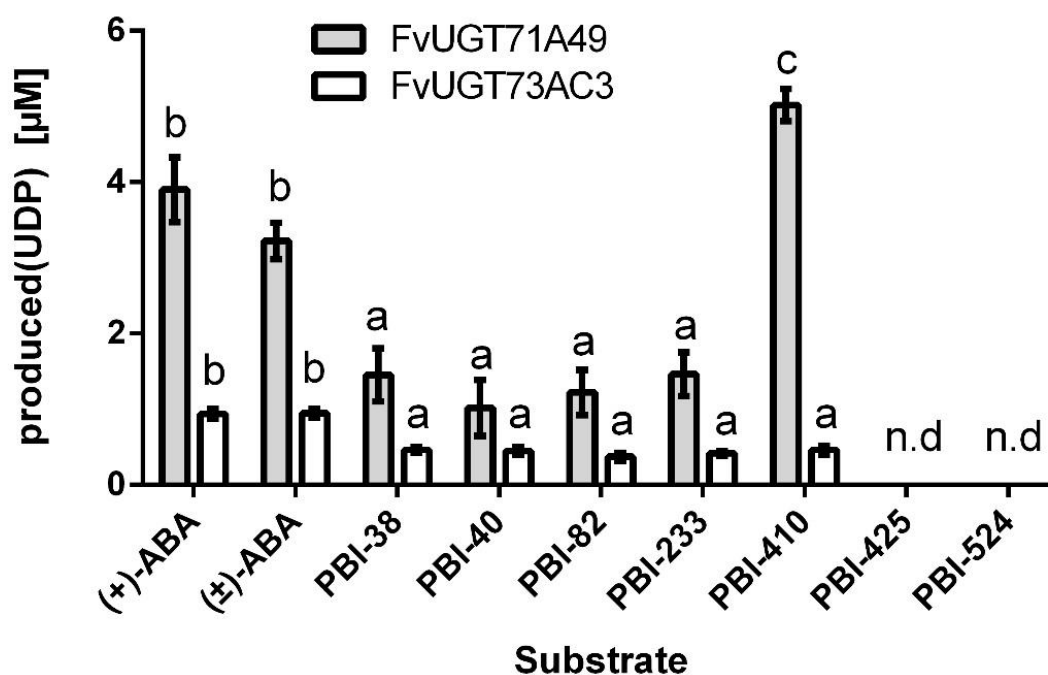


Figure 13. Enzymatic activity of FvUGT71A49 and FvUGT73AC3 towards different ABA analogues analyzed by UDP-Glo assay. The results are expressed as produced UDP, which equals glucoside production. Data indicate the mean \pm SD of four independent reactions. Different letters indicate statistically significant differences in produced UDP among different substrates for the same tested enzyme ($p < 0.05$; Tukey HSD test); n.d. not detected.

Besides, it can be seen that the racemic mixtures PBI-40 and (\pm)-ABA produced a similar amount of product as the corresponding enantiomers (+)-ABA and (+)-PBI-82, respectively, after the period employed for this assay.

4.3 Enzymatic activity of *FaCYP707A1/3* and *FaCYP7074a*

To functionally characterize cytochrome P450s putatively involved in the oxidation of ABA, the coding sequences of *FaCYP707A1/3* and *FaCYP7074a* were expressed in the yeast strain INVSc1. For *in vitro* analysis, the microsomal fractions of the cells transformed with pYES-*FaCYP707A1/3*, pYES-*FaCYP7074a*, or pYES2-empty vector were incubated with NADPH and (+)-ABA or (\pm)-ABA. The products were isolated and analyzed by LC-MS (Figure 14). Both enzymes produced a single and identical product, which showed a

pseudomolecular mass of m/z 279 $[M-H]^-$. The product ion spectrum indicated a hydroxylated ABA derivative.

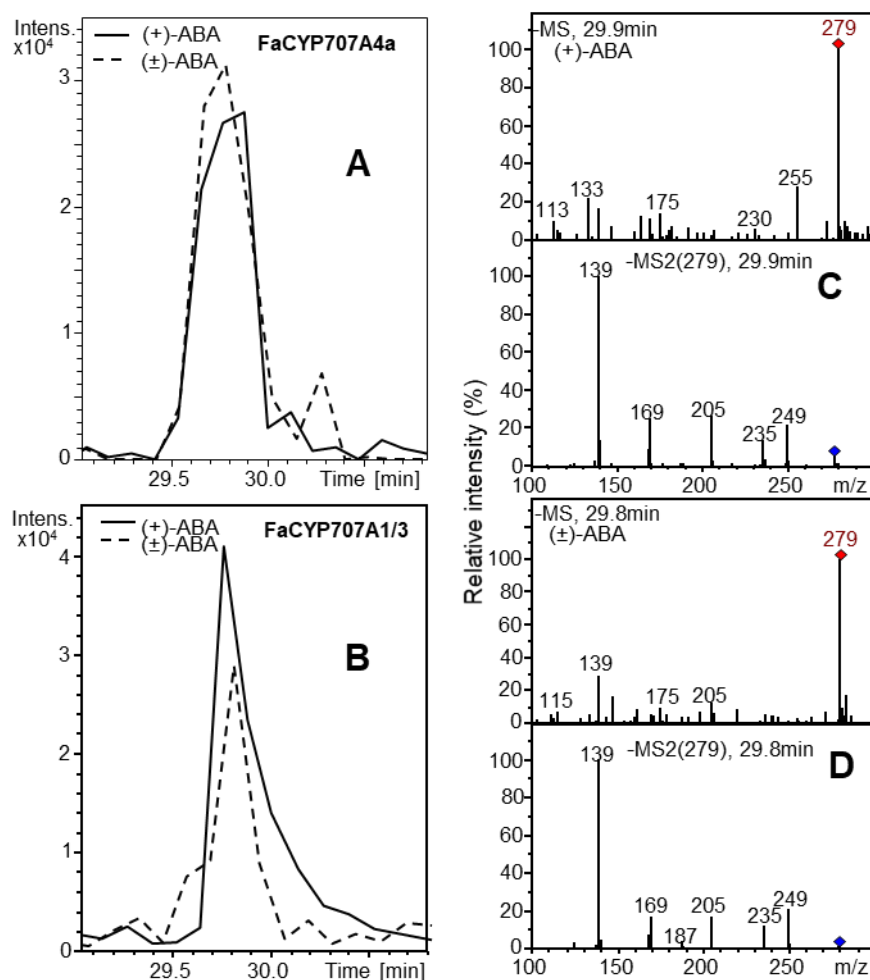


Figure 14. Extracted ion chromatogram of the products formed by FaCYP707A4a (A) and FaCYP707A1/3 (B) after incubation with NADPH and (+)-ABA or (±)-ABA or (±)-ABA. MS and MS2 spectra of the products resulting from the oxidation of ABA when (+)-ABA (C) or (±)-ABA (D) is added.

The metabolite was identified as phaseic acid (PA) using authentic reference material. Thus, the CYP707s hydroxylate (+)-ABA and (±)-ABA at the C-8' position. While *FaCYP707A4a* showed no preference for an optical isomer of ABA, *FaCYP707A1/3* seems to exhibit a slight preference for the natural (+)-ABA (Figure 14).

In a biotransformation experiment, (+)-ABA or (±)-ABA were directly added to culture media containing yeast cells transformed with pYES-*FaCYP707A1/3*, pYES-*FaCYP707A4a*, or the empty pYES2-vector after induction by galactose and

were incubated for two days. Cells were removed, and the products were extracted from the supernatant with ethyl acetate and analyzed by LC-MS (Figure 15).

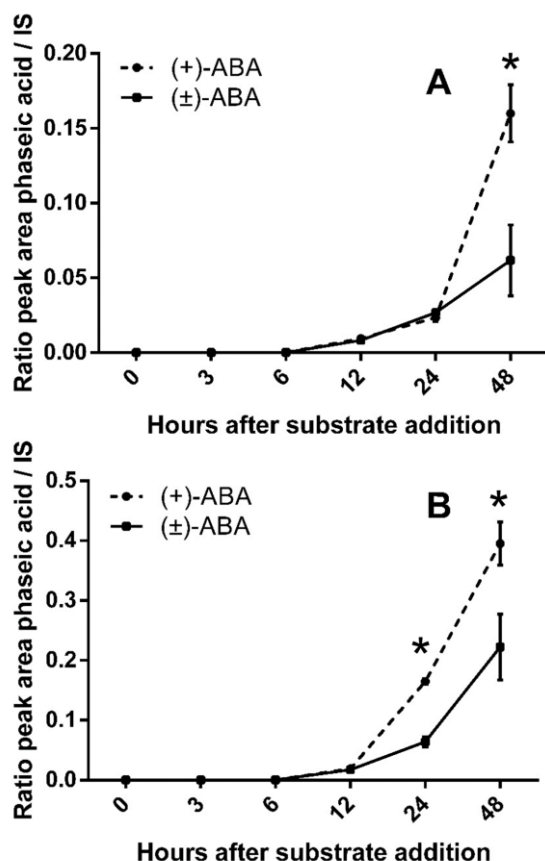


Figure 15. Time curve of phaseic acid formation in biotransformation systems with FaCYP707A4a (A) and FaCYP707A1/3 (B) after induction by galactose. Data indicate the means \pm SD of three independent biotransformation systems. Asterisks indicate statistically significant differences at the same sampling point ($p < 0.05$; t-test)

Cells containing pYES-FaCYP707A1/3 and pYES-FaCYP7074a produced only PA when supplemented with (+)-ABA and (±)-ABA. PA was not formed by the empty vector controls. At the beginning of the incubation period, the cells produced similar amounts of PA from (+)-ABA and (±)-ABA, but after a prolonged incubation time (48 h), the cultures to which (+)-ABA was added yielded about 2 times more (Figure 15).

4.4 Extended incubation of UGT71A49 with ABA

Since the *in vitro* (short-term experiment) and *in vivo* (long-term experiment) incubations yielded different results regarding the enantioselectivity of the CYP707 enzymes, we decided to perform *in vitro* long-term experiments with UGT71A49 and the stereoisomers of ABA to re-analyze its enantioselectivity. The same conditions as in 4.2.3 were used, but the samples were incubated for a period of 16 h instead of 30 min. The amount of product in the samples incubated with (+)-ABA was about 2 times higher than in the samples incubated with the racemic mixture (Figure 16). These results are similar to those obtained in the experiments described in section 4.3 with the CYP707 enzymes.

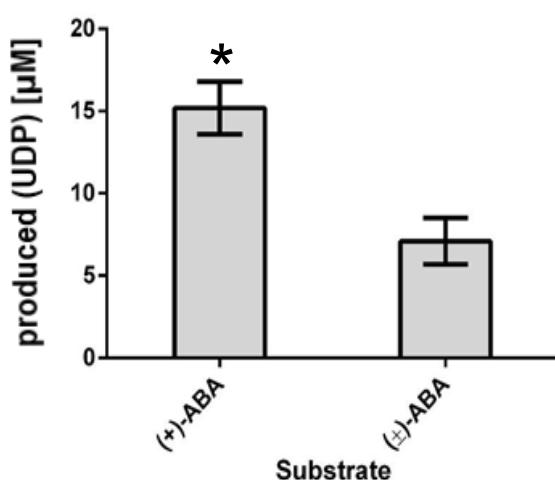


Figure 16. In vitro activity of UGT71A49 towards (+)-ABA and (±)-ABA after 16 hours of incubation. The results are expressed as produced UDP, which equals glucoside production. Data indicate the mean \pm SD of four independent reactions. Asterisks indicate statistically significant difference ($p < 0.05$; t-test)

4.5 Quantification of ABA and its metabolites during strawberry ripening

To obtain an overview of the ABA metabolism during strawberry ripening, the endogenous content of ABA and its derivatives ABA-GE, PA, dihydrophaseic acid (DPA), 7'-hydroxy-ABA and neophaseic acid (neoPA) was quantified by LC-MS. Five *F. vesca* varieties (receptacle and achenes were analyzed separately), and one *F. x ananassa* cultivar (whole fruit) were analyzed (Figures 17-19). The MS spectra and retention times of the ABA metabolites neophaseic acid, phaseic

acid, dihydrophaseic acid, and 7'-hydroxy-ABA were obtained by analysis of authentic reference material (Figure 20). Chemically synthesized references were kindly provided by the Department of Chemistry, University of Saskatchewan, Canada (PA and 7'-hydroxy-ABA), and purchased from the National Research Council of Canada (neoPA and DPA).

In all six studied genotypes, the (+)-ABA content increased throughout the ripening in the receptacle tissue as well as in achenes (Figures 17-19). At the same time, in all *F. vesca* varieties, the ABA-GE content increased considerably during ripening, with a dramatic increase at the late developmental stage (Figure 17). No difference in the ABA metabolite pattern between white- and red-fruited varieties was observed. The same pattern of increasing content of ABA-GE during ripening was found in achenes but to a much lesser extent (Figure 18). In contrast, the ABA-GE content decreased in *F. x ananassa* cv. Elsanta during ripening and the proportion of ABA-GE/free ABA at the late developmental stage was significantly lower compared with *F. vesca* varieties (Figure 19).

In all analyzed receptacles and achenes, the concentration of 7'-hydroxy-ABA remained stable or exhibited only a minor increase throughout the ripening process. Noticeably, in receptacles and achenes of HW4 and RdV 7'-hydroxy-ABA is one of the major ABA metabolites in terms of quantity compared with its concentration in the other *F. vesca* varieties (Figures 17 and 18). Similarly, 7'-hydroxy-ABA is an abundant ABA metabolite in *F. x ananassa* cv. Elsanta and the ripening process does not affect its level (Figure 19).

PA peaked at the white developmental stage in receptacle tissue from all analyzed strawberry samples, while the DPA content increased during the ripening except for *F. vesca* var. RdV, where PA increased during ripening and

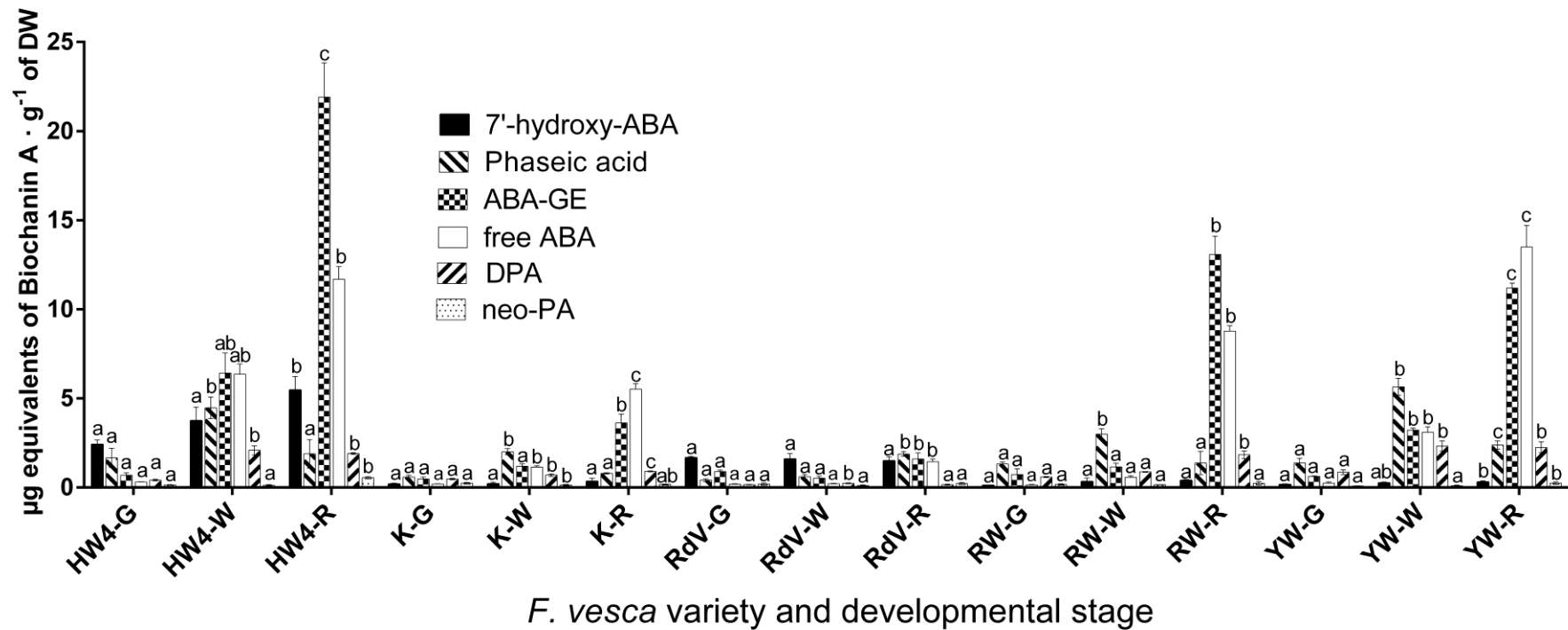


Figure 17. Quantification of ABA and its catabolites in receptacle tissue from *F. vesca* varieties Hawaii4 (HW4), Korsika (K), Reine des Vallées (RdV), Red Wonder (RW) and Yellow Wonder (YW) at green (G), white (W) and ripe (R) developmental stages by LC-MS. Data indicate the mean \pm SD ($n = 3$). Different letters indicate a statistically significant difference in the amount of the corresponding ABA metabolite at different developmental stages within the same analyzed variety ($p < 0.05$; Tukey HSD test).

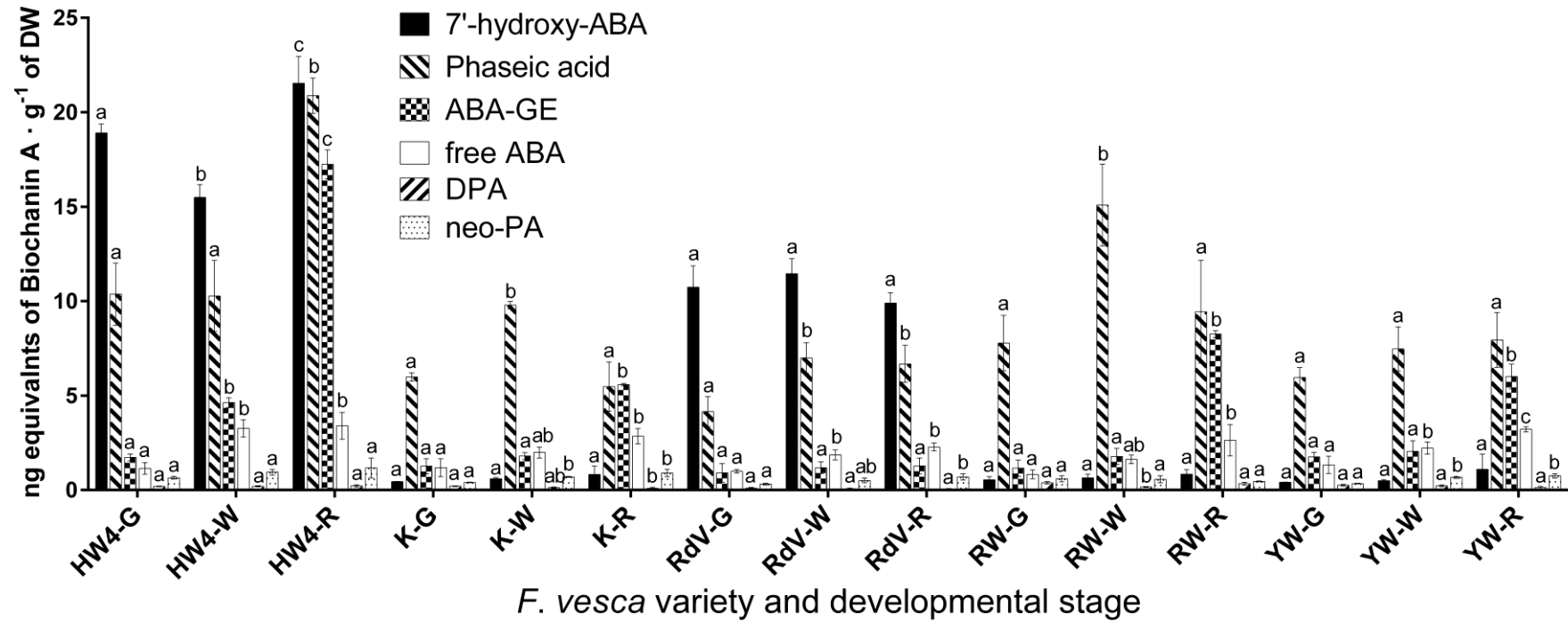


Figure 18. Quantification of ABA and its catabolites in achenes tissue from *F. vesca* varieties Hawaii4 (HW4), Korsika (K), Reine des Vallées (RdV), Red Wonder (RW) and Yellow Wonder (YW) at green (G), white (W) and ripe (R) developmental stages by LC-MS. Data indicate the mean \pm SD ($n = 3$). Different letters indicate a statistically significant difference in the amount of the corresponding ABA metabolite at different developmental stages within the same analyzed variety ($p < 0.05$; Tukey HSD test).

DPA exhibited a peak at the white developmental stage (Figure 17). This increase in DPA content was also clearly visible for *F. x ananassa* cv. Elsanta (Figure 19). In achenes, PA appears as the most important catabolite in varieties K, RW, and YW, and the second most important in HW4 and RdV after 7'-hydroxy-ABA. In K and RW achenes, PA peaked at the white developmental stage but increased throughout ripening in other varieties. The DPA content showed a decreasing trend in achenes of all varieties except for HW4, where it exhibited a slight increase during ripening.

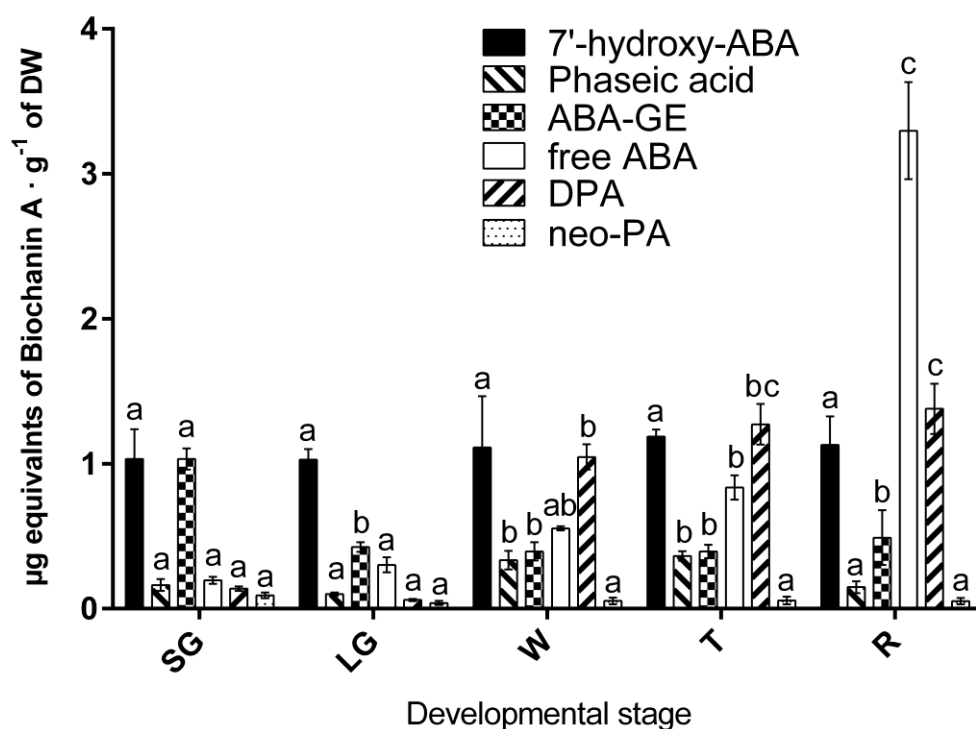


Figure 19. Quantification of ABA and its catabolites in *F. x ananassa* cv. Elsanta at small green (SG), large green (LG), white (W), turning (T) and ripe (R) developmental stages by LC-MS. Data indicate the mean \pm SD ($n = 3$). Different letters indicate a statistically significant difference in the amount of the corresponding ABA metabolite at different developmental stages within the same analyzed variety ($p < 0.05$; Tukey HSD test).

In the receptacle tissue of all analyzed samples, the content of neoPA was insignificant compared to the other ABA catabolites. In achenes, neoPA levels increased during ripening in all genotypes except for RW, where a decrease was observed; however, neoPA and DPA concentrations in achenes were relatively low compared with PA, 7'-hydroxy-ABA or ABA-GE levels (Figures 17 and 18).

Overall, the level of ABA metabolites was generally 100 times higher in the receptacle than in the achenes.

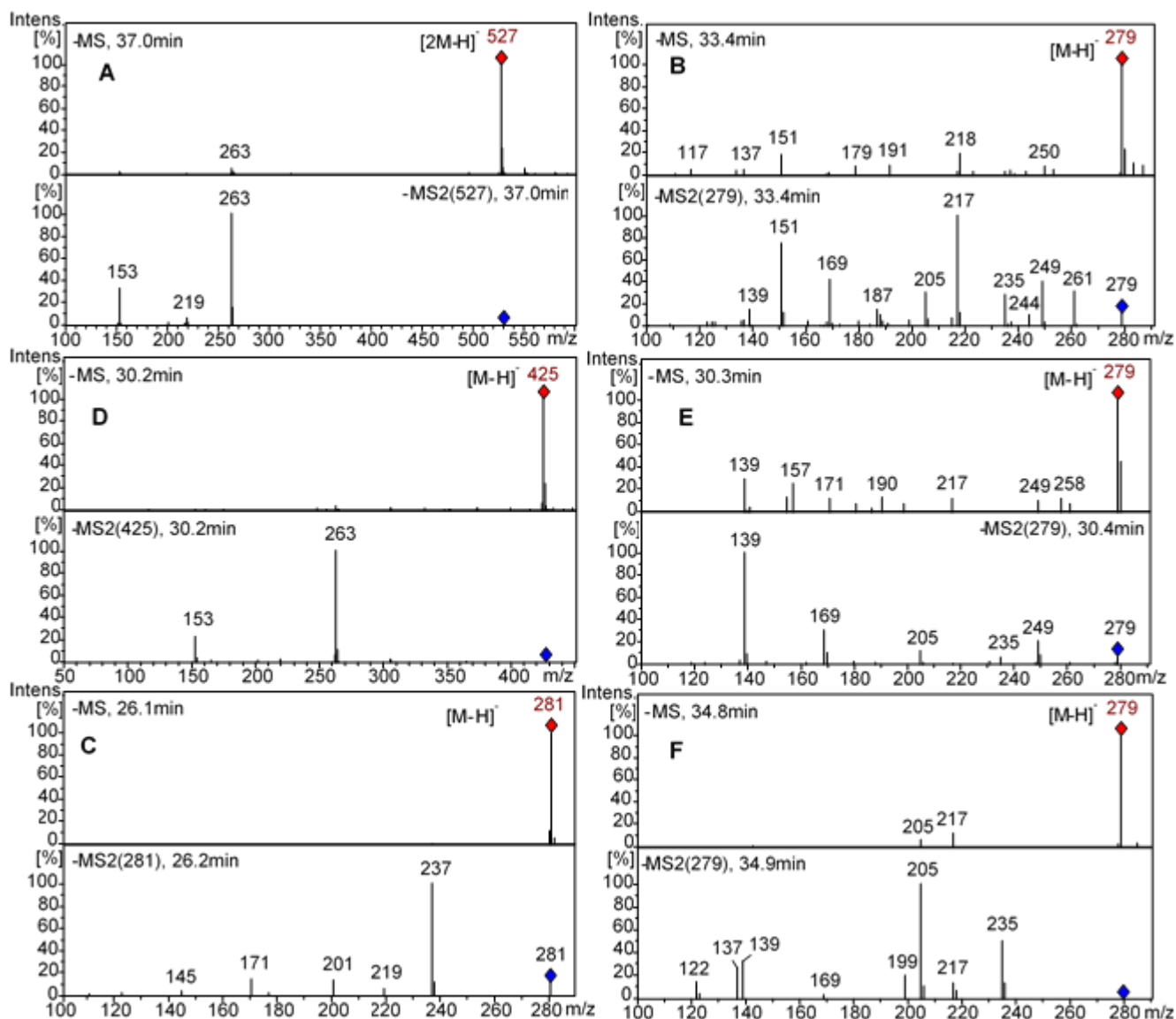


Figure 20. MS and MS2 spectra of (+)-ABA (**A**) and its metabolites ABA glucose ester (**B**), dihydrophaseic acid (**C**), 7'-hydroxy-ABA (**D**), PA (**E**) and neophaseic acid (**F**).

4.6 Analysis of ABA and ABA-GE content in agroinfiltrated fruits

The *in planta* function of *FvUGT71A49* was tested by *Agrobacterium*-mediated transient overexpression of *F. x ananassa* cv. Elsanta fruits. The expression level of *FvUGT71A49* was significantly increased in agroinfiltrated fruits injected with

the pBI121-2x35S:FvUGT71A49 vector compared with fruits infiltrated with the empty pBI121-2x35S vector (Figure 21A). At the same time, a significant decrease in free ABA was observed in fruits agroinfiltrated with pBI121-2x35S:FvUGT71A49 (Figure 21B), however no phenotypic changes were visible, and the content of ABA-GE PA, DPA, neoPA or 7'-OH-ABA was not altered compared with the control.

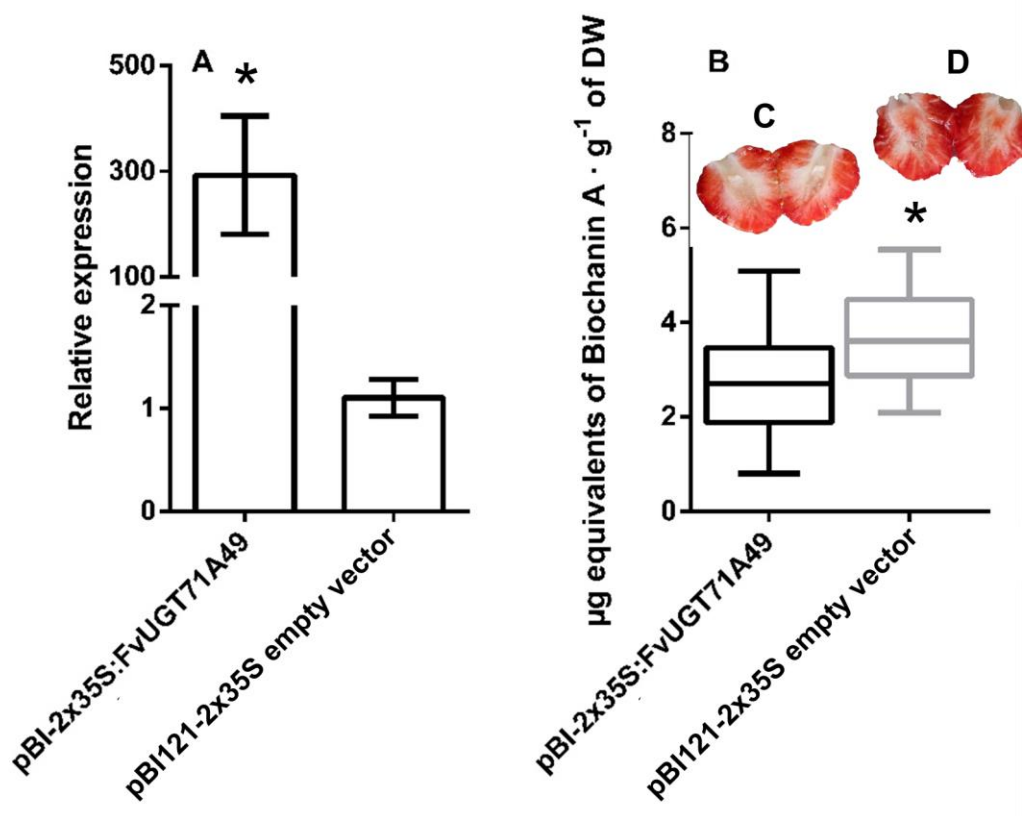


Figure 21. Changes in relative mRNA levels of FvUGT71A49 (A) and (+)-ABA content (B) in agroinfiltrated fruits. (C) and (D) represent the phenotypes of harvested fruits agroinfiltrated with pBI-2x35S:FvUGT71A49 and pBI121-2x35S empty vector, respectively. Data represent the means \pm SD of six (A) or eleven (B) biological replicates (different fruits from the same or different plants). Asterisks indicate a statistically significant difference ($p < 0.05$; Wilcoxon-Mann-Whitney U test).

4.7 Phylogenetic tree

FvUGT71A49 (with the highest specificity constant value) is grouped with previously isolated UGTs (FaUGT71A33, 34 and 35), which showed *in vitro* activity towards ABA but also a broad *in vitro* substrate tolerance (Song et al.

2015). All those UGTs form a clade with ABA-specific UGTs from *Arabidopsis* (UGT71B6, B7, and B8). In addition to those enzymes, a closely related group comprised of InGTase1 (Suzuki et al. 2007), FaUGT71W2 (Song et al. 2015), and AtUGT71C5 (Liu et al. 2015) is observed. FaUGT71W2 and AtUGT71C5 have been functionally *in planta* characterized, and particularly AtUGT71C5 exhibited a predominant role in the regulation of free ABA levels in *A. thaliana*, unlike the other UGTs from *A. thaliana* or *Fragaria* spp with activity towards ABA included in this group. On the other hand, FvUGT73AC3, which displayed a reduced *in vitro* activity towards ABA compared with FvUGT71A49, is clustered in the same group with ABA-specific UGTs from *Vigna angularis* (Willd.) Ohwi & Ohashi (VaQ8W3P8; Xu et al. 2002), *Pisum sativum* (L.) (PsABAUGT1; Zdunek-Zastocka and Grabowska 2019) and *Phaseolus vulgaris* (L.) (PvABA-GT; Palaniyandi et al. 2015).

Interestingly, this group of enzymes is closely related not only to GhUGT73C14, which showed *in planta* activity towards ABA (Gilbert et al. 2013) but also to AtUGT73C5, which catalyzes the glucosylation of brassinosteroids in *Arabidopsis* (Poppenberger et al. 2005). The P450s FaCYP707A4a and FaCYP707A1/3 are grouped with their orthologs from *F. vesca* (Figure 22; Liao et al. 2018) at the same time that they form a clade with the other enzymes from CYP707A subfamily. Among all the enzymes with activity towards ABA used for the construction of the phylogenetical tree, the activity of only a few of them (AtCYP707A1, 3 and the three P450s from *P. vulgaris*) has been studied by heterologous expression and enzyme-substrate assays. In this work, we provide the first direct evidence of the 8'-hydroxylase activity of P450s isolated from strawberry by *in vitro* and biotransformation assays.

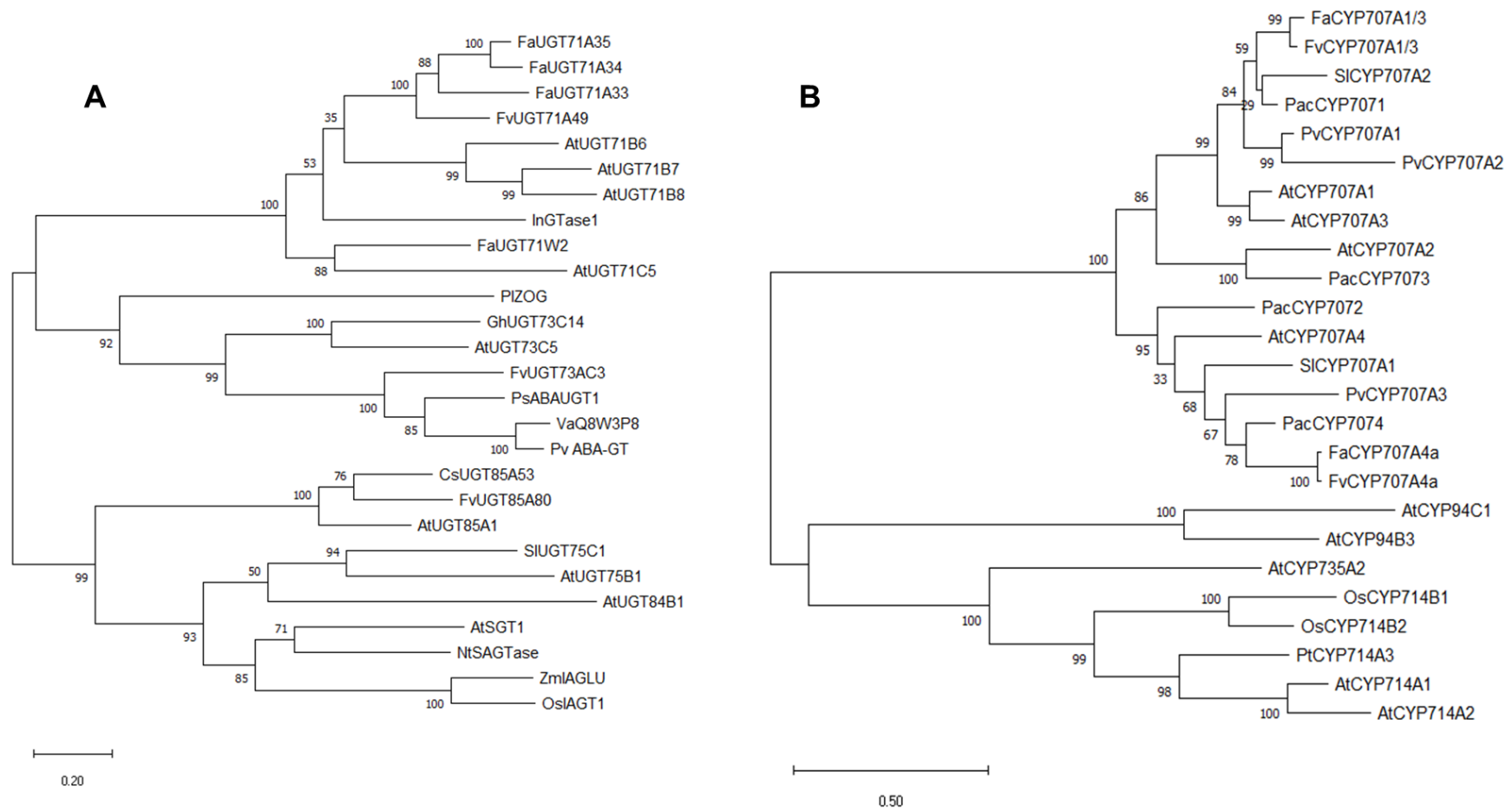


Figure 22. Phylogenetic trees using full-length aminoacidic sequences of biochemically characterized phytohormone-related UGTs (A) and P450 hydroxylases (B) (Table 28) constructed by Maximum Likelihood method of MEGA X software (Kumar et al. 2018). Next to the branches are shown the bootstrap values based on 1,000 replicates. Branch lengths are measured in number of substitutions per site.

4.8 Cytokinins quantification during strawberry ripening

Considering a previous report of very low CKs content in achene tissue (Gu et al. 2019) we quantified *trans*-zeatin (tZ), *trans*-zeatin-glucoside (tZG), and N₆-isopentenyladenine (iP) in receptacle tissue of the aforementioned *F. vesca* varieties and whole fruit of *F. x ananassa* at different developmental stages (Figures 23-25). For quantification, chemically synthesized references of tZ and iP were used (Figure 23; Supplementary Figure 1). In all samples of *F. vesca* as well as in *F. x ananassa* cv. Elsanta, the tZ content was lowest at the late-ripening stage. Similarly, the tZG content decreased during the ripening process in all analyzed samples except for *F. vesca* var. HW4 where tZG increased during strawberry ripening. Remarkably, in *F. vesca* the content of iP was between 5- and 40-times higher in ripe receptacle compared to the green receptacle. However, in *F. x ananassa* cv. Elsanta, the content of iP remained stable throughout the entire ripening process (Figures 24 and 25).

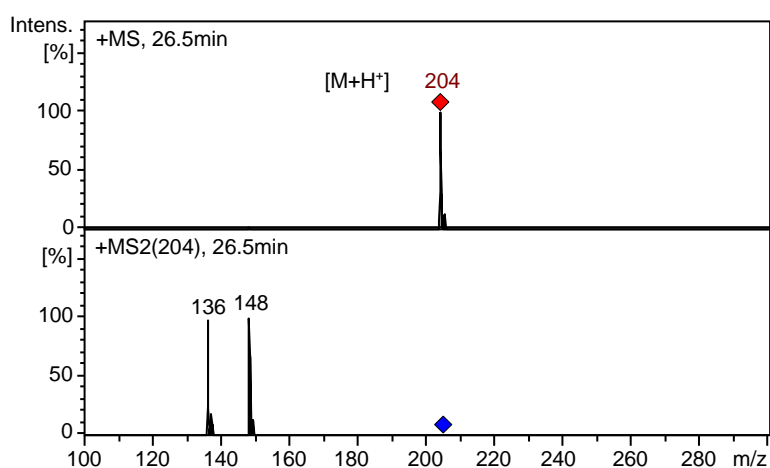


Figure 23. MS and MS2 spectra of N₆-isopentenyladenine (iP)

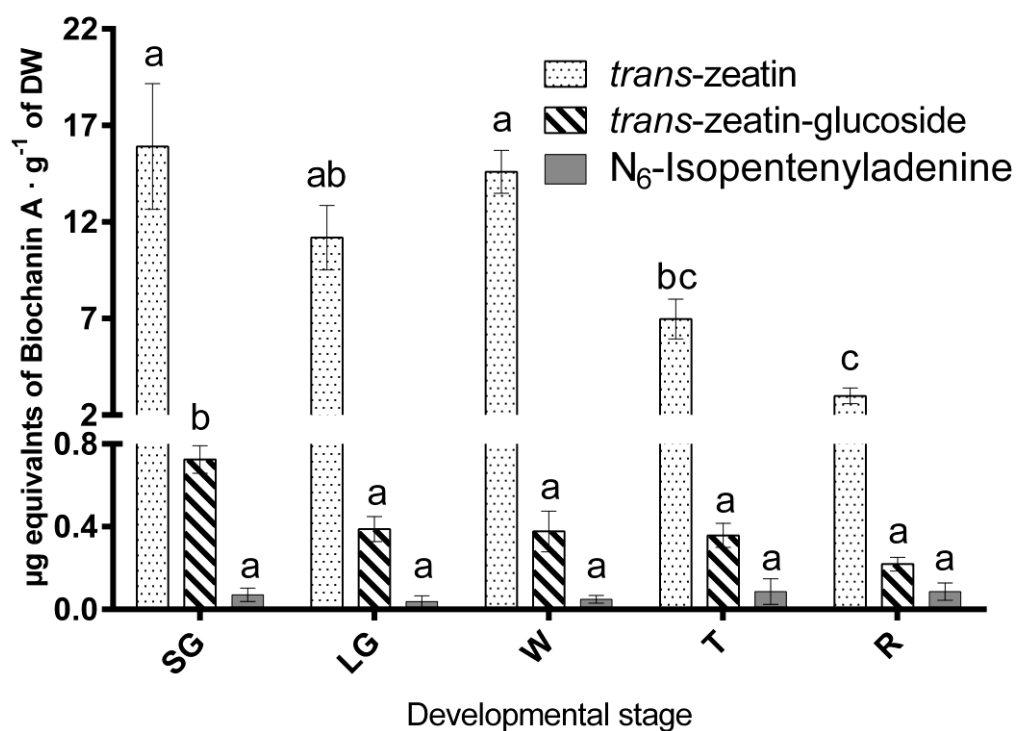


Figure 24. Quantification of tZ, tZG, and iP in *F. x ananassa* cv. Elsanta at small green (SG), large green (LG), white (W), turning (T) and ripe (R) developmental stages by LC-MS. Data indicate the mean \pm SD ($n = 3$). Different letters indicate a statistically significant difference in the amount of the corresponding ABA metabolite at different developmental stages within the same analyzed variety ($p < 0.05$; Tukey HSD test).

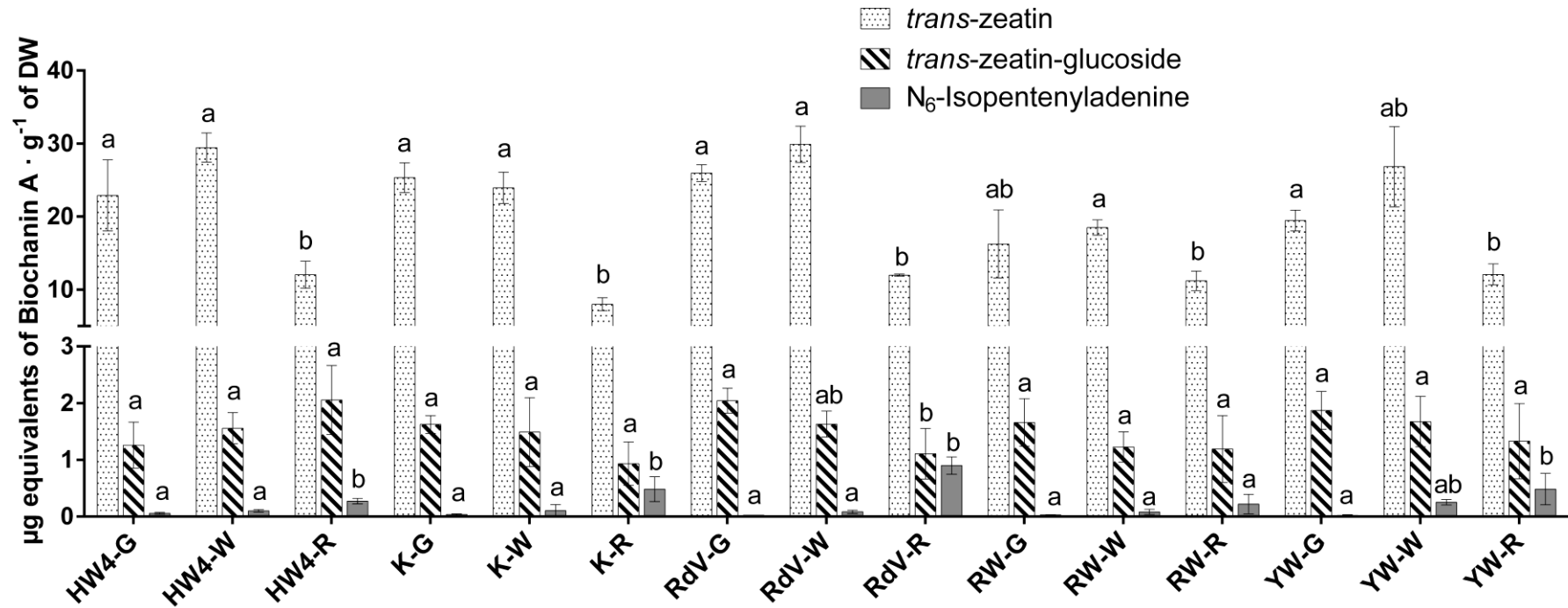


Figure 25. Quantification of tZ, tZG and iP in receptacle tissue from *F. vesca* varieties Hawaii4 (HW4), Korsika (K), Reine des Vallées (RdV), Red Wonder (RW) and Yellow Wonder (YW) at green (G), white (W) and ripe (R) developmental stages by LC-MS. Data indicate the mean \pm SD ($n = 3$). Different letters indicate a statistically significant difference in the amount of the corresponding ABA metabolite at different developmental stages within the same analyzed variety ($p < 0.05$; Tukey HSD test).

5. DISCUSSION

5.1 Enzymatic activity of isolated UGTs

The use of ABA analogs as a tool for the analysis of substrate tolerance and properties of ABA UGTs has already been demonstrated with enzymes from *Arabidopsis* (Priest et al. 2005). We studied the activity of UGT71A49 and UGT73AC3 from *Fragaria* towards (+)-ABA and some of its structural analogs (Figure 12). While *At*UGT71B6 from *Arabidopsis* showed higher catalytic activity towards PBI-82 (with an acetylene-containing side chain) and PBI-410 (a racemic mixture with an aromatic ring fused to the ABA ring) than (+)-ABA (Priest et al. 2005), UGT71A49 preferred PBI-410 over (+)-ABA, but not PBI-82 (Figure 13). Also, we found that no analog was a better substrate than (+)-ABA for UGT73AC3. Remarkably, PBI-524 (8'-acetylene-ABA) was not a substrate for *At*UGT71B6 (Priest et al. 2005), *Fv*UGT71A49, and *Fv*UGT73AC3. Moreover, no activity was found with PBI-425, which is also chemically modified at C-8' like PBI-524. Analogs with modifications at C-8' or 9' were also poor substrates for *At*UGT71B6 (Priest et al. 2005).

Due to the only partial characterization of most of the UGTs with activity towards ABA, only a little information is available on the kinetic properties of these enzymes. *At*UGT71B6 exhibited a K_m of 280 μM , while *Gh*UGT73C14 showed a K_m of 61 μM with ABA (Priest et al. 2005; Gilbert et al. 2013). The enzymes UGT73AC3, UGT71A33, and UGT71A35 examined in this work showed considerably higher K_m values, except for UGT71A49, which has a K_m value of 101 μM (Table 31). The K_{cat}/K_m values obtained for the analyzed enzymes (1 to 13 $\text{s}^{-1} \text{M}^{-1}$) were lower than those of *At*UGT71B6 (500 $\text{s}^{-1} \text{M}^{-1}$) and *Gh*UGT73C14 (115000 $\text{s}^{-1} \text{M}^{-1}$).

Regarding the activity of *Fv*UGT85A80, no previous reference of UGTs isolated from *Fragaria* species with activity towards *cis*- or *trans*-zeatin is available. Three enzymes from *Arabidopsis* with *in vivo* cytokinin activity have been reported. UGT85A1 shows *O*-glucosylation activity towards *trans*-zeatin and putative activity towards a broad range of cytokinins (Šmehilová et al. 2016), UGT76C1 and UGT76C2 also glucosylate a broad range of cytokinins but at the N-7 and N-9 positions (Hou et al. 2004). UGT76C1 and UGT76C2 showed K_m values of 240

μM and $220 \mu\text{M}$, respectively, when *trans*-zeatin was used as acceptor substrate (Hou et al. 2004), while the K_m value of the stereospecific cytokinin-O-glucosyltransferase ZOG1 from *P. lunatus* was determined with $50 \mu\text{M}$ (Mok et al. 2005). These values are lower than the Michaelis-Menten constant of $635 \mu\text{M}$ calculated for FvUGT85A80. However, since different buffers and analytical methods were used in the studies, the reference values can only serve as a rough guide.

5.2 Enzymatic activity of P450s enzymes

In vitro and biotransformation assays confirmed the regiospecific C-8' hydroxylation activity of FaCYP707A4a and FaCYP707A1/3 (Figure 14). Minor C-9' hydroxylase activity was demonstrated by *in vitro* assays for AtCYP707A1/2/3 and 4 (ABA 8'-hydroxylases; Okamoto et al. 2011). Overexpression and downregulation of FvCYP707A4a led to a decrease and increase of the ABA level, respectively in agroinfiltrated fruits (Liao et al. 2018), but the authors did not test if these changes were due to specific activity at C-8' of (+)-ABA and/or by unspecific activity at C-7' and/or C-9' (Liao et al. 2018). In *Xhantium sp.* and *Vicia faba* (-)-ABA is oxidized to 7'-hydroxy-ABA instead of PA (Zeevaart et al. 1990). We could not detect any other product such as 7'-hydroxy-ABA or neoPA acid after incubation of FaCYP707A4a and FaCYP707A1/3 with (+)-ABA. Besides, in the biotransformation system and the *in vitro* assays, we could detect only PA as a product (the cyclization product resulting from 8'-hydroxy-ABA), excluding any unspecific activity or interaction with yeast metabolism. On the other hand, we observed that after prolonged incubation periods, the transformation of ABA to ABA-GE or PA is about 2 times higher in samples supplemented with (+)-ABA than in samples with (\pm)-ABA (Figure 15 and 16). It appears that UGT71A49, FaCYP707A4a and FaCYP707A1/3 are not active towards (-)-ABA present in the mixture, but at the same time their activities are not inhibited by the presence of (-)-ABA in the reaction.

At high substrate concentration at the beginning of the enzymatic reaction, the enzymes (P450s and UGTs) probably work at maximum velocity. Although there is twice as much productive substrate available in (+)-ABA, the same amount of

product is formed as with racemic ABA. Only when (+)-ABA is limited in the racemic mixture formation of product slows down for racemic ABA but continues for (+)-ABA because enough productive substrate is still available. Therefore, the results support the hypothesis that both P450 and UGT enzymes prefer (+)-ABA over (-)-ABA as in long-term experiments (+)-ABA produced twice as much product than (-)-ABA (Figures 15 and 16). However, it is not possible to calculate exact ratios due to the above-mentioned reason.

5.3 Dynamic of ABA and ABA metabolites during strawberry ripening

Our results show that the (+)-ABA and ABA-GE content increases during fruit ripening in all analyzed *F. vesca* varieties both in the receptacle and in achenes. This increase confirms data obtained with *F. vesca* var. Rügen (Gu et al. 2019). The concentration of PA reached a peak in the white development stage, which was also observed by Gu et al. 2019. This pattern correlates with the expression level of *CYP707A4a*, as this gene is mainly expressed at early and intermediate developmental stages of fruit development in both *F. vesca* and *F. x ananassa* (Figure 26; Sánchez-Sevilla et al. 2017) and seems to be the most important gene for 8'-hydroxylation of ABA in the strawberry fruit (Liao et al. 2018).

All investigated UGTs with activity towards ABA showed increasing transcript levels during ripening of *F. vesca* (Figure 26) and *F. x ananassa* cv Camarosa (Sánchez-Sevilla et al. 2017). While *FvUGT71A49* is mainly expressed in achenes tissue, *FvUGT73AC3* is highly expressed in receptacle tissue (Figure 26). The expression pattern correlates with the increase in ABA-GE observed in *F. vesca* samples; however, there is no relation with the decrease detected in *F. x ananassa* cv Elsanta.

On the other hand, the β -glucosidases with activity towards ABA-GE identified in *F. x ananassa* cv Camarosa (Zhang et al. 2014) and cv Albion (Li et al. 2013) also exhibited increasing transcript levels during strawberry fruit ripening in our transcriptomic data sets (Härtl et al. 2017) and of others (Sánchez-Sevilla et al. 2017). The expression pattern correlates with the ABA-GE decrease in *F. x ananassa* cv. Elsanta, but not in the investigated *F. vesca* varieties.

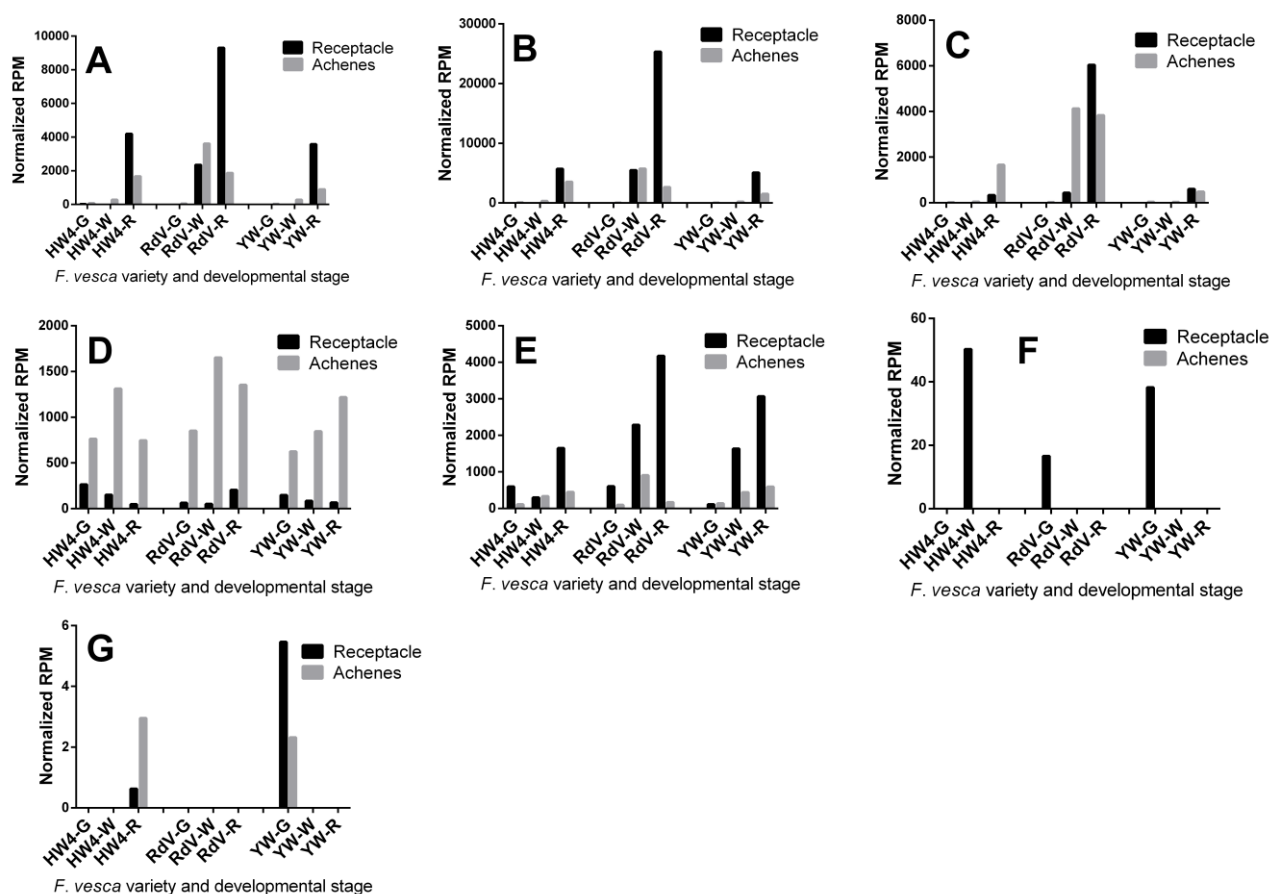


Figure 26. Expression profiles of the genes *FvUGT71A33* (A), *FvUGT71A34* (B), *FvUGT71A35* (C), *FvUGT71A49* (D), *FvUGT73AC3* (E), *FvCYP707A4a* (F) and *FvCYP707A1/3* (G) in receptacle tissue from *F. vesca* varieties Hawaii4 (HW4), Reine des Vallees (RdV) and Yellow Wonder (YW) at green (G), white (W) and ripe (R) developmental stages obtained from RNA-Seq data (Härtl et al., 2017).

The presence of ABA-GE, PA, and DPA in *F. x ananassa* cv. Camarosa has been quantified only at the ripe developmental stage (Perin et al. 2018). The amount of PA+DPA was between 6 to 11 times higher than ABA-GE at this developmental stage, depending on the extraction method. We also observed that the oxidative pathway was preferred over the conjugation pathway in fruits of *F. x ananassa* cv. Elsanta. In the absence of previous reports on the content of neoPA or 7'-OH-ABA in *F. x ananassa* fruits, this study provides the first report on the dynamics of all known ABA metabolites throughout the ripening process in *F. x ananassa* species.

The content of the metabolite 7'-OH-ABA showed several differences between tissues and cultivars. In cultivars K, RW, and YW, it seems to be a minor metabolite in receptacle tissue, as was already shown (Gu et al. 2019). In contrast, we found that in cultivars HW4 and RdV as well as in *F. x ananassa*, 7'-OH-ABA is often more abundant than the other metabolites. Similarly, very low levels of 7'-OH-ABA were reported in achenes, compared to ABA-GE and DPA (Gu et al. 2019). We found that 7'-OH-ABA is the most important ABA metabolite along with PA in achenes of varieties HW4 and RdV, and only extremely low levels of DPA were detected in all achenes samples.

Although it has been reported that PA and DPA are hormonally inactive (Cutler and Krochko 1999), there is clear evidence that ABA catabolites from the oxidative pathway may play a physiological role. In half seeds of *Hordeum vulgare* (L.) 7'-OH-ABA repressed gibberellic acid-induced α -amylase activity (Hill et al. 1995). Moreover, 8'-hydroxy-ABA was as effective as ABA in the induction of lipid modification genes in microspore-derived embryos (MDE) of *Brassica napus* (L.) (Zou et al. 1995) and 7'-, 8'- and 9'-hydroxy ABA have similar effects to ABA inducing expression of oleosin and fatty acid elongase genes and increasing the accumulation of triacylglycerols and very long chain fatty acids in MDE of *Brassica napus* (Jadhav et al. 2008). Results in Arabidopsis show that PA possesses ABA-like hormonal activity since it can be recognized by a subset of the PYR/PYL/RCAR family of ABA receptors (Weng et al. (2016); consequently, it is conceivable that the other ABA catabolites in plants may show similar properties. A homolog to the Arabidopsis ABA receptor PYR, named *FaPYR1* has been described in *F. x ananassa* (Chai et al. 2011). It is, therefore, possible that PA also plays a physiological role in strawberry fruits.

Our results support the thesis that the receptacle is the main tissue for ABA biosynthesis but also for ABA metabolism of the strawberry fruit (Gu et al. 2019). On the other hand, we propose that both, an increase in ABA biosynthesis and a decrease in ABA oxidation in ripening fruits (Gu et al. 2019), cause the remarkable increase of the ABA content in receptacles during ripening. In some varieties, the decrease in the PA content correlated with an increase in the DPA content, a product derived from PA by C-8' hydroxylation; however, exceptions

were found, e.g., in RdV where the PA content increased during ripening along with a stable high content of 7'-OH-ABA.

In achenes of all *F. vesca* samples, the hydroxylation seems to be the preferred metabolism pathway throughout the whole ripening process, unlike in the receptacle tissue, where ABA-GE is the metabolite with the most dramatic change during the transition from green to the ripe developmental stage. It appears that *Fragaria spp.* prefer a certain metabolism pathway in a tissue-, variety- or species-depending manner.

5.4 Transient overexpression of UGT71A49 in strawberry fruit

Considering the decreasing pattern of ABA-GE in *F. x ananassa* cv. Elsanta, we decided to overexpress *FvUGT71A49*. Although significant changes in ABA content between fruits agroinfiltrated with pBI-2x35S:*FvUGT71A49* and empty pBI121-2x35S vector was detected and was confirmed by untargeted analysis, no changes in ABA-GE content was detected. Similarly, when the gene *FaUGT71W2* (also with activity towards ABA) was down-regulated by *Agrobacterium*-mediated transient gene silencing, only a slight decrease in ABA-GE content was observed, but ABA was not measured (Song et al. 2015). Thus, it appears that the redundancy of the ABA UGTs compensates for the down-, and up-regulation of individual UGTs.

5.5 CKs content and metabolism during strawberry ripening

Kang et al. (2013) provided first insights of a putative role of CKs in strawberry ripening. These authors compared transcriptomes of post- and pre-fertilized *F. vesca* var. Rügen fruits, finding 17 genes related to cytokinin biosynthesis, signaling, and degradation. Among them, *FvLOG6*, *FvLOG9*, and *FvIPT5* (all of them involved in biosynthesis) were upregulated in the cortex and/or pith tissue, suggesting that cytokinins may play a role at the early developmental stages of the strawberry fruit.

Recently, Gu et al. (2019) quantified cytokinins during fruit ripening of *F. vesca* var. Rügen and performed transcriptomic analyses focusing on genes related to CK biosynthesis and degradation. Of the bioactive free-base CKs, only tZ and iP

were found in the receptacle tissue. Specifically, tZ was detected at all developmental stages and showed slightly lower levels in the ripe fruit, while a remarkable 60-fold increase in the iP level from intermediate to red developmental stage was observed. The results showed a conserved pattern of the tZ content in receptacle tissue during ripening in *F. vesca* and *F. x ananassa*, which was characterized by a peak at the intermediate developmental stage (Figures 24 and 25). Moreover, we confirmed the increase in iP content reported by Gu et al. (2019), which, however, was exclusively observed in *F. vesca* varieties, while the iP content remained stable during the ripening of *F. x ananassa* cv. Elsanta.

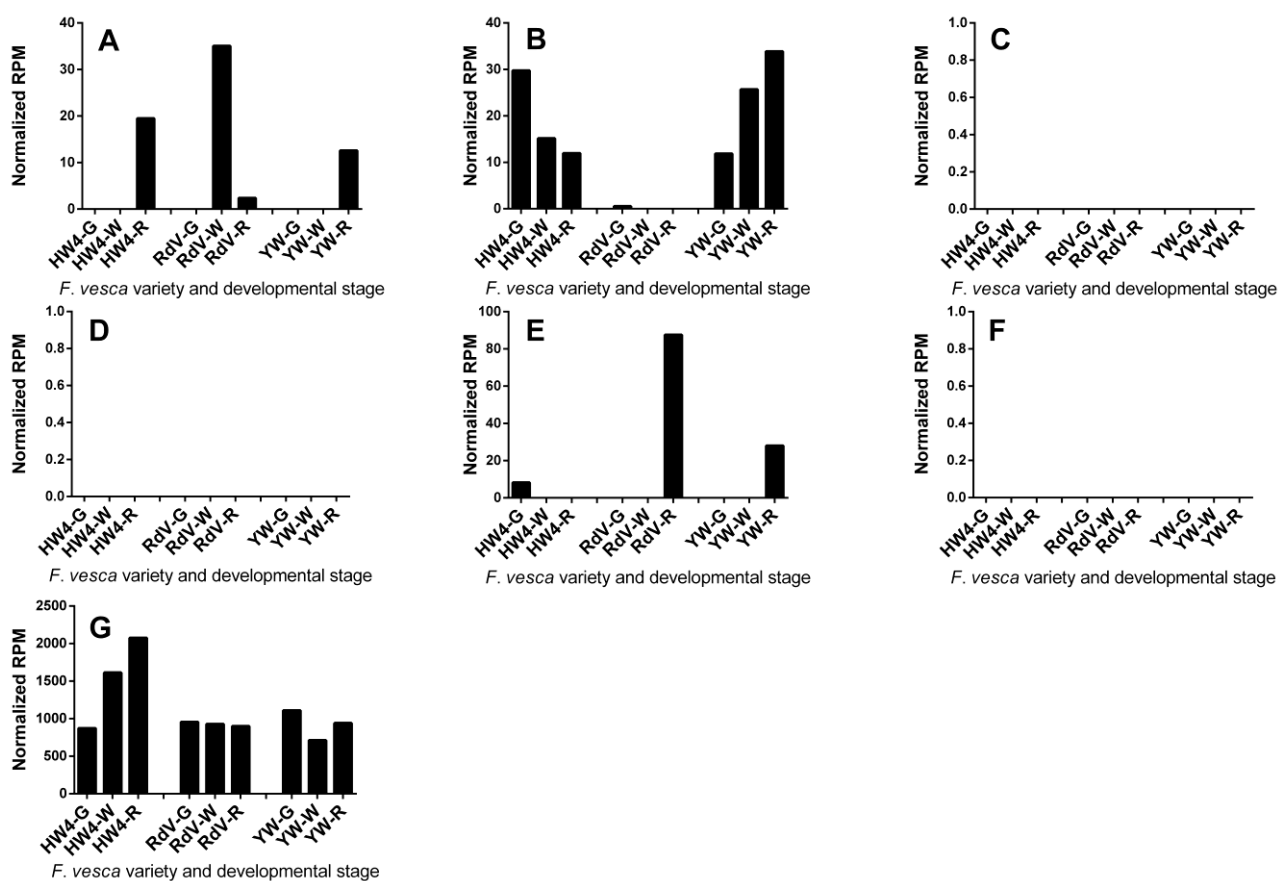


Figure 27. Expression profiles of the *IPT* genes *FvIPT1* (A), *FvIPT2* (B), *FvIPT3* (C), *FvIPT4* (D), *FvIPT5* (E), *FvIPT6* (F) and *FvIPT7* (G) in receptacle tissue from *F. vesca* varieties Hawaii4 (HW4), Reine des Vallées (RdV) and Yellow Wonder (YW) at green (G), white (W) and ripe (R) developmental stages obtained from RNA-Seq data (Härtl et al., 2017).

Eight *FvCKX* genes, 7 *FvIPT*, and 9 *FvLOG* genes were found in the *F. vesca* genome by bioinformatic analyses (Jiang et al 2016; Mi et al 2017). The

expression patterns of genes putatively involved in CK biosynthesis were analyzed in different organs and tissues of *F. vesca* var. Hawaii 4 (Jiang et al. 2016; Mi et al. 2017). *FvCKX1*, *FvCKX4*, *FvCKX6*, and *FvCKX8*, *FvLOG6*, and *FvLOG9* were strongly expressed in the receptacle tissue compared to other organs. However, the expression levels of these genes were not studied at intermediate or ripe fruit developmental stages. These results are consistent with our transcriptomic data, where mentioned genes showed high expression levels in the receptacle tissue (Figures 27, 28, and 29). Gu et al. (2019) provided transcriptomic data of genes related to the biosynthesis and metabolism of CKs during the ripening of *F. vesca* var. Rügen. *FvIPT7* showed the highest expression level of all IPTs in the receptacle tissue, which increased during the ripening, like the transcript levels of most *IPT* genes. Our transcriptomic data and the transcriptomic data for *F. x ananassa* provided by Sánchez-Sevilla et al. (2017) confirm the high abundance of *FvIPT7* transcripts; however, the expression pattern is variety-dependent (Figure 27).

Similar to the *IPT* genes, the *LOG* genes showed varying transcript levels and patterns. *LOG9* exhibited the highest expression levels, followed by *LOG6* and *LOG8*. These genes were expressed at all developmental stages in all *F. vesca* varieties studied and the variety analyzed by Gu et al. (2019). *LOG1* displayed a conserved decreasing pattern in our transcriptomic data (Figure 28), in the data reported by Gu et al. (2019), and in the data published by Sánchez-Sevilla et al. (2017). The contrasting expression patterns of the *LOG* genes could be involved in the opposite changes of the tZ and iP content during strawberry ripening (Figures 24 and 25).

In contrast to the increased expression pattern reported for *CKX6* by Gu et al. (2019), our transcriptomic data (Figure 29) and the data reported by Sánchez-Sevilla et al. (2017) show a decrease in the transcript abundance of *CKX6* at the intermediate developmental stage. This decrease could be related to the observed peak of the tZ content at the intermediate developmental stage of the analyzed fruits (Figures 24 and 25).

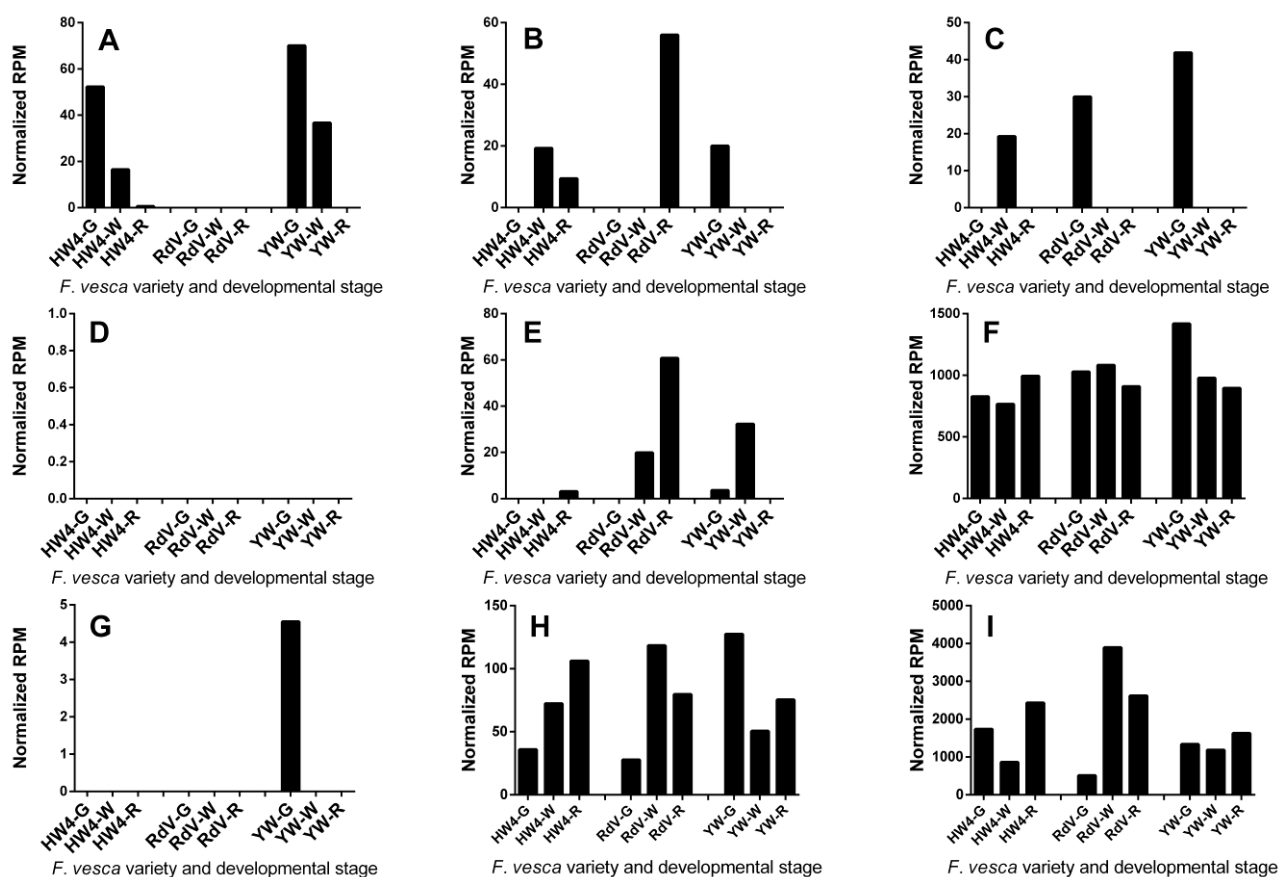


Figure 28. Expression profiles of LOG genes *FvLOG1* (A), *FvLOG2* (B), *FvLOG3* (C), *FvLOG4* (D), *FvLOG5* (E), *FvLOG6* (F), *FvLOG7* (G), *FvLOG8* (H) and *FvLOG9* (I) in receptacle tissue from *F. vesca* varieties Hawaii4 (HW4), Reine des Vallees (RdV) and Yellow Wonder (YW) at green (G), white (W) and ripe (R) developmental stages obtained from RNA-Seq data (Härtl et al., 2017).

Interestingly, Jiang et al. (2016) and Mi et al. (2017) noticed that in strawberry leaves, almost all *FvCKX* genes were upregulated after ABA application, while *FvIPT* and *FvLOG* were downregulated by the exogenous ABA application. Similarly, the expression of *CYP735A1* and *CYP735A2*, two genes crucial for the biosynthesis of tZ were downregulated by auxin and ABA in roots of *Arabidopsis* (Takei et al. 2004), and *CKX* genes were upregulated by ABA in maize (Brugiére et al. 2003).

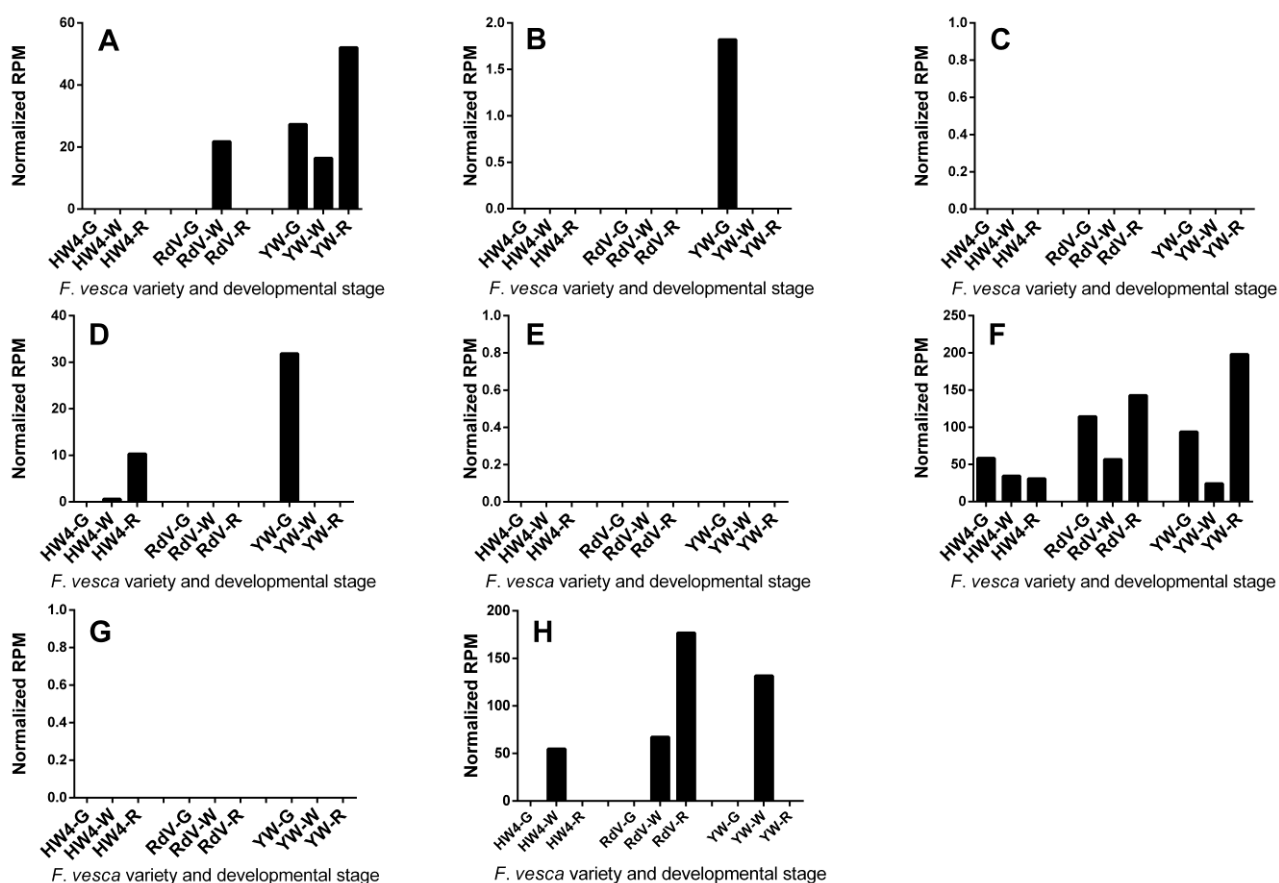


Figure 29. Expression profiles of CKX genes *FvCKX1* (A), *FvCKX2* (B), *FvCKX3* (C), *FvCKX4* (D), *FvCKX5* (E), *FvCKX6* (F), *FvCKX7* (G) and *FvCKX8* (H) in receptacle tissue from *F. vesca* varieties Hawaii4 (HW4), Reine des Vallees (RdV) and Yellow Wonder (YW) at green (G), white (W) and ripe (R) developmental stages obtained from RNA-Seq data (Härtl et al., 2017).

Given the low ABA and high *trans*-zeatin levels found in green fruits, the increase in ABA during ripening, and the previously reported transcriptomic data, we propose a likely antagonistic relationship between *trans*-zeatin and ABA during strawberry fruit ripening. Key genes involved in the biosynthesis and metabolism of CKs mediate this relationship.

Finally, we could observe that the tZG content decreased during the ripening in all strawberry genotypes (except for HW4). However, changes in tZG were not as significant as changes in tZ or iP content. The changes in tZG content do not correlate with changes in the expression levels of *FvUGT85A80* (Figure 30),

suggesting that similar to the ABA-GE content, its level is regulated by the coordinated action of a group of UGTs with redundant function.

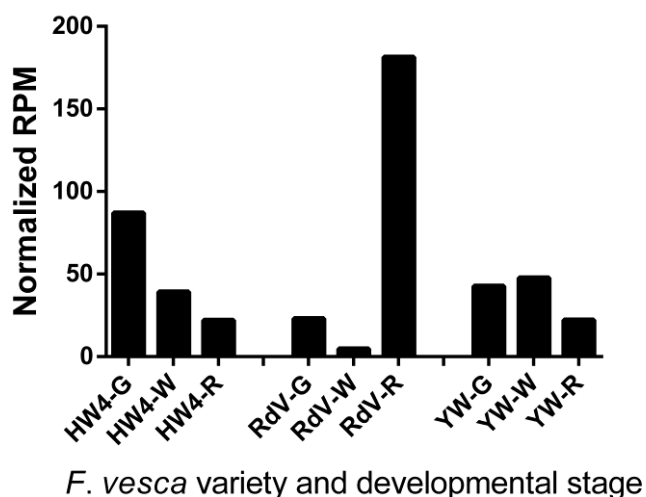


Figure 30. Expression profiles of *FvUGT85A80* in receptacle tissue from *F. vesca* varieties Hawaii4 (HW4), Reine des Vallees (RdV) and Yellow Wonder (YW) at green (G), white (W) and ripe (R) developmental stages obtained from RNA-Seq data (Härtl et al., 2017).

5.6 Phylogenetic tree

Currently, the UGTs are named by UGT Nomenclature Committee. They are named as follows: the prefix UGT, an Arabic number which corresponds to the family (in the case of plants between 71 and 100), a letter to represent the subfamily, and finally an Arabic number for the individual gene (Mackenzie et al. 1997). UGTs show >40% or >60% amino acid sequence identity within a family or a sub-family, respectively (Mackenzie et al. 1997; Bock 2016). The division of UGTs families is clearly visible in the phylogenetic tree (Figure 22A). In general, lower bootstrap values are observed just in the division of subclades within a UGT family, as in the case of family 71 and its subdivision into families A and B, mainly represented here by members from *Fragaria* and *Arabidopsis*. However, the separation in different UGTs families is supported by strong bootstrap values. It is interesting to note that UGTs able to disturb either ABA or ABA-GE homeostasis can belong to different UGTs families (as in the case of families 71

and 75 from Arabidopsis) or even subfamilies (71B and 71C from Arabidopsis or 71A and 71W from Fragaria), contributing to regulating the final pools of ABA and ABA-GE in plants. Furthermore, as alternative to the current classification of UGTs, Yonekura-Sakakibara and Hanada (2011) proposed a classification into 24 orthologous groups, using UGTs families from *A. thaliana*, *Arabidopsis lyrata* (L.) O'Kane & Al-Shehbaz, *Populus trichocarpa* Torr. & Gray ex Hooker, *Oryza sativa* L., *Selaginella moellendorffii* Hieron and *Physcomitrella patens* (Hedw.) Bruch & Schimp. They defined an orthologous group (OG) as a group containing genes that had diverged in each species from those of their common ancestor. This classification may explain for example, the clustering of UGTs from families 75 and 84, since they were grouped together in the orthologous OG14 (Yonekura-Sakakibara and Hanada 2011). In addition, according to this classification, the family 71 and 73 belong to the OG7 and OG1, respectively. Recently, Jing et al. (2020) reported that UGT85A53 from *Camellia sinensis* is involved in flowering via ABA glucosylation. In our tree, CsUGT85A53 is clustered with other members of UGT85 family, which showed activity mainly toward zeatin (Supplementary Figure 1; Hou et al. 2004). At the same time, according to the classification of Yonekura-Sakakibara and Hanada (2011), the UGT85 family belongs to the OG2 along with the UGT76 family, which also include members with activity towards cytokinins (Wang et al. 2011). This data would support the hypothesis that UGTs belonging to different families or groups according to different systems of classification are involved in the regulation of ABA levels in plants.

Like the UGTs, the P450s are also named with a family number and subfamily letter but using the same number for orthologs in different species and unique numbers for paralogs in the same species (Xu et al. 2015). Moreover, if the aminoacidic sequence identity is higher than 40%, the enzymes are grouped in the same family, while if the identity is higher than 55%, they are classified in the same subfamily (Xu et al. 2015). Unlike the UGTs, it seems that the modification of ABA is restricted to just members from subfamily CYP707A, which formed a clade in our phylogenetic tree (Figure 22B).

6. CONCLUSION

Unlike the ABA biosynthesis, a genotype-specific ABA metabolism was detected during strawberry ripening. However, it was also possible to identify conserved patterns for the ABA-GE, PA, and DPA content. Most of the variability in ABA metabolism is due to the hydroxylation pathways of ABA, whereby neoPA seems to be the least important metabolite of ABA in strawberry fruit. On the other hand, a conserved pattern of tZ content was observed in all samples analyzed, but a contrasting pattern between *F. vesca* and *F. x ananassa* fruits was observed for the iP content, similarly to the results observed for the ABA-GE content. Moreover, no significant changes were detected in the content of tZG during ripening, indicating a minor role in regulating the active pool of CKs in strawberry fruit. The variability of ABA metabolism and CKs content does not correlated with white or red fruit coloration and may be determined at species- or even at cultivar-level. Further studies involving more strawberry varieties, in particular, *F. x ananassa* may help to confirm the existence of conserved patterns in the metabolism of ABA and CKs during strawberry fruit ripening and contribute to globally understand the relationship between hormonal changes and the ripening process.

7. REFERENCES

- Bajguz A, Piotrowska A (2009) Conjugates of auxin and cytokinin. *Phytochemistry* 70(8): 957-969.
- Bastías A, López-Climent M, Valcárcel M, Rosello S, Gómez-Cadenas A, Casaretto JA (2011) Modulation of organic acids and sugar content in tomato fruits by an abscisic acid-regulated transcription factor. *Physiologia Plantarum* 141(3): 215-226.
- Bock KW (2016) The UDP-glycosyltransferase (UGT) superfamily expressed in humans, insects and plants: Animal-plant arms-race and co-evolution. *Biochemical Pharmacology* 99: 11–17.
- Bray EA, Zeevaart JA (1985) The compartmentation of abscisic acid and β -D-glucopyranosyl abscisate in mesophyll cells. *Plant Physiology* 79(3): 719-722.
- Brugiere N, Jiao S, Hantke S, Zinselmeier C, Roessler JA, Niu X, Jones RJ, Habben JE (2003) Cytokinin oxidase gene expression in maize is localized to the vasculature, and is induced by cytokinins, abscisic acid, and abiotic stress. *Plant Physiology* 132:1228-40.
- Brzobohaty B, Moore I, Kristoffersen P, Bako L, Campos N, Schell J, Palme K. 1993. Release of active cytokinin by a beta-glucosidase localized to the maize root meristem. *Science* 262:1051–54.
- Chai YM, Jia HF, Li CL, Dong QH, Shen YY (2011) FaPYR1 is involved in strawberry fruit ripening. *Journal of Experimental Botany* 62(14): 5079-5089.
- Cherian S, Figueroa CR, Nair H (2014) 'Movers and shakers' in the regulation of fruit ripening: a cross-dissection of climacteric versus non-climacteric fruit. *Journal of Experimental Botany* 65(17): 4705-4722.
- Chervin C, Tira-umphon A, Terrier N, Zouine M, Severac D, Roustan JP (2008) Stimulation of the grape berry expansion by ethylene and effects on related gene transcripts, over the ripening phase. *Physiologia Plantarum* 134(3): 534-546.
- Cutler AJ, Krochko JE (1999) Formation and breakdown of ABA. *Trends in Plant Science* 4(12): 472-478.
- Darrow GM (1966) *The strawberry. History, Breeding and Physiology*. Holt, Rinehart and Winston, New York, 1996.
- Davis TM, Denoyes-Rothan B, Lerceteau-Köhler E (2007) Strawberry. In *Fruits and nuts* (pp. 189-205). Edited by Kole C. Springer, Heidelberg, 2007.
- del Refugio Ramos M, Jerz G, Villanueva S, López-Dellamary F, Waibel R, Winterhalter P (2004) Two glucosylated abscisic acid derivatives from avocado

seeds (*Persea americana* Mill. Lauraceae cv. Hass). *Phytochemistry* 65(7): 955-962.

Dietz KJ, Sauter A, Wichert K, Messdaghi D, Hartung W (2000) Extracellular β -glucosidase activity in barley involved in the hydrolysis of ABA glucose conjugate in leaves. *Journal of Experimental Botany* 51(346): 937-944.

Dong T, Xu ZY, Park Y, Kim DH, Lee Y, Hwang I (2014) Abscisic acid uridine diphosphate glucosyltransferases play a crucial role in abscisic acid homeostasis in *Arabidopsis*. *Plant Physiology* 165(1): 277-289.

Dunn B, Wobbe CR (1993) Preparation of protein extracts from yeast. In *Current Protocols in Molecular Biology* 23(1): 13.13. Edited by Chanda VB. John Wiley & Sons, New York, 2001

Endo A, Okamoto M, Koshiba T (2014) ABA biosynthetic and catabolic pathways. In *Abscisic acid: Metabolism, transport and signaling* (pp. 21-45). Springer, Dordrecht.

Fait A, Hanhineva K, Beleggia R, Dai N, Rogachev I, Nikiforova VJ, Fernie AR, Aharoni A (2008) Reconfiguration of the achene and receptacle metabolic networks during strawberry fruit development. *Plant Physiology* 148(2): 730-750.

Falk A, Rask L (1995) Expression of a zeatin-o-glucoside-degrading β -glucosidase in *Brassica napus*. *Plant Physiology* 108(4): 1369-1377.

FAOSTAT (2019) Accessed in February 2020
<http://www.fao.org/faostat/en/#search/strawberries>

Finkelstein R (2013) Abscisic acid synthesis and response. *The Arabidopsis book*. American Society of Plant Biologists 11.

Galuszka P, Frébort I, Šebela M, Sauer P, Jacobsen S, Peč P (2001) Cytokinin oxidase or dehydrogenase? Mechanism of cytokinin degradation in cereals. *European Journal of Biochemistry* 268(2): 450-461.

Galuszka P, Popelková H, Werner T, Frébortová J, Pospíšilová H, Mik V, Köllmeier I, Schmülling T, Frébort, I. (2007) Biochemical characterization of cytokinin oxidases/dehydrogenases from *Arabidopsis thaliana* expressed in *Nicotiana tabacum* L. *Journal of Plant Growth Regulation*, 26(3), 255-267.

Garrido-Bigotes A, Figueroa PM, Figueroa CR (2018) Jasmonate metabolism and its relationship with abscisic acid during strawberry fruit development and ripening. *Journal of Plant Growth Regulation* 37(1): 101-113.

Gasic K, Hernandez A, Korban SS (2004) RNA extraction from different apple tissues rich in polyphenols and polysaccharides for cDNA library construction. *Plant Molecular Biology Reporter* 22(4): 437-438.

Gilbert, MK, Bland JM, Shockey JM, Cao H, Hinchliffe DJ, Fang DD, Naoumkina M (2013) A transcript profiling approach reveals an abscisic acid-specific glycosyltransferase (UGT73C14) induced in developing fiber of Ligon lintless-2 mutant of cotton (*Gossypium hirsutum* L.). *PloS one* 8(9): e75268.

Giovannoni JJ (2001) Molecular biology of fruit maturation and ripening. *Annual Review of Plant Physiology and Plant Molecular Biology* 52: 725-749.

Giovannoni JJ (2004) Genetic regulation of fruit development and ripening. *The Plant Cell*, 16: S170-S180.

Gu T, Jia S, Huang X, Wang L, Fu W, Huo G, Gan L, Ding J, Li Y (2019) Transcriptome and hormone analyses provide insights into hormonal regulation in strawberry ripening. *Planta*: 1-18.

Hall TA (1999) BioEdit: a user-friendly biological sequence alignment editor and analysis program for Windows 95/98/NT. *Nucleic Acids Symposium Series* 41: 95-98.

Han SY, Kitahata N, Sekimata K, Saito T, Kobayashi M, Nakashima K, Yamaguchi-Shinozaki K, Shinozaki K, Yoshida S, Asami T (2004) A novel inhibitor of 9-cis-epoxycarotenoid dioxygenase in abscisic acid biosynthesis in higher plants. *Plant Physiology* 135(3): 1574-1582.

Hancock JF, Sjulín TM, Lobos GA (2008) Strawberries. In *Temperate fruit crop breeding* (pp. 393-437). Edited by Hancock JF. Springer, Dordrecht, 2008.

Hart A (2001) Mann-Whitney test is not just a test of medians: differences in spread can be important. *BMJ*, 323(7309): 391-393.

Härtl K, Denton A, Franz-Oberdorf K, Hoffmann T, Spornraft M, Usadel B, Schwab W (2017) Early metabolic and transcriptional variations in fruit of natural white-fruited *Fragaria vesca* genotypes. *Scientific Reports* 7:45113.

Hill RD, Liu JH, Durnin D, Lamb N, Shaw A, Abrams SR (1995) Abscisic acid structure-activity relationships in barley aleurone layers and protoplasts (biological activity of optically active, oxygenated abscisic acid analogs). *Plant Physiology* 108(2): 573-579.

Hirai N, Yoshida R, Todoroki Y, Ohigashi H (2000) Biosynthesis of abscisic acid by the non-mevalonate pathway in plants, and by the mevalonate pathway in fungi. *Bioscience, Biotechnology, and Biochemistry* 64(7): 1448-1458.

Hirayama T, Shinozaki K (2007) Perception and transduction of abscisic acid signals: keys to the function of the versatile plant hormone ABA. *Trends in Plant Science* 12(8): 343-351.

Hirose N, Takei K, Kuroha T, Kamada-Nobusada T, Hayashi H, Sakakibara H. 2008. Regulation of cytokinin biosynthesis, compartmentalization and translocation. *Journal of Experimental Botany* 59(1): 75-83.

Hoffman CS (1997) Preparation of yeast DNA. In *Current Protocols in Molecular Biology* 39(1): 13.11. Edited by Chanda VB. John Wiley & Sons, New York, 2001

Hou B, Lim EK, Higgins GS, Bowles DJ (2004) N-glycosylation of cytokinins by glycosyltransferases of *Arabidopsis thaliana*. *Journal of Biological Chemistry* 279(46): 47822-47832.

Huang FC, Peter A, Schwab W (2014) Expression and characterization of CYP52 genes involved in the biosynthesis of sophorolipid and alkane metabolism from *Starmerella bombicola*. *Applied and Environmental Microbiology* 80(2): 766-776.

Jadhav AS, Taylor DC, Giblin M, Ferrie AMR, Ambrose SJ, Ross AR, Nelson KM, Zaharia IL, Sharma N, Anderson M, Fobert PR, Abrams SR (2008) Hormonal regulation of oil accumulation in Brassica seeds: metabolism and biological activity of ABA, 7'-, 8'-and 9'-hydroxy ABA in microspore derived embryos of *B. napus*. *Phytochemistry* 69(15): 2678-2688.

Ji K, Chen P, Sun L, Wang Y, Dai S, Li Q., Li P, Sun Y, Wu Y, Duan C, Leng P (2012) Non-climacteric ripening in strawberry fruit is linked to ABA, FaNCED2 and FaCYP707A1. *Functional Plant Biology* 39(4): 351-357.

Ji K, Kai W, Zhao B, Sun Y, Yuan B, Dai S, Li Q, Chen P, Wang Y, Pei Y, Wang H, Guo Y, Leng P (2014). SINCED1 and SICYP707A2: key genes involved in ABA metabolism during tomato fruit ripening. *Journal of Experimental Botany* 65(18): 5243-5255.

Jia HF, Chai YM, Li CL, Lu D, Luo JJ, Qin L, Shen YY (2011) Abscisic acid plays an important role in the regulation of strawberry fruit ripening. *Plant Physiology* 157(1): 188-199.

Jiang Y, Joyce DC (2003) ABA effects on ethylene production, PAL activity, anthocyanin and phenolic contents of strawberry fruit. *Plant Growth Regulation* 39(2): 171-174.

Jing T, Zhang N, Gao T, Wu Y, Zhao M, Jin J, Du W, Schwab W, Song C (2020) UGT85A53 promotes flowering via mediating abscisic acid glucosylation and FLC transcript in *Camellia sinensis*. *Journal of Experimental Botany*. In Press.

Kakimoto T. 2001. Identification of plant cytokinin biosynthetic enzymes as dimethylallyl diphosphate: ATP/ADP isopentenyltransferases. *Plant and Cell Physiology* 42(7): 677-685.

Kang C, Darwish O, Geretz A, Shahan R, Alkharouf N, Liu Z (2013) Genome-scale transcriptomic insights into early-stage fruit development in woodland strawberry *Fragaria vesca*. *The Plant Cell* 25(6): 1960-1978.

Kang D, Gho YS, Suh M, Kang C (2002) Highly sensitive and fast protein detection with coomassie brilliant blue in sodium dodecyl sulfate polyacrylamide gel electrophoresis. *Bulletin of the Korean Chemical Society* 23(11): 1511-1512.

Kano Y, Asahira T (1981) Roles of cytokinin and abscisic acid in the maturing of strawberry fruits. *Journal of the Japanese Society for Horticultural Science* 50(1): 31-36.

Kasahara H, Takei K, Ueda N, Hishiyama S, Yamaya T, Kamiya Y, Yamaguchi S, Sakakibara H. 2004. Distinct isoprenoid origins of cis- and trans-zeatin biosyntheses in *Arabidopsis*. *Journal of Biological Chemistry* 279(14): 14049-14054.

Kim HJ, Ryu H, Hong SH, Woo HR, Lim PO, Lee IC, Sheen J, Nam HG, Hwang I. 2006. Cytokinin-mediated control of leaf longevity by AHK3 through phosphorylation of ARR2 in *Arabidopsis*. *Proceedings of National Academy of Sciences USA* 103: 814-819.

Krochko JE, Abrams GD, Loewen MK, Abrams SR, Cutler AJ (1998) (+)-Abscisic acid 8'-hydroxylase is a cytochrome P450 monooxygenase. *Plant Physiology* 118(3): 849-860.

Kumar S, Stecher G, Li M, Knyaz C, Tamura K (2018) MEGA X: molecular evolutionary genetics analysis across computing platforms. *Molecular Biology and Evolution* 35(6): 1547-1549.

Kurakawa T, Ueda N, Maekawa M, Kobayashi K, Kojima M, Nagato Y, Sakakibara H, Kyojuka J (2007) Direct control of shoot meristem activity by a cytokinin-activating enzyme. *Nature* 445: 652-655.

Kushiro T, Okamoto M, Nakabayashi K, Yamagishi K, Kitamura S, Asami T, Hirai N, Koshiba T, Kamiya Y, Nambara E (2004) The *Arabidopsis* cytochrome P450 CYP707A encodes ABA 8'-hydroxylases: key enzymes in ABA catabolism. *EMBO Journal* 23(7): 1647-1656.

Lazo GR, Stein PA, Ludwig RA (1991) A DNA transformation-competent Arabidopsis genomic library in *Agrobacterium*. *Nature Biotechnology* 9(10): 963-967.

Lee KH, Piao HL, Kim HY, Choi SM, Jiang F, Hartung W, Hwang I, Kwak JM, Lee IJ, Hwang I (2006) Activation of glucosidase via stress-induced polymerization rapidly increases active pools of abscisic acid. *Cell* 126(6): 1109-1120.

Li Q, Ji K, Sun Y, Luo H, Wang H, Leng P (2013) The role of FaBG 3 in fruit ripening and *B. cinerea* fungal infection of strawberry. *The Plant Journal* 76(1): 24-35.

Liao X, Li M, Liu B, Yan M, Yu X, Zi H, Liu R, Yamamuro C (2018) Interlinked regulatory loops of ABA catabolism and biosynthesis coordinate fruit growth and ripening in woodland strawberry. *Proceedings of the National Academy of Sciences* 115(49): E11542-E11550.

Lim EK, Bowles DJ (2004) A class of plant glycosyltransferases involved in cellular homeostasis. *The EMBO Journal* 23(15): 2915-2922.

Lim EK, Doucet CJ, Hou B, Jackson RG, Abrams SR, Bowles DJ (2005) Resolution of (+)-abscisic acid using an *Arabidopsis* glycosyltransferase. *Tetrahedron: Asymmetry* 16(1): 143-147.

Liston A, Cronn R, Ashman TL (2014) *Fragaria*: a genus with deep historical roots and ripe for evolutionary and ecological insights. *American Journal of Botany* 101(10): 1686-1699.

Liu Z, Yan JP, Li DK, Luo Q, Yan Q, Liu ZB, Ye LM, Wang JM, Li XF, Yang Y (2015) UDP-glucosyltransferase71c5, a major glucosyltransferase, mediates abscisic acid homeostasis in Arabidopsis. *Plant Physiology* 167(4): 1659-1670.

Lorenc-Kukuła K, Korobczak A, Aksamit-Stachurska A, Kostyń K, Łukaszewicz M, Szopa, J (2004) Glucosyltransferase: the gene arrangement and enzyme function. *Cellular & Molecular Biology Letters* 9: 935-946.

Mackenzie PI, Owens IS, Burchell B et al. (1997) The UDP glycosyltransferase gene superfamily: recommended nomenclature update based on evolutionary divergence. *Pharmacogenetics and Genomics* 7(4): 255-269.

Martin RC, Mok MC, Habben JE, Mok DW (2001) A maize cytokinin gene encoding an O-glucosyltransferase specific to cis-zeatin *Proceedings of National Academy of Sciences USA* 98:5922-26.

Martin RC, Mok MC, Mok DW (1999) Isolation of a cytokinin gene, ZOG1, encoding zeatin O-glucosyltransferase from *Phaseolus lunatus*. *Proceedings of National Academy of Sciences USA* 96: 284-89.

Martinez GA, Chaves AR, Anon MC (1996) Effect of exogenous application of gibberellic acid on color change and phenylalanine ammonia-lyase, chlorophyllase, and peroxidase activities during ripening of strawberry fruit (*Fragaria x ananassa* Duch.). *Journal of Plant Growth Regulation* 15(3): 139.

Masada S, Terasaka K, Mizukami H (2007) A single amino acid in the PSPG-box plays an important role in the catalytic function of CaUGT2 (Curcumin glucosyltransferase), a Group D Family 1 glucosyltransferase from *Catharanthus roseus*. *FEBS Letters* 581(14): 2605-2610.

Merchante C, Vallarino JG, Osorio S, Aragüez I, Villarreal N, Ariza MT, Martínez GA, Medina-Escobar N, Civello MP, Fernie AR, Botella MA, Valpuesta V (2013) Ethylene is involved in strawberry fruit ripening in an organ-specific manner. *Journal of Experimental Botany* 64(14): 4421-4439.

Milborrow BV, Vaughan GT (1982) Characterization of dihydrophaseic acid 4'-O- β -d-glucopyranoside as a major metabolite of abscisic acid. *Functional Plant Biology* 9(3): 361-372.

Mok DW, Mok MC (2001) Cytokinin metabolism and action. *Annual Review of Plant Biology* 52(1): 89-118.

Mok MC, Martin RC, Dobrev PI, Vanková R, Ho PS, Yonekura-Sakakibara K, Sakakibara H, Mok DW (2005) Topolins and hydroxylated thidiazuron derivatives are substrates of cytokinin O-glucosyltransferase with position specificity related to receptor recognition. *Plant Physiology* 137(3): 1057-1066.

Nambara E, Marion-Poll A (2005) Abscisic acid biosynthesis and catabolism. *Annual Review of Plant Biology* 56:165-185.

Nishiyama R, Watanabe Y, Fujita Y, Le DT, Kojima M (2011) Analysis of cytokinin mutants and regulation of cytokinin metabolic genes reveals important regulatory roles of cytokinins in drought, salt and abscisic acid responses, and abscisic acid biosynthesis. *Plant Cell* 23:2169-2183.

Nitsch LMC, Oplaat C, Feron R, Ma Q, Wolters-Arts M, Hedden P, Mariani C, Vriezen WH (2009) Abscisic acid levels in tomato ovaries are regulated by LeNCED1 and SICYP707A1. *Planta* 229(6): 1335-1346.

Okamoto M, Kuwahara A, Seo M, Kushiro T, Asami T, Hirai N, Kamiya Y, Koshiba T, Nambara E (2006) CYP707A1 and CYP707A2, which encode abscisic acid 8'-hydroxylases, are indispensable for proper control of seed dormancy and germination in *Arabidopsis*. *Plant Physiology* 141(1): 97-107.

Okamoto M, Kushiro T, Jikumaru Y, Abrams SR, Kamiya Y, Seki M, Nambara E (2011) ABA 9'-hydroxylation is catalyzed by CYP707A in *Arabidopsis*. *Phytochemistry* 72(8): 717-722.

Olsen KM, Hehn A, Jugdé H, Slimestad R, Larbat R, Bourgaud F, Lillo C (2010) Identification and characterisation of CYP75A31, a new flavonoid 3'5'-hydroxylase, isolated from *Solanum lycopersicum*. *BMC Plant Biology* 10(1): 21.

Osmani SA, Bak S, Møller BL (2009) Substrate specificity of plant UDP-dependent glycosyltransferases predicted from crystal structures and homology modeling. *Phytochemistry* 70(3): 325-347.

Ostrowski M, Jakubowska A (2014) UDP-glycosyltransferases of plant hormones. *Advances in Cell Biology* 4(1): 43-60.

Palaniyandi SA, Chung G, Kim SH, Yang SH (2015) Molecular cloning and characterization of the ABA-specific glucosyltransferase gene from bean (*Phaseolus vulgaris* L.). *Journal of Plant Physiology* 178: 1-9.

Perin EC, Crizel RL, Galli V, da Silva Messias R, Rombaldi CV, Chaves FC (2018) Extraction and quantification of abscisic acid and derivatives in Strawberry by LC-MS. *Food Analytical Methods* 11(9): 2547-2552.

Priest DM, Ambrose SJ, Vaistij FE, Elias L, Higgins GS, Ross AR, Abrams SR, Bowles DJ (2006) Use of the glucosyltransferase UGT71B6 to disturb abscisic acid homeostasis in *Arabidopsis thaliana*. *The Plant Journal* 46(3): 492-502.

Priest DM, Jackson RG, Ashford DA, Abrams SR, Bowles DJ (2005) The use of abscisic acid analogues to analyse the substrate selectivity of UGT71B6, a UDP-glycosyltransferase of *Arabidopsis thaliana*. *FEBS Letters* 579(20): 4454-4458.

Ramos P, Parra-Palma C, Figueroa CR, Zuñiga PE, Valenzuela-Riffo F, Gonzalez J, Gaete-Eastman C, Morales-Quintana L (2018) Cell wall-related enzymatic activities and transcriptional profiles in four strawberry (*Fragaria x ananassa*) cultivars during fruit development and ripening. *Scientia Horticulturae*, 238: 325-332.

Ren J, Sun L, Wu J., Zhao S, Wang C, Wang Y, Ji K, Leng P (2010) Cloning and expression analysis of cDNAs for ABA 8'-hydroxylase during sweet cherry fruit maturation and under stress conditions. *Journal of Plant Physiology* 167(17): 1486-1493.

Ring L, Yeh SY, Hücherig S, Hoffmann T, Blanco-Portales R, Fouche M, Villatoro C, Denoyes B, Monfort A, Caballero JL, Muñoz-Blanco J, Gershenson J, Schwab W (2013) Metabolic interaction between anthocyanin and lignin biosynthesis is associated with peroxidase FaPRX27 in strawberry fruit. *Plant Physiology* 163(1): 43-60.

Sakakibara H (2006) Cytokinins: activity, biosynthesis, and translocation. *Annual Review of Plant Biology* 57: 431-449.

Sánchez-Sevilla JF, Vallarino JG, Osorio S, Bombarely A, Posé D, Merchante C, Botella MA, Amaya I, Valpuesta V (2017) Gene expression atlas of fruit ripening and transcriptome assembly from RNA-seq data in octoploid strawberry (*Fragaria x ananassa*). *Scientific Reports* 7(1): 13737.

Sauter A, Dietz K, Hartung W (2002) A possible stress physiological role of abscisic acid conjugates in root-to-shoot signalling. *Plant, Cell & Environment* 25(2): 223-228.

Šmehilová M, Dobrušková J, Novák O, Takáč T, Galuszka P (2016) Cytokinin-specific glycosyltransferases possess different roles in cytokinin homeostasis maintenance. *Frontiers in Plant Science* 7: 1264.

Song C, Gu L, Liu J, Zhao S, Hong X, Schulenburg K, Schwab W (2015) Functional characterization and substrate promiscuity of UGT71 glycosyltransferases from strawberry (*Fragaria x ananassa*). *Plant and Cell Physiology* 56(12): 2478-2493.

Stewart PJ (2011) *Fragaria* history and breeding. In *Genetics, genomics and breeding of berries* (pp. 114–137) Edited by Folta KM and Kole C. Science Publishers, Enfield, 2011.

Strnad M (1997) The aromatic cytokinins. *Physiologia Plantarum* 101(4): 674-688.

Symons GM, Chua YJ, Ross JJ, Quittenden LJ, Davies NW, Reid JB (2012) Hormonal changes during non-climacteric ripening in strawberry. *Journal of Experimental Botany* 63(13): 4741-4750.

Takei K, Takahashi T, Sugiyama T, Yamaya T, Sakakibara H (2002) Multiple routes communicating nitrogen availability from roots to shoots: a signal transduction pathway mediated by cytokinin. *Journal of Experimental Botany* 53: 971-977.

Takei K, Yamaya T, Sakakibara H (2004) Arabidopsis CYP735A1 and CYP735A2 encode cytokinin hydroxylases that catalyze the biosynthesis of trans-zeatin. *Journal of Biological Chemistry* 279: 41866–41872.

Tanaka M, Takei K, Kojima M, Sakakibara H, Mori H (2006) Auxin controls local cytokinin biosynthesis in the nodal stem in apical dominance. *The Plant Journal* 45: 1028-1036.

- Tiwari P, Sangwan RS, Sangwan NS (2016) Plant secondary metabolism linked glycosyltransferases: an update on expanding knowledge and scopes. *Biotechnology Advances* 34(5): 714-739.
- Veach YK, Martin RC, Mok DW, Malbeck J, Vankova R, Mok MC (2003) O-Glucosylation of cis-zeatin in maize. Characterization of genes, enzymes, and endogenous cytokinins. *Plant Physiology* 131:1374-1380.
- Villarreal NM, Bustamante CA, Civello PM, Martínez GA (2010) Effect of ethylene and 1-MCP treatments on strawberry fruit ripening. *Journal of the Science of Food and Agriculture* 90(4): 683-689.
- Wang J, Ma XM, Kojima M, Sakakibara H, Hou BK (2011) N-glucosyltransferase UGT76C2 is involved in cytokinin homeostasis and cytokinin response in *Arabidopsis thaliana*. *Plant Cell Physiology* 52: 2200–2213.
- Weng JK, Ye M, Li B, Noel JP (2016) Co-evolution of hormone metabolism and signaling networks expands plant adaptive plasticity. *Cell* 166(4): 881-893.
- Werner T, Motyka V, Laucou V, Smets R, Van Onckelen H, Schmülling T (2003) Cytokinin-deficient transgenic *Arabidopsis* plants show multiple developmental alterations indicating opposite functions of cytokinins in the regulation of shoot and root meristem activity. *Plant Cell* 15: 2532-50.
- Xu J, Wang XY, Guo WZ (2015) The cytochrome P450 superfamily: Key players in plant development and defense. *Journal of Integrative Agriculture* 14(9): 1673-1686.
- Xu ZJ, Nakajima M, Suzuki Y, Yamaguchi I (2002) Cloning and characterization of the abscisic acid-specific glucosyltransferase gene from adzuki bean seedlings. *Plant Physiology* 129(3): 1285-1295.
- Xu ZY, Lee KH, Dong T, Jeong JC, Jin JB, Kanno Y, Kim DH, Youn S, Seo M, Bressan RA, Yun DJ, Hwang I (2012) A vacuolar β -glucosidase homolog that possesses glucose-conjugated abscisic acid hydrolyzing activity plays an important role in osmotic stress responses in *Arabidopsis*. *The Plant Cell* 24(5): 2184-2199.
- Yang SH, Zeevaart JA (2006) Expression of ABA 8'-hydroxylases in relation to leaf water relations and seed development in bean. *The Plant Journal* 47(5): 675-686.
- Yonekura-Sakakibara K, Hanada K (2011) An evolutionary view of functional diversity in family 1 glycosyltransferases. *The Plant Journal* 66(1): 182-193.

Zdunek-Zastocka E, Grabowska A (2019) The interplay of PsABAUGT1 with other abscisic acid metabolic genes in the regulation of ABA homeostasis during the development of pea seeds and germination in the presence of H₂O₂. *Plant Science* 285: 79-90.

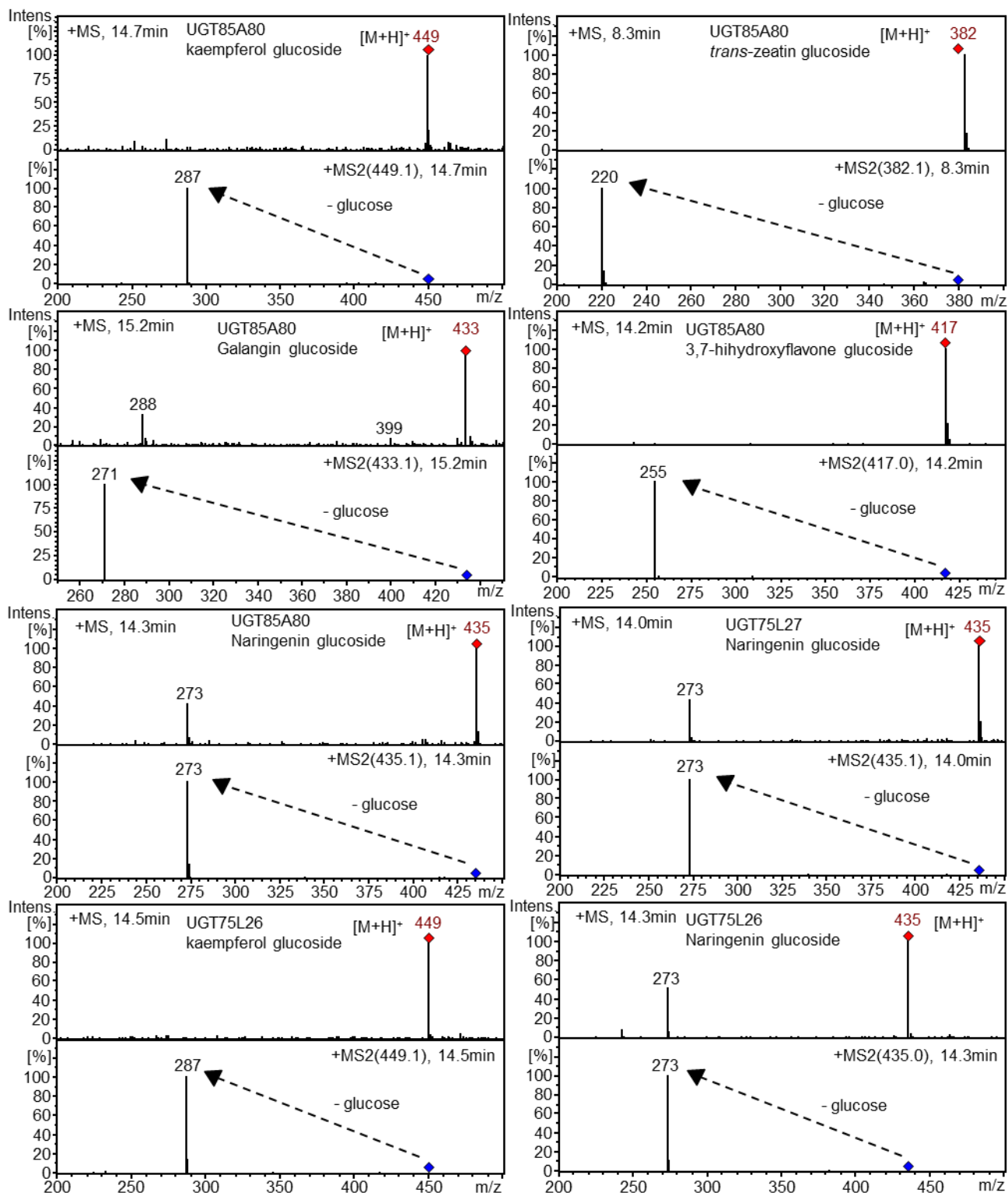
Zeevaart, JAD, Gage DA, Creelman RA (1990) Recent studies of the metabolism of abscisic acid. In *Plant Growth Substances 1988* (pp. 233-240). Springer, Berlin, Heidelberg.

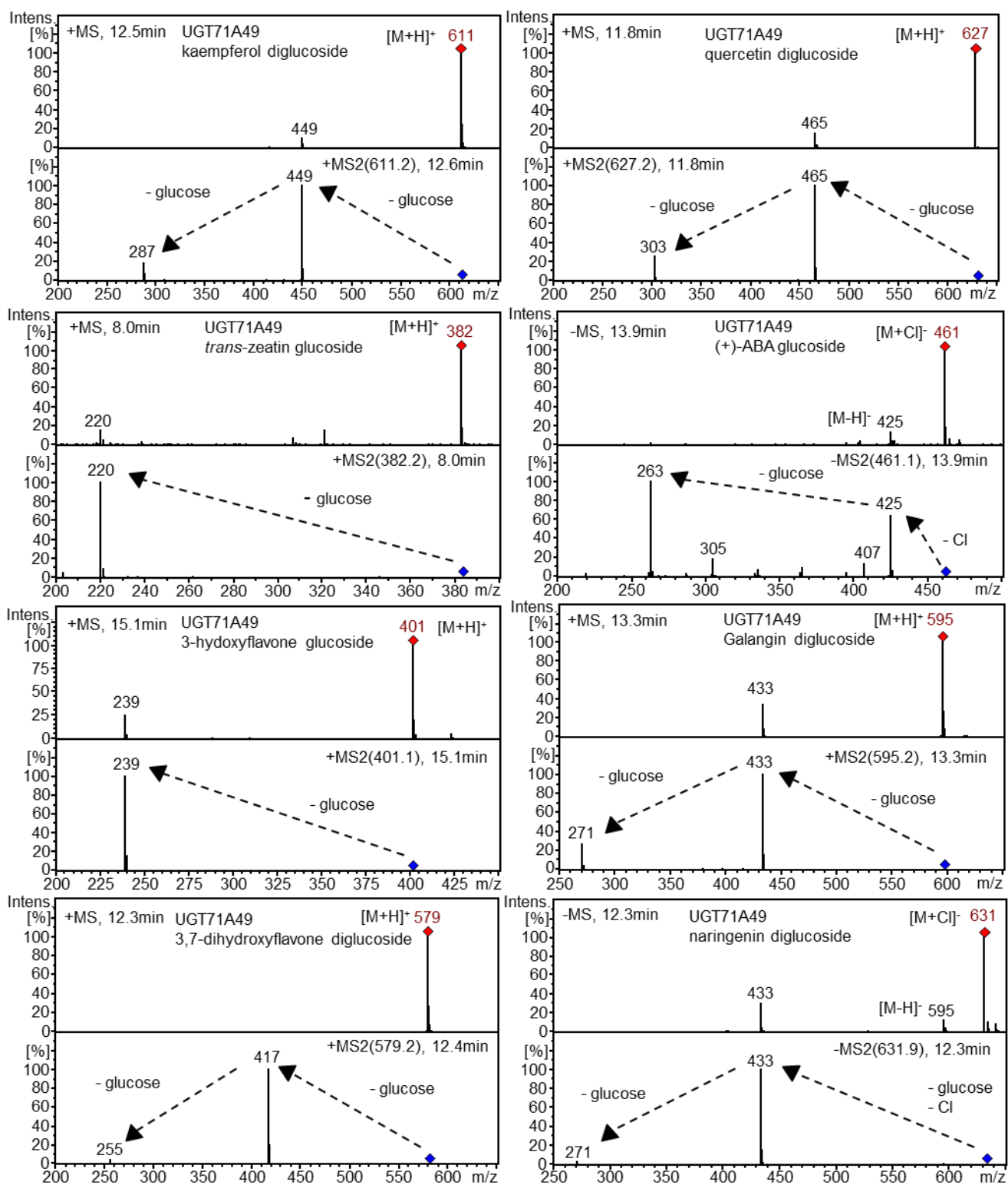
Zhang SH, Sun JH, Dong YH, Shen YY, Li CL, Li YZ, Guo JX (2014) Enzymatic and functional analysis of-glucosidase FaBG1 during strawberry fruit ripening. *The Journal of Horticultural Science and Biotechnology* 89(6): 733-739.

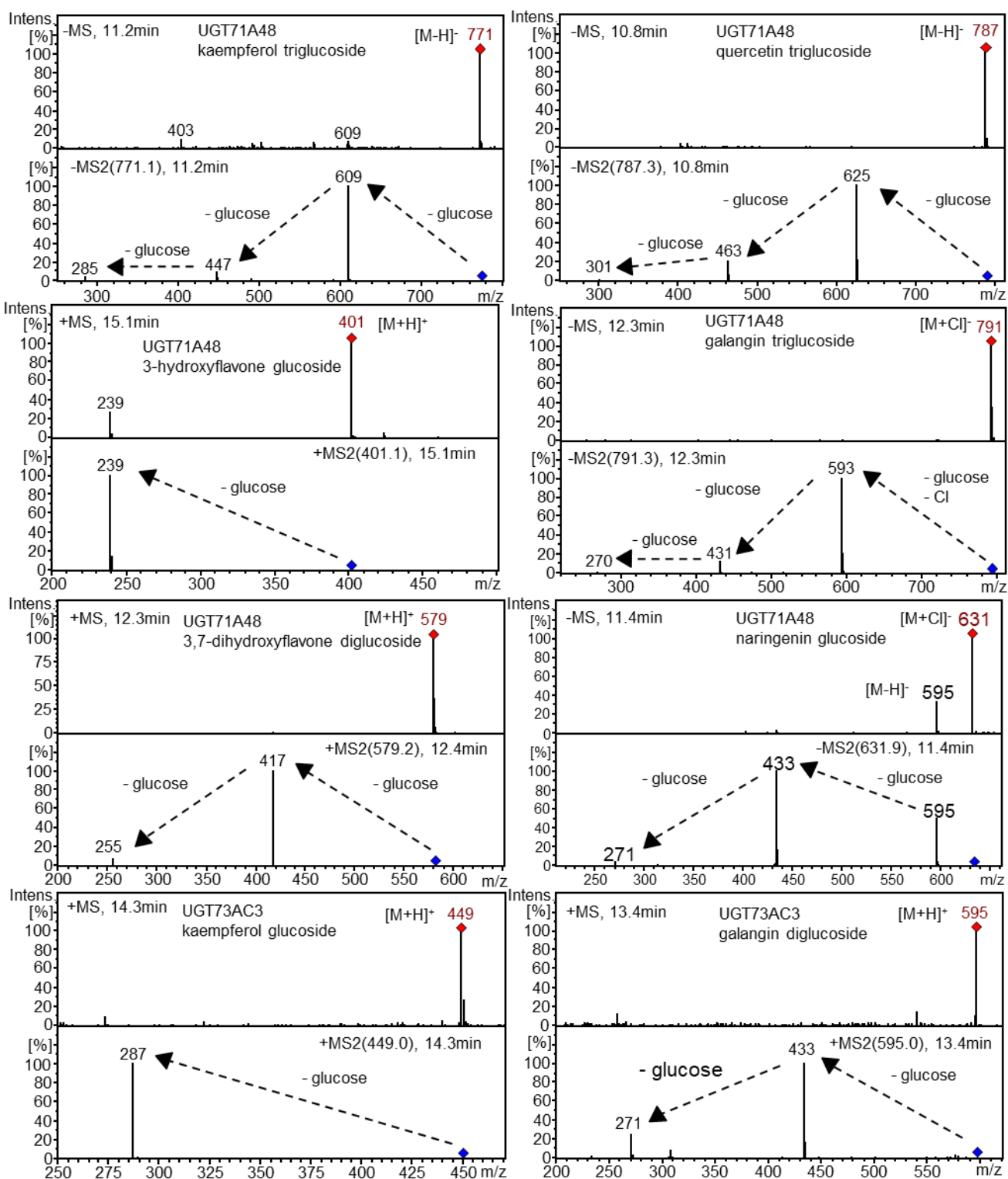
Zhou R, Cutler AJ, Ambrose, SJ, Galka, MM, Nelson, KM, Squires, TM, Loewen MK, Jadhav AS, Ross ARS, Taylor DC, Abrams, SR (2004) A new abscisic acid catabolic pathway. *Plant Physiology* 134(1): 361-369.

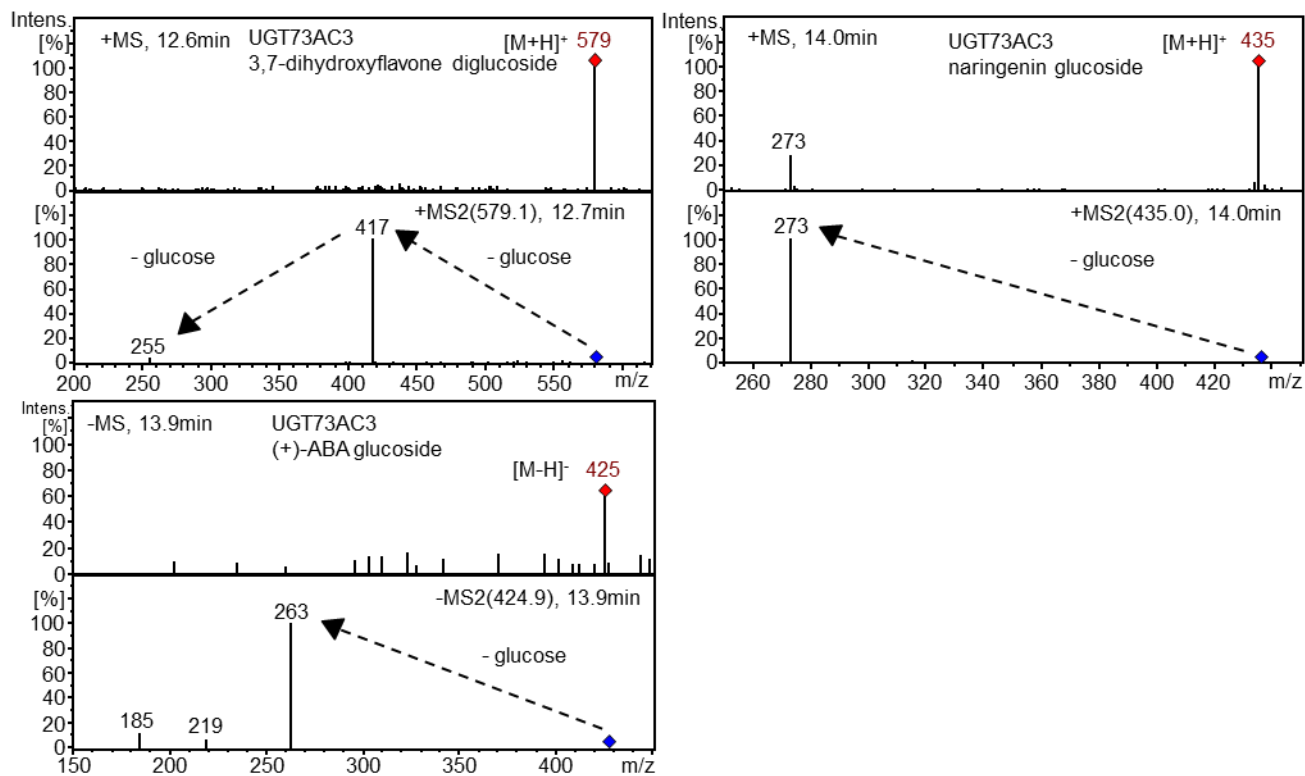
Zou J, Abrams GD, Barton DL, Taylor DC, Pomeroy MK, Abrams SR (1995) Induction of lipid and oleosin biosynthesis by (+)-abscisic acid and its metabolites in microspore-derived embryos of *Brassica napus* L. cv Reston (biological responses in the presence of 8'-hydroxyabscisic acid. *Plant Physiology* 108(2): 563-571.

8. SUPPLEMENTAL DATA









Supplementary Figure 1. MS and MS2 analysis of all tested combinations of UGTs and substrates.


```

AtUGT71B6  LLLLLHIQFMYDAEDIYDMS--ELEDSD--DVELVPSLTSPYP-LKCLPYIFKS---KEWLTFVFTQARRFR-----ETKGILVNTVPDLEPQALTF
AtUGT84B1  YSVYYRYMKTNSFPDLEDLNQT-----VELPALPILLEVRDLPSFMLP--SGGAHFYNLMAEFAD-----CLRYVKWVLVNSFYELESEIIES
AtUGT85A1  FLAYLHFYLFIEKGLCPKDESILTK-EYLEDTVIDFIPTMKNVKLKDIPSIIRTNNPDDVMISFALRETER-----AKRASAILNTFDDLEHDVVHA
AtUGT75B1  FNIYYT-HFMGNK-----SVFELPNLSSLEIRDLPSFLTSPSNTNG---AYDAFOEMMEFLIKETKPKILINTFDSLEPEALTA
AtUGT73C5  LLCMHVLRKNRE-----ILDNLKSD--KELFTVPDFPDRVEFTRTQVPVETVYVPAAGDWKIDFDGMVEANE-----TSYGVIVNSFOELEPAYAKD
          310          320          330          340          350          360          370          380          390          400
FaUGT71W2  IFRVGEQDQDQWPVAVYPVGPPLIDTKG-----EHQVRSRDRIMEFLDNQPPKSVVFLCFGSGFSFDEAQLREIAIGLEKSGHRFLWS
FaUGT71A33  LS-----SDAETIPPVYPVGPILLVNS-----NESR-----VDSDEVKKNNDILKWLDDQPPLSVVFLCFGSMGFSFDENOVREIAKALEHAGHRFLWS
FaUGT71A35  LS-----SDGKLPPVYPVGPILNLKSDD-----NNDQ-----VNSKQ---KSDILNWLDDQPPSSVVFLCFGSMGFSFSEDQVKEIACALEQGGFRFLWS
AtUGT71B7  LS-----SS-DTPPVYPVGPILLHLEN-----Q-----RDDSKDEKLEIIRWLDDQPPSSVVFLCFGSMGGFGEEQVREIAIALERSGHRFLWS
AtUGT71B8  LH-----SSGDTPRAYPVGPILLHLEN-----H-----VDGSKDEKGSILRWLDEQPPKSVVFLCFGSIGGFNEEQAREMAIALERSGHRFLWS
AtUGT71C5  FS-----QGRDYPHVYPVGPVNLNLTGR-----T-----NPLASAQYKEMMKWLDEQDSSVFLCFGSMGVFPAPQITEIAHALELIGCRFIWA
VaQ8W3P8  IK-----SKWGNKAWIVGPVSFCNRSKEDKTERGK-----PPTIDEQN---CLNWLNSKPPSSVLYASFGSLARLPPEQLKEIAYGLEASEQSFVIW
Pv ABA-GT  LK-----DKWGNKAWIVGPVSLCNRTKQDKTERGK-----PPTVDEEK---CLNWLNSKPPSSVLYISFGSLARLPPEQLKEIAYGLEASDQSFVWV
FvUGT73AC3  FK-----KDLGKKAWGIGPVSICNRDEADKVERGQ-----AASVDEEKLKWCLDWLDSQEPDSVVYISFGSLARLSYKQLIEIAHGVTNCFVWV
FvUGT71A49  LS-----SDGKIPPVYPVGPILNVKS-----EGNQ-----VSSEKSKQKSDILEWLDDQPPSSVVFLCFGSMGCFGEDQVKEIAHALEQGGIRFLWS
PsABAUGT1  IR-----NELGKKRWLVGPVSLYNSSVEDKTERGK-----QPTIDEQS---CLNWLNSKKSNSVLYISFGSVAACLPMKQLKEIAYGLEASDQPFVIW
GhUGT73C14  YR-----KEK--KAWCIGPVSLSHKDELDAERGN-----KTSIDGQK---CLKWLDSSQPGSVIYAACLGSIGTIKPELIELEGLGLEASNKPFVIW
FaUGT71A34  LS-----SDGKLPPVYPVGPILNLKSDD-----NNDQ-----VDSKQKQTSIDILKWLDDQPPSSVVFLCFGSMGFSFSEDQVKEIARALEQGGFRFLWS
CsUGT85A53  LSSM-----FPPIYTIIGPLHILMN-QIN-DDSLK--LIGSNLWKEETE---CLEWLDTKGPNSSVVYVNFSGITVMTPNQMVFEAWGLANSNMTFLWV
SlUGT75C1  IEK-----YNLIG-IGPLIPSSFLGGKSLLESS---FGDDLFOKSNDD--YMEWLNTKPKSSIVYISFGSLLNLSRNQKEEIAKGLIEIQRPFLWV
AtSGT1  WSKA-----CPVLT-IGPTIPSIYLDQRIKSDTG--YDLNLFESKDDSF CINWLDRPQGSVVYVAFGSMQTLNVQMEELASAVSN--FSFLWV
NtSAGTase  MAKI-----YPIKT-IGPTIPSMYLDKRLPDDKE--YGLSVFKPMTN-ACLNWLNHQPVSSVVYVVSFGSLAKLEAQMEELAWGLSNSNKNFLWV
InGTase1  LS-----HYPNSPPVYPVGPILNLAG-----AGKDSQQILEWLDDQPEGSVVFLCFGSEGYFPEEQVKEIAIALERSGKRFLWT
FvUGT85A80  FSSL-----LPPVYSIGPLHQQLS-HIQEDDDSK--TIGSNLWKEEPE--CLEWLESKEPNSSVVYVNFSGITVMTDEQLIEFAWGLANSNMTFLWV
PlZOG  LELFN-----GGKKVWALGPFNPLAVE-----KKDSIGFRHPCMEWLKQEPSSVIYISFGTTTALRDEIQQIATGLEQSKQKFIWV
ZmIAGLU  LTKY-----LKARA-IGPCVP-LPTAGRTAGANGRITYGANLVKPEDA--CTKWLDTKPDRSVAYVSFGSLASLGNAQKEELARGLLAAGKPFLLWV
OsIAGT1  LSTQ-----WKARA-IGPCVP-LPAG--DGATGRFTYGANLLDPEDT--CMQWLDTKPSSVAYVSFGSFASLGAQTTELARGLLAAGRPFLWV
AtUGT71B6  LS-----NG-NIPRAYPVGPILLHLKN-----V-----NCDYVDKQKSEILRWLDEQPPRSVVFLCFGSMGGFSEEQVRETALALDRSGHRFLWS
AtUGT84B1  MADL-----KPVIP-IGPLVSPFLLGDGEEETLD---GKNLDFCKSDCCMEWLKQARSSVVYISFGSMLETLENQVETIAKALKNRGLPFLWV
AtUGT85A1  MQSI-----LPPVYSVGPILLHANREIEEGSEIG--MSSNLWKEEME--CLDWLDTKTQNSVIYINFGSITVLSVKQLVEFAWGLAGSGKEFLWV
AtUGT75B1  FPN-----IDMVA-VGPLLPTEIFSG--STNKS--VK-----DQSSS-YTLWLDSKTESSVIYVSFGTMVELSKKQIEELARALIECKRPFLLWV
AtUGT73C5  YK-----EVRSKAWTIGPVSICNVKVGADKAERGN-----KSDIDQDE--CLKWLDKSKHGSVLYVCLGSI CNLPLSOLKELGLGLEESQRPFIWV
          410          420          430          440          450          460          470          480          490          500
FaUGT71W2  VRQRPPK GKTEFPGEYKNYEDFLPQGFLERTKGVGMLCG- WAPQVEVLGHKSTGGFVSHCGWNSILESLWYGVPIVWTPLYAEQOVNAFLIARDLGLGVE
FaUGT71A33  LRRPPPTGKIAFPSDYDDHTGVLPEGFLDRTGGIGKVG- WAPQVAVLAHPSVGGFVSHCGWNSTLESWLHGVVPVATWPLYAEQQLNAFQLVKELELAVE
FaUGT71A35  LRQPPP KGNVPSDYADHTGVLPEGFLDRTAGVGVKVG- WAPQVAILGHPAVGGFVSHCGWNSTLESWLFGVPVATWPLYAEQOVNAFQLVKELGIAVE
AtUGT71B7  LRRASPNIFKELPGEFTNLEEVLPEGFFDRTKDIGKVG- WAPQVAVLANPAIGGFVTHCGWNSTLESWLFGVPTAAWPLYAEQKFNFAFLMVEELGLAVE
AtUGT71B8  LRRASRDIDKELPGEFKNLEEILPEGFFDRTKDKGVKVG- WAPQVAVLAKPAIGGFVTHCGWNSILESLWFGVPIAPWPLYAEQKFNFAFVMVEELGLAVK

```



```

InGTase1      LKMDYKRDFKDATKFSEMVREEIERGIRSVMDPLN-----PIRLKAKEMSEKRSAI-VEGGSSYTNVGRFTQDVFSNIN-----
FvUGT85A80   IEGDVR-----RNYIEVLVLRKLMEGQE-----GKQMRKKSLEWKKLEEAVTAPNGSSFLNLNKMVNQVLLSPKN-----
PlZOG        VKDWAQRNS-----LVSASVVENGVRRLMETKEG-----DEMRQRAVRLKNAIHRSM-DEGGVSHMEMGSFIAHISK-----
ZmIAGLU      ARR-----DAGAG-----VFLRGEVERCVRAVMDGGE-----AASAARKAAGEWRDRARAAV-APGGSSDRNLDEFVQFVRAG-----ATEK-----
OsIAGT1      ARRGDADADDAAGGTAAMFLRGDIERCVRAVMDGEEQEAARARARGEARRWSDAARAAV-SPGGSSDRSLDEFVEFLRGGSGADAGEKWKTLVWEGSEAA
AtUGT71B6    IKKHWRGDLLLG-R-SEIVTAEIEKGIICLMEQDS-----DVRKRVNEISEKCHVAL-MDGGSETALKRFIQDVTENIAWSETES-----
AtUGT84B1    MRNDS---VDGELK-----VEEVERCIEAVTEGPA-----AVDIRRAAELKRVARLAL-APGGSSSTRNLDLFISDITIA-----
AtUGT85A1    IGGDVK-----REEVEAVVRELMDGEK-----GKKMREKAVEWQRLAEKATEHKLGSSVMNFETVVSKFLLGQKSQD-----
AtUGT75B1    VREN---KDGLVE-----RGEIRRCLEAVME--EK--SVELRENAKKWKRLAMEEAG-REGGSSDKNMEAFVEDICGESLIQNLCEAEEVKVK-----
AtUGT73C5    SVEQPMKWGEEEKIGVLVDKEGVKKAVEELMGESDD--AKERRRRAKELGDSAKAV-EEGGSSHSNISFLLQDIMELAEPNN-----

          . . . .
FaUGT71W2    -----
FaUGT71A33   -----
FaUGT71A35   -----
AtUGT71B7    -----
AtUGT71B8    -----
AtUGT71C5    -----
VaQ8W3P8     -----
Pv ABA-GT    -----
FvUGT73AC3   -----
FvUGT71A49   -----
PsABAUGT1    -----
GhUGT73C14   -----
FaUGT71A34   -----
CsUGT85A53   -----
SlUGT75C1    -----
AtSGT1       -----
NtSAGTase    -----
InGTase1     -----
FvUGT85A80   -----
PlZOG        -----
ZmIAGLU      -----
OsIAGT1      ASEM
AtUGT71B6    -----
AtUGT84B1    -----
AtUGT85A1    -----
AtUGT75B1    -----
AtUGT73C5    -----

```

Supplementary Figure 2. Amino acid sequence alignment of UGTs with activity towards ABA used for building the phylogenetic tree. Red box contains the PSPG (Plant Secondary Product Glycosyltransferase) motif. Red arrow indicates the catalytic His20

```

      10      20      30      40      50      60      70      80      90     100
.....|.....|.....|.....|.....|.....|.....|.....|.....|.....|.....|.....|.....|.....|.....|.....|
FaCYP707A4a  -----M-----MKKSKGGGEEDPHDDHG-----HKNRAAQLPP-----GSFGWPYIGETLQLY
FaCYP707A1/3 -----MFAASALIFFFFSPIIKLFLI-----SARHKIPLPP-----GSLGWPYIGETFQLY
AtCYP707A1  -----MDISALFLTLFAGSLFLYFLRCLISQRR-----FGSSKLPLPP-----GTMGWPYVGETFQLY
SlCYP707A1  -----MVNYFEIFLYIISMFLVGLYLSYFFCFGKNNNSS-----SKKNAYKLPP-----GSMGWPYIGETLQLY
SlCYP707A2  -----MEFVSMCLLFTFISLTLLLIHSIFKFLA-----FASKKLPLPP-----GTLGLPYIGETFQLY
AtCYP707A2  -----MQISSSSSSNFFSSLYADEPALITLTIVVVVVLLFKWWLH-----WKEQRLRLPP-----GSMGLPYIGETLRLY
AtCYP707A3  -----MDFSGFLFLTLSAAALFLCLLRFIAGVRR-----SSSTKLPLPP-----GTMGYPYVGETFQLY
AtCYP707A4  -----MAEIWFLVVPILILCLLLVVRVIVSKK-----KKNSRQKLPP-----GSMGWPYIGETLQLY
FvCYP707A1/3 -----MELLSLNSMFCMFAASALIFFFFSPIIKLFLI-----SARHKIPLPP-----GSLGWPYIGETFQLY
FvCYP707A4a  -----MVAIFTYVVFVSLTLIF-LYIFMKKSKGGGEEDPHDDHG-----HKNRAAQLPP-----GSFGWPYIGETLQLY
PacCYP707A1  -----
PacCYP707A2  -----PR-----GSE-----
PacCYP707A3  -----
PacCYP707A4  -----
PvCYP707A1  -----MELSTILCLGASFLFIFLFRTLIKQFLS-----KRPH-FPLPP-----GTMGWPYIGETFQMY
PvCYP707A2  -----MDLSAILLLGARGLEFFFLFRRLIKSFRS-----FGSH-FPLLP-----GTMVCPYFGETFQMY
PvCYP707A3  -----MAELVLFVSVPAAVLAFGVPVAFKVCCTSEYRWRDVG LHGGRDWRKKTCLRFP-----GSMGWPYFGETLQLY
OsCYP714B1  ---MVVVVAAMAASLCCG---VAAYLYVWLWLAPELRAHLRRQGI GGPTSPFPYGNLADMRSHAAAAAG-----GKATGEGRQEGDIVHDY
OsCYP714B2  MEVGMVVVVAAKVLVSLWCVGACCLAAYLYRVVWVAPRRVLA EFRRQGI GGPRSPFPYGNLADMRSHAAAAAG-----GKATGEGRQEGDIVHDY
AtCYP714A1  --MENFMVEMAKTISWIVVIGVGLGIRVYGKVMAEQWRMRRLTMOGKVGPPPSLFRGNVPEMOKIOS-----QIMSNSKHYSGDNIIAHDY
AtCYP714A2  --MESLVVHTVNAIWCIVIVIGIFSVGYHYGRAVVEQWRMRRLSLKQGVKPPPSIFNGNVSEMORIQ-----SEAKHCSDGNIISHDY
AtCYP735A2  ---MMVTLVLKYVLVIVMTLILRVLYDSICCYFLT PRRIKKEMERQGITGPKRLLTGNIIDISKMLS-----HSASNDCCSIHNI
PtCYP714A3  ---MEVSLPCLRLVSSLTLLALVFFLVHVCYTVLLKSERIKRKLRMQGIQPPPSFLYGNLPEMOKIQ-----N-TLKASSFQAPDFIAHDY
AtCYP94C1  -----MLLIISFTIVSFFFIIIFSLFHLLEFLQKLRYNCEICHAYLTS---SWKKDFIN-----LSDWY
AtCYP94B3  -----MAFLLSFLILAFILTIIFFLSSSSSTKKVQENTTYGPPSYPLIGSILSFNKNRHR-----LLQWY
      110     120     130     140     150     160     170     180     190     200
.....|.....|.....|.....|.....|.....|.....|.....|.....|.....|.....|.....|.....|.....|.....|.....|
FaCYP707A4a  SQDPNTFFSSRQKRYGKNFKTHILGSPCVMLASPEAAKFVLV TQAHLFKP-TYPKSKEALIGPSALFFHHGDYHFRLKRLVQRSLSPDAIRNLVPHINAT
FaCYP707A1/3 SQDPNVFFFASKIKRFGSIFKTHILGCPVMISSPEAAKFVLLTKAHLFKP-TFPASKERMLGKQAIFFHQGDYHAKLRKLVLAQAFMPTALKNKVGDIEAI
AtCYP707A1  SQDPNVFFQSKQKRYGSVFKTHVLGCPVMISSPEAAKFVLVTKSHLFKP-TFPASKERMLGKQAIFFHQGDYHAKLRKLVLAQAFMPTALKNKVGDIEAI
SlCYP707A1  SQDPNAFFINRQRRFGEIFKTKILGCPVMLASPEAAKFVLVNQANLFKP-TYPKSKENLIGQSAIFFHQGDYHNHLRKLVAQPLNPESIRNQIPYIEEL
SlCYP707A2  SQDPNVFFFASKVKKYGSIFKTYILGCPVMISSPEAAKQVLVTKANHLFKP-TFPASKERMLGKQAIFFHQGDYHAKLRKLVLAQAFKPD SIRNIIPDIESI
AtCYP707A2  TENPNSEFFATRQNKYGDIFKTHILGCPVMISSPEAAKRMVLVSKAHLFKP-TYPPASKERMLGQAEALFFHQGPYHSTLKRKLVSQSSFMPSALRPTVSHIELL
AtCYP707A3  SQDPNVFFFAAKQRRYGSVFKTHVLGCPVMISSPEAAKFVLVTKSHLFKP-TFPASKERMLGKQAIFFHQGDYHAKLRKLVLAQAFMPTAIRNMPHIESI
AtCYP707A4  SQDPNVFFFTSKQKRYGEIFKTRILGYPCVMLASPEAAKFVLVTHAHMFKP-TYPRSKKELIGPSALFFHQGDYHSHIRKLVQSSFFPETIRKLIPIDIEHI
FvCYP707A1/3 SQDPNVFFFASKIKRFGSIFKTHILGCPVMISSPEAAKFVLLTKSHLFKP-TFPASKERMLGKQAIFFHQGDYHAKLRKLVLAQAFMPTALKNKVGDIEAI
FvCYP707A4a  SQDPNTFFSSRQKRYGKIFKTHILGSPCVMLASPEAAKFVLV TQAHLFKP-TYPKSKEALIGPSALFFHHGDYHFRLRKLVQRSLSPDAIRNLVPHIDAT
PacCYP707A1  -----LGCPVMISSPEAAKFVLVTRSHLFKP-TFPASKERMLGKQAIFFHQGDYHAKLGLVLAQAFMPEAIRSIVPAIESI
PacCYP707A2  -----RFVLV TQAHLFKP-TYPPQSKKELIGPSALFFHQNDYHAQIRRLVQSSLSLDVNRNLVPHIDIEAI

```



```

          310          320          330          340          350          360          370          380          390          400
...|...|...|...|...|...|...|...|...|...|...|...|...|...|...|...|...|...|...|...|...|...|
FaCYP707A4a  LRNIIGDIIHERKEKR---LPEKDLLGCLLSSINEGG-EVLSDDDQ-----IADNII GILFAAQD TTASVMTWIFKYLHDEPKII EAVKAEQN AIRI SN
FaCYP707A1/3 LAQILAKIISTRRESK---LDDHNDLLGSFMGDKE-----GLTDEQ-----IADNVI GVIFAARD TTASVLTWIMKYLGENPSVLEAVTEEQEAIMK LK
AtCYP707A1  LSQILARILSERRQNG---SSHNDLLGSFMGDKE-----ELTDEQ-----IADNII GVIFAARD TTASVMSWILKYLAENPNVLEAVTEEQMAIRKDK
SlCYP707A1  LGKILSEIIREMKKK---TLEKDLLSCFLNAKEEKGFVLNEDQ-----IADNII GVLFAAQD TTASVLTWIIKYLHDNPKLLECVKAEQKVIWQSN
SlCYP707A2  LAKIVAKIISTRREMK---IDHGDLGSGFMGDKE-----GLTDEQ-----IADNVI GVIFAARD TTASVLTWILKYLGENPSVLQAVTEEQENIMRKK
AtCYP707A2  LSEELRKVIEKRRENG---REE-GGLLVLLGAKDQKRN-GLSDSQ-----IADNII GVIFAATD TTASVLTWLLKYLHDHPNLLQEVSRQFSIRQKI
AtCYP707A3  LAQILANILSKRRQNP---SSH TDLLGSFMEDKA-----GLTDEQ-----IADNII GVIFAARD TTASVLTWILKYLADNPTVLEAVTEEQMAIRKDK
AtCYP707A4  LKTIVSEIICERREKR---ALQTD FLGHLLNFKNEKG-RVLTQE Q-----IADNII GVLFAAQD TTASCLTWILKYLHDDQKLEAVKAEQKAIYEEN
FvCYP707A1/3 LAQILAKIISTRRESK---LDDHNDLLGSFMGDKE-----GLTDEQ-----IADNVI GVIFAARD TTASVLTWIMKYLGENPSVLEAVTEEQEAIMK LK
FvCYP707A4a  LRHIIGDIIHERKEKR---LPEKDLLGCLLRSINEGG-EVLSDDDQ-----IADNII GVLFAAQD TTASVMTWIFKYLHDEPKILEAVKAEQN AIRLSN
PacCYP707A1  LAQILAKIISTRQRKQ---VEDHKDLLGSFMGDKE-----GLTDQQ-----IADNVI GVIFAARD TTASVLTWIVKYLGENPSVLQAVTEEQEAIMR TK
PacCYP707A2  LSLIVSEIIKEREKES---LVQRDLLGSLNFKDEKG-QTLTHNQ-----IVDNII GVMFAAQD TTASLLTWMIKYLHDDSN TREAIQIEQKAI FESN
PacCYP707A3  LNETLRGLIAKRRKSD---EEESGGLLRVLLGKDQNKPNLQLSDSQ-----IADNII GVIFAAHD TTASTLTWLIKYLHDNADLLEAVTREQEGIRRKL
PacCYP707A4  LREILGDIISERKEKR---LLEKDLLGCLLNSKDKKG-EVLTDDQ-----IADNII GVLFAAQD TTASVMTWILKYLHDEPKLLEAVKAEHNAIRESN
PvCYP707A1  LAQIVAQIISRRQRK---QDYKDLLGSFMGEKA-----GLTDEQ-----IADNVI GVIFAARD TTASVLTWIVKYLGENPSVLEAVTEEQE CILKTK
PvCYP707A2  LAEILAQKISTRKMK---XRT HDLMGSFMNEKA-----GFTDEQ-----IICYIIGCIFAARD TTASVLTWVMVWYLG RNP SVLETA TATEEKCILETK
PvCYP707A3  LGKIISDII CERKEKK---LVERD LLSCLLNWKGGEGG-EVLSDDDQ-----IADNII GVLFAAQD TTASAMTWVVKYLHDEPKLLESVKAEQKAIH KSN
OsCYP714B1  VRALILDVGENGEED---GGNLLSAMLRSARGGGGGGEEVAA-AAEDFVVDNCKSIYFAGYESTAVTAAWCLMLLALHPEWQDRVDEVQEAACCGG
OsCYP714B2  VHKLILEIVKESGEE-----RNLLRAILLSASSS---KVELA-EAENFIVDNCKSIYFAGYESTAVTAAWCLMLLGLHPEWQDRVEEVQEV CAG-
AtCYP714A1  IESLIWETVKERERE CVGDH---K KDLMLQ LILEGARSSCDGNLEDKTQSYKSFVVDNCKSIYFAGHETS AVAVSWCLM LLLALNPSWQTRIRDEVFLHCKNG
AtCYP714A2  LESSIWETVKEREIECKDTH---K KDLMLQ LILEGAMRSCDGNLWDKS-AYRRFVVDNCKSIYFAGHDSTAVSVSWCLM LLLALNPSWQVKIRDEILSSCKNG
AtCYP735A2  VERLLMEIIDS RKDSVEIGR---SSSYGDDLLGLLLNQMDSNKNNLN---VQMIMDECKTFFFTGHETT SLLL TWTMLLALHNPTWQDNVREVRQVCGQD
PtCYP714A3  VESLILGAVKET SQEMSETNSSEKDLMLLLEGA IN--DQSLGKDA---SKSFVVDNCKTIYFAGHESTAVAASWCLM LLLALHPEWQGGIRKELAEISKDG
AtCYP94C1  INRLAGDLIKQR-----LTGLMGKNDLISRMAVVAEDDEYLRD IVVSFLLAGRDTVAAGLTGFFWLLTRHPEVENRIREELD RVMGTG
AtCYP94B3  VHVIVSEIVRAKKKSL E-----IGTGAEAKQD LLSRFLAAGHNG--EAVRDMVISFIMAGRDTTSAAMTWLFWLLTENDDVERKILEEVDPLVSLG
          410          420          430          440          450          460          470          480          490          500
...|...|...|...|...|...|...|...|...|...|...|...|...|...|...|...|...|...|...|...|...|...|
FaCYP707A4a  EQA-----GNQPLSWADTRNMPISYKVVLESRLSSII SFLFREAVDVEYKG-YLIPKGWKV MPLFRNIH HNPEFFA---DPQKFDLSRFEVA-----
FaCYP707A1/3 EES-----GEEKVLNWEDTKKMPITSRVLOETLRVASILSFTFREAVEDVEYEG-YLIPKGWKV LPLFRNIH HSPEIFP---EPEKFDPTRF EVA-----
AtCYP707A1  EEG-----ESLTWGDTKKMPITSRVIOETLRVASILSFTFREAVEDVEYEG-YLIPKGWKV LPLFRNIH HSADIFS---NPGKFDPSRFEVA-----
SlCYP707A1  E-Q-----ENHG L TWQT RKM PITSRVVLETLRMA SII SFAFREAVDVEYKG-YLIPKGWKV MPLFRNIH HNPEFFP---DPQKFDPSRFEVA-----
SlCYP707A2  EVN-----GEEKVLNWQDTRQMPMTTRVIOETLRVASILSFTFREAVEDVEYEG-YLIPKGWKV LPLFRNIH HS PDNFP---EPEKFDPSRFEVS-----
AtCYP707A2  KKE-----NRRISWEDTRKMP LTRVIOETLR AASILSFTFREAVDVEYDG-YLIPKGWKV LPLFRNIH HSSEFFP---DPEKFDPSRFEVA-----
AtCYP707A3  KEG-----ESLTWEDTKKMP LTYR VIOETLRAATILSFTFREAVEDVEYEG-YLIPKGWKV LPLFRNIH HNADIFS---DPGKFDPSRFEVA-----
AtCYP707A4  S-R-----EKKPLTW RQTRNMP LTHKVI VESLRMA SII SFTFREAVDVEYKG-YLIPKGWKV MPLFRNIH HNPKYFS---NPEVFDPSRFEVN-----
FvCYP707A1/3 EES-----GEEKVLNWEDTKKMPITSRVLOETLRVASILSFTFREAVEDVEYEG-YLIPKGWKV LPLFRNIH HSPEIFP---EPEKFDPTRF EVA-----
FvCYP707A4a  EQA-----GNQPLSWADTRNMPISYKVVLESRLSSII SFLFREAVDVEYKG-YLIPKGWKV MPLFRNIH HNPEFFT---DPQKFDLSRFEVA-----
PacCYP707A1  EEEEGDDEGNQKALSWADTKKMPMTSRVIOETLRVASILSFTFREAVEDVEYEG-YLIPKGWKV LPLFRNIH HSPEIFP---EPEKFDPSRFEVA-----
PacCYP707A2  D-G-----GNRTL SWAQTRNMP LTSRAIKESLRMA SII SFTFREAVEDVEYKG-YLIPKGWKV LPLFRNIH HNP DFFV---DPHKFD PSTF-----

```


box contains Cytochrome P450 cysteine heme-iron ligand signature.